Engineering and Urology Society

38th Annual Meeting

Monday, April 28, 2025

Las Vegas, NV

https://engineering-urology.org/

ENDOUROLOGICAL SOCIETY

"Endourology Society Day"
MEETING GUIDE

Monday, April 28th, 2025
7:00am – 6:00pm EDT
The Venetian Resort & Expo
Room: Palazzo Ballroom EF
Las Vegas, Nevada

7:30am – 10:00am

Engineering & Urology Society (EUS)
Engineering & Urology Society President: Jihad Kaouk, MD
Executive Director: Dan Stoianovici, PhD
http://engineering-urology.org/

10:00am – 12:00pm

Focal Therapy Society (FTS)
Focal Therapy Society President: Rafael Sanchez-Salas, MD
https://focaltherapy.org

1:00pm – 5:30pm

Society of Urologic Robotic Surgeons (SURS) Meeting
President: Michael Stifelman, MD
https://sursroboticsurgery.org/

The Engineering and Urology Society proudly announces its 38th Annual Meeting: **"Pioneering the Future of Urology: Precision, Innovation, and Accessibility",** April, 2025 | Las Vegas, Nevada

As we continue our mission to drive the development and application of cutting-edge technologies in urology, the Engineering and Urology Society — an affiliate of the Endourological Society — remains committed to fostering collaboration between engineers, physicists, and urologists. Our goal is to bridge the gap between technical innovation and clinical application, ultimately improving patient care and outcomes.

This year's program has been expanded to showcase groundbreaking advancements across multiple disciplines within urology. Highlights include next-generation robotic surgical platforms, and AI-enhanced intraoperative guidance. Our distinguished speakers—leading urologic surgeons, engineers, and rising star investigators—will present on the development, validation, and integration of these transformative technologies. Additionally, we will emphasize the importance of standardizing research methodologies and outcome reporting to ensure the clinical adoption of these innovations. Key topics will include:

- New robotic systems: First look at cutting-edge robotic technologies in urology.
- Artificial intelligence applications: Exploring AI's role in surgical education, kidney stone management, prostate cancer detection, and bladder cancer treatment.

Two **poster sessions** in the afternoon provide researchers with the opportunity to present their work and update the attendees on the progress on the field and latest innovations. Overall, the review of the abstracts for the poster sessions was performed by a group of 42 international reviewers. We would like to thank the reviewers, listed at the end of this program book, for their essential contribution to the quality of the meeting and their constructive comments that they made for the research.

Based on the review scores, the Society **awards** two closely ranked top abstracts this year. These are listed at the end of this program book, together with the Top 10 abstracts, and Best Reviewer Awards. The authors of all awarded abstracts are invited to submit full length articles to the Journal of Endourology on the respective topics. We gratefully thank all reviewers for their hard work, objective scoring, and contribution to the success of the meeting.

Please visit the website https://engineering-urology.org/ for a complete version of this program including the abstracts presented.

We welcome all urologists, engineers, scientists from industry and academia to join us for this cross-disciplinary experience.

Jihad Kaouk, M.D.
President, Engineering and Urology Society
Dan Stoianovici, Ph.D.
Executive Director, Engineering and Urology Society

The Focal Therapy Society (FTS) in partnership with the Endourological Society, aims to advance and position minimally invasive, image-targeted cancer treatment in a safe, effective, gland-preserving manner to extend and maintain quality of life. Our vision is to control or eradicate prostate or kidney cancer in a minimally invasive, image-targeted manner while optimizing the preservation of organ function. Focal therapy is gaining importance in medicine for several reasons:

- Precision Medicine: Focal therapy allows for targeted treatment of diseased tissue while preserving surrounding healthy tissue, minimizing side effects, and preserving organ function.
- Quality of Life: By preserving organ function, focal therapy can improve a patient's quality of life compared to more aggressive treatments like surgery or whole-gland treatments.
- Reduced Side Effects: Focal therapy typically results in fewer side effects compared to whole-gland treatments, such as urinary incontinence and erectile dysfunction in prostate cancer treatment.
- Patient Selection: Focal therapy is suitable for select patients with localized disease, providing a middle ground between active surveillance and radical treatments.
- Advancements in Technology: Advances in imaging and ablation technologies have improved the accuracy and effectiveness of focal therapy procedures, making them more viable treatment options.

Overall, focal therapy offers a promising treatment alternative reaching its tipping point, which refers to the moment when this approach to treating Prostate Cancer becomes widely accepted and adopted as a standard of care. Several factors will contribute to this tipping point and the Focal Therapy Society strives to address every aspect:

- Clinical Evidence: Accumulating clinical evidence demonstrating the effectiveness and safety of focal therapy compared to traditional treatments like surgery or radiation therapy.
- Advancements in Technology: Continued advancements in imaging, diagnostic tools, and ablative technologies that improve the accuracy and precision of focal therapy procedures.
- Patient Awareness and Demand: Increased awareness among patients about the benefits of focal therapy, leading to greater demand for this treatment option.
- Physician Training and Expertise: Expanded training and expertise among healthcare providers in performing focal therapy procedures, leading to greater confidence in recommending and performing these treatments.
- Guidelines and Recommendations: Inclusion of focal therapy as a recommended treatment option in clinical practice guidelines and consensus statements by professional medical societies.
- Healthcare System Acceptance: Acceptance and integration of focal therapy into healthcare systems, including reimbursement policies and infrastructure support.

The FTS supports and maintains an international registry open to all participating collaborators for the collection of real-world physician experience utilizing FT including outcomes and complications. The FTS will feature state-of-the-art presentations on FT topics of interest during the Endourological Societies' Specialty Day on Sunday, May 5th, 2024 in San Antonio. We have a rich and exciting agenda in 2024 with our next FTS annual meeting, the ***14th International Symposium on Focal Therapy and Imaging in Prostate and Kidney Cancer in conjunction with the Singapore Urological Association*** will be held in Singapore July 25th-26th, 2024. **The World Congress of Endourology 2024** will feature a dedicated Focal Therapy Session in Seoul, South Korea, August 12th-16th, 2024. On September 26th-28th we will hold the FTS-SURS combined Symposium with a unique approach combining Focal Therapy, Imaging, Artificial Intelligence, and Robotics, along with a special session with the FDA on these technologies. We welcome all stakeholders interested in these topics to join us and visit our website www.focaltherapy.org.

Rafael Sanchez-Salas, M.D.
President and Program Chair, Focal Therapy Society

Dear Colleagues and Friends,

On behalf of the Society of Urologic Robotic Surgeons, it is our pleasure to welcome you to the AUA SURS meeting this year, to be held in San Antonio, TX on Sunday, May 5, 2024 (1:00pm–5:30pm). The Society of Urologic Robotic Surgeons (SURS) strives to help surgeons and their teams advance robotic surgery techniques with a goal of promoting innovative treatments and improved outcomes.

The meeting will provide useful information for surgeons and teams at all levels of training and experience in robotic surgery. A diverse faculty will be featured, with both rising and established stars in robotic surgery giving video-based presentations and with expert robotic surgeons moderating and providing commentary. Sessions will include techniques using both Xi and SP robotic approaches and will discuss new and upcoming robotic technologies.

The Young Urologist/Rising Stars session includes video presentations from rising stars as well as presentations on approaches to robotic surgery training and a presentation on building a surgical practice, innovation, and balance. The GU robotic reconstruction session will cover upper and lower urinary tract reconstruction techniques. The prostate surgery session will feature presentations focusing on management of challenging scenarios as well as extraperitoneal and retzius sparing approaches. This session will also feature a presentation from the Focal Therapy Society on why to consider including focal therapy into your robotic surgery practice and how. The robotic kidney surgery session will tips for complex robotic partial nephrectomy, retroperitoneal approaches, tumor excision techniques, and managing complex situations. The robotic cystectomy session will cover cystectomy and diversion techniques and tips to improve efficiency and minimize complications. We look forward to a productive afternoon of learning at the AUA SURS meeting from a diverse faculty of robotic experts and rising stars demonstrating their techniques to improve outcomes in robotic urologic surgery. Thank you all for your dedication to advancing robotic surgery techniques and for your support.

Craig Rogers, MD
President and Program Chair, Society of Urologic Robotic Surgeons

PROGRAM

Engineering & Urology Society Meeting

Program Chair: Jihad Kaouk

7:00AM	**Registration**	**Presenter / Moderator**
7:30AM	**Welcome**: Pioneering the Future of Urology: Precision, Innovation, and Accessibility	Jihad Kaouk
		Craig Rogers Jennifer Lineha
	Session 1: Emerging Robotic Surgical Platforms	David Lee
	Single Port Robotic Platform (5 minute video)	
7:35AM	Da Vinci SP Transvesical Radical Prostatectom	Jihad Kaouk
7:40AM	Da Vinci SP Low Anterior Access Retroperitoneal Partial Nephrectomy	Simone Crivallero
7:45AM	Shurui SP Retroperitoneal Partial Nephrectomy	Zhenjie Wu
	Multi-Modular Robotic Platforms (5 minute video)	
7:50AM	HUGO RAS Retzius-Sparing Radical Prostatectomy	Antonio Galfano
7:55AM	HUGO RAS Cystectomy with Intracorporeal Neobladder	Bernardo Rocco
	Endoluminal Robotic Platform (5 minute video)	
8:00AM	Redefining Endoscopic Surgery with Novel Transurethral Concentric Tube Robotic Platform	S. Duke Herrell
8:05AM	Advancing Minimally Invasive Urological Surgery with Flexible Transurethral Robotic Platform	Peter Chiu
8:10AM	Discussion	
		Alexa Meyer Casey Seideman
	Session 2: Emerging Technologies in Surgical Robotics	
8:20AM	The Future of Innovation in Urology: Integrating the Latest in Biomedical Technology	Margot Damaser
8:27AM	Navigating Challenges and Evolving Landscape in Innovation and Academic Urology	Jennifer Miles-Thomas
8:34AM	Innovations in Endourology & Building Successful Clinical Programs	Amy Krambeck
		Jorge Gutierrez Deepak Agrawal
	Session 3: Advances in Endourology	Bristol Whiles
8:41AM	Emerging Ureteral Access Sheath for Lithotripsy	Anna Zampini
8:48AM	Impact of Intra-Renal Temperature Elevation on Kidney Injury During Ureteroscopic Laser Lithotrispy	Mantu Gupta
8:55AM	Advancing Clinical Outcomes of PCNL with Preoperative Immersive Virtual Reality	Jaime Landman

	Session 4: Innovations in Image-Guided Surgery, Artificial Intelligence, and Telesurgery	Giovanni Cacciamani John Weaver Riccardo Autorino
9:02AM	Contemporary Applications and Future Directions of Augmented Reality with Real-Time Intraoperative Images Overlay	Daniele Amparore
9:09AM	Visualizing the Invisible: The Utility of PSMA-Radioguided Surgery	Giorgio Gandaglia
9:16AM	Telesurgery for Focal Therapy: The First Transcontinental Clinical Application	Ruben Olivares
9:23AM	The Role of Artificial Intelligence & Machine Learning in Urology	Andrew Hung
9:30AM	Telesurgery: The Next Frontier in Surgical Education & Healthcare Equity	Vipul Patel
9:40AM	**Best Abstract Awards**	Dan Stoianovici
9:50AM	Robotic Transurethral Bladder Tumor Resection: A New Era of Natural Orifice Transluminal Endoscopic Surgery (Notes)	Nicolas A Soputro
9:55AM	Biopsy Needle Design Matters: 96% Reduced Bacterial Transfer and Significantly Improved Targeting May Challenge TR vs TP Prostate Biopsy Paradigms	Andreas Forsvall
	Poster Sessions	
1:00PM – 2:00PM	Session 1	Thomas Polascik Atieh Ashkezari
2:30PM – 3:30PM	Session 2	Koon Ho Rha Andreas Forsvall

The Growing Significance of Focal Therapy

Dear Colleagues,

We are pleased to invite you to the Focal Therapy Society Session, which will take place during the Endourological Society Day at the AUA 2025 Annual Meeting on Monday, April 28, 2025. This session will spotlight one of the most promising and rapidly evolving approaches in prostate cancer care: focal therapy.

As the management of localized prostate cancer continues to shift towards precision and personalization, focal therapy has emerged as a cornerstone of this evolution. By balancing cancer control with the preservation of quality of life, focal therapy represents a paradigm shift in treatment—offering minimally invasive options that address the disease while minimizing unnecessary harm to surrounding tissues.

This session will explore how advancements in diagnostics, imaging technologies, and innovative treatments are shaping the future of focal therapy. We aim to provide attendees with a comprehensive understanding of the current standards, the latest research, and the exciting potential of these approaches.

Our carefully curated program features renowned international experts who will delve into critical aspects of focal therapy:

- The evolving standards in diagnosis, risk stratification, and the integration of cutting-edge imaging techniques.
- A focus on the latest technologies in micro-ultrasound, artificial intelligence, and their role in focal therapy planning and monitoring.
- Updates on the most advanced therapeutic modalities, including cryotherapy, irreversible electroporation, and robotic partial prostatectomy.

The session is designed to combine practical, evidence-based lectures with opportunities for dialogue through interactive Q&A segments, ensuring a dynamic exchange of ideas and insights.

As practitioners, researchers, and innovators, we are at a critical juncture in redefining prostate cancer treatment, Focal Therapy is moving toward its tipping point. The work we do today will set the standards for future care, and this session provides a unique platform to advance our shared mission of delivering optimal outcomes for our patients.

We look forward to welcoming you to this pivotal event and to continuing the important conversations that will drive progress in focal therapy and beyond.

Warm regards,

Rafael Sanchez-Salas, M.D.
President and Program Chair, Focal Therapy Society

Focal Therapy Society

FTS Program Chair: Rafael Sanchez-Salas, MD

Objective: To offer a comprehensive overview of the aspects currently under development in partial gland ablation for prostate cancer treatment.

10:00am – 10:05am Welcome and Introduction
Rafael Sanchez-Salas, M.D.

Session 1: **Diagnosis, Risk Stratification and Imaging Integration**
Chairs: Lara Rodriguez-Sanchez, MD
Kae Jack Tay, MD
Ardeshir Rastinehad, DO

10:05am – 10:20am Prostate Cancer Diagnosis and Stratification in 2024
Hashim Ahmed, MD

10:20am – 10:35am Role of Micro-Ultrasound in Prostate Cancer Diagnosis
Laurence Klotz, MD

10:35am – 10:50am Imaging for Focal Therapy Planning and Monitoring
Kara Watts, MD

10:50am – 11:05am Artificial Intelligence in Prostate Imaging and Diagnosis
André Abreu, MD

11:05am – 11:10am Q & A

Session 2: **Focal Therapy: Treatment and Evolution**
Chairs: Alice Yu, MD
Thomas Polascik, MD
Fernando Bianco, MD

11:15am – 11:30am Cryotherapy and Beyond
Herbert Lepor, MD

11:30am – 11:45am Irreversible Electroporation and Beyond
Phillip Stricker, MD

11:45am – 12:00pm Robotic Partial Prostatectomy
Jihad Kaouk, MD

12:00pm – 12:05pm Q & A

POSTER SESSION 1

1:00 PM – 2:00 PM

Moderators:
Thomas Polascik
Atieh Ashkezari

No	Title	Presenting Author
1	SPONTANEOUS URETERAL RUPTURE MANAGED WITH NOVEL NON-REFLUXING RELIEF STENT	George Gheordunescu
2	**BEST ABSTRACT AWARD** BIOPSY NEEDLE DESIGN MATTERS: 96% REDUCED BACTERIAL TRANSFER AND SIGNIFICANTLY IMPROVED TARGETING MAY CHALLENGE TR vs TP PROSTATE BIOPSY PARADIGMS	Andreas Forsvall
3	**TOP 10 ABSTRACT** A STEERABLE KIDNEY STONE BASKET	Peter Connor
4	**TOP 10 ABSTRACT** OPTIMIZATION OF GOLD-SILVER NANOPARTICLE COATINGS WITH ANTIMICROBIAL AND ANTIBIOFILM PROPERTIES	Alejandro Bautista-Perez-Gavilan
5	**TOP 10 ABSTRACT** A NEW ULTRASOUND PROBE AND ROBOT FOR PROSTATE BIOPSY	Dan Stoianovici
6	**TOP 10 ABSTRACT** THE EFFECT OF PROSTATE SIZE AND NUMBER OF CORES AT SYSTEMATIC PROSTATE BIOPSY – STUDY UPDATE	Dan Stoianovici
7	A FIBER-STEERING DEVICE TO REDUCE LASER LITHOTRIPSY PROCEDURE TIME	Peter Connor
8	A 3D-PRINTED DUAL-MODEL TRAINING PLATFORM FOR PEDIATRIC HYPOSPADIAS REPAIR: ENHANCING SURGICAL SKILL DEVELOPMENT	Akash Chauhan
9	PROSTATE CANCER EXTRACAPSULAR INVASION DETECTION VIA NON-CONTACT LASER INDUCED FLUORESCENCE SPECTROSCOPY	Tanner J Zachem
10	SIMULATION OF DIAPHRAGMATIC DISPLACEMENT DURING PERCUTANEOUS NEPHROLITHOTOMY: A COMPUTATIONAL APPROACH FOR OPTIMIZING AIRWAY MANAGEMENT	Atieh Ashkezari
11	HIGH-FIDELITY PHYSICAL SIMULATOR MODEL FOR TRAINING MALE INFANT FOLEY CATHETERIZATION WITH INTEGRATION INTO OPERATING ROOM NURSING TECHNICAL SKILLS CURRICULUM	Lauren Poniatowski
12	ELUCIDATING THE PHYSICAL PROPERTIES OF URETERAL STENTS	Felix Yiu
13	NOVEL FOLEY CATHETER WITH TOROIDAL BALLOON SHEATH REDUCES URETHRAL TRAUMA	Grant Steele
14	A NOVEL PLATFORM FOR REMOTE MICROSCOPIC URINALYSIS: THE U-CHECK SYSTEM	André F Santos

15	VISUAL EXPLANATION OF DEEP LEARNING MODELS FOR AUTOMATIC KIDNEY STONE DETECTION USING MULTIPLE CT SOURCES DATASET	Gabriel Nunes Missima
16	A TALE OF TWO PERCS: A CAUSAL ANALYSIS OF PAPILLARY PERCUTANEOUS ACCESS USING THE MONARCH™ PLATFORM, UROLOGY	Lauren Friend
17	A BENCHTOP KIDNEY MODEL FOR MEASURING SPATIAL VARIATION IN TEMPERATURE DURING SIMULATED LITHOTRIPSY	Alycia Abbott
18	MATHEMATICAL MODELING OF INTRA-RENAL PRESSURE DURING SCOPE WITHDRAWAL THROUGH A FANS	Jessica Williams
19	USE OF ARTIFICIAL INTELLIGENCE AND NOVEL ELECTROMAGNETIC DEVICE IN PROSTATE CANCER DETECTION: DEVELOPMENT OF A MODEL OF PCA RISK ASSESSMENT	Carlo Bellorofonte
20	INITIAL EXPERIENCE OF ARTIFICIAL INTELLIGENCE-GUIDED CORRELATION BETWEEN MPMRI AND ELECTROMAGNETIC DIAGNOSTIC TOOL IN MANAGEMENT OF PI-RADS 3 LESIONS	Carlo Bellorofonte
21	COMPARATIVE EVALUATION OF THE PHYSICOCHEMICAL PROPERTIES OF ADHESIVE AGENTS FOR THE ENHANCEMENT OF POST-LITHOTRIPSY STONE CLEARANCE	Harel Sims
22	AFTER ONE YEAR OF EXPERIENCE: COULD DISS (3.6 FR WORKING CHANNEL) MAKE EVERYTHING THAT SUCTIONING BENDABLE ACCESS SHEATH DOES?	Bogdan Geavlete
23	CONCOMITANT URETERO-RENAL STONES TREATED WITH DISPOSABLE RIWO D-URS – FIRST EXPERIENCE	Bogdan Geavlete
24	OPTIMIZING RADIOFREQUENCY THERAPY FOR OVERACTIVE BLADDER: IDENTIFYING HIGH NERVE DENSITY ZONES IN A CADAVERIC STUDY	Gamal Ghoniem

POSTER SESSION 2

2:30 PM – 3:30 PM

Moderators:
Koon Ho Rha
Andreas Forsvall

No	Title	Presenting Author
25	ENHANCING SURGICAL SAFETY IN TELEOPERATED ROBOTICS RIRS SYSTEMS USING FORCE FEEDBACK	Jin-Hyeok Bae
26	THE EFFECT OF CONTINUOUS FLOW IRRIGATION ON INTRARENAL PRESSURE DURING *EX VIVO* PORCINE RETROGRADE INTRARENAL SURGERY	Yezan F Hadidi
27	ROBO-CYSTO: FEASIBILITY OF A COMPUTER VISION MODEL TO IDENTIFY ANATOMIC LANDMARKS DURING CYSTOSCOPY	Maya Srinath
28	MEDIC: MACHINE LEARNING-BASED FEATURE EXTRACTION FOR INTELLIGENT CLIPPING IN ENDOSCOPIC KIDNEY SURGERY VIDEOS	Bradley French
29	AUTOMATED PREDICTION OF KIDNEY STONE-FREE STATUS USING DIGITAL URETEROSCOPY VIDEO ANALYSIS	Bradley French
30	**TOP 10 ABSTRACT** FEASIBILITY OF WIRELESS CATHETER-FREE AMBULATORY URODYNAMICS IN MALE PATIENTS	Tyler Trump
31	*EX-VIVO* COMPARISON OF PIRANHA™ VS. CYBER BLADE™ MORCELLATORS IN A VALIDATED PROSTATE MODEL	Chloe Michel
32	A NOVEL CORE NEEDLE BIOPSY (CNB) INSTRUMENT DESIGNED FOR TARGETED PROSTATE BIOPSY	Eric Gwynn
33	EVALUATION OF A NOVEL WIRELESS MOTORIZED SINGLE-USE FLEXIBLE URETEROSCOPE IN PORCINE MODEL	Runhan Ren
34	UNDERSTANDING BIOMECHANICAL DIFFERENCES IN PENILE IMPLANT CYLINDER MATERIALS	Irwin Goldstein
35	WHAT IS “TENSION-FREE”? UTILIZING BLACK LIGHT ASSESSMENT OF SURGICAL TECHNIQUE (BLAST) TO QUANTIFY SUTURE TENSION IN AN ADVANCED URETERAL REPAIR SIMULATOR	Judith Hagedorn
36	CAN A SURGEON WEAR A MONITOR: PHYSICAL ATTRIBUTES OF AN EXTENDED REALITY (XR) NEAR-EYE HEADSET	Steven Griffith
37	TRANSPACIFIC TELESURGERY: A PRECLINCAL FEASIBILITY STUDY OF LONG-DISTANCE ROBOTIC SURGERY BETWEEN THE USA AND CHINA	Marcio Covas Moschovas
38	PRESSURE CHARACTERIZATION OF BENCHTOP MODEL WITH SIMULATED FANS OPERATION	Anya Chase
39	AUTOMATED DETECTION OF LASING ACTIVITY FOR POST-OPERATIVE CASE ANALYSIS IN MINIPCNL PROCEDURES WITH THE MONARCH™ PLATFORM	Saif Sayed
40	DOES LUBRICATION OF BRAIDED AND MONOFILAMENT SUTURE WITH BACITRACIN-PETROLATUM AND SALINE, RESPECTIVELY, REDUCE SUTURE DRAG AND, PRESUMABLY, TISSUE TRAUMA? A QUANTITATIVE PULL-FORCE MEASUREMENT STUDY	Alejandro D Lopez

41	**TOP 10 ABSTRACT** HIGH-PRECISION DETECTION OF DIFFICULT-TO-DETECT LESIONS IN BLADDER CANCER DIAGNOSIS USING A LIGHTWEIGHT AI MODEL	Ryotaro Okazaki
42	THE FIRST-IN-HUMAN TRANSCONTINENTAL TELESURGERY COLLABORATION FOR HIGH-INTENSITY FOCUSED ULTRASOUND (HIFU): A NEW ERA IN GLOBALIZING FOCAL CANCER TREATMENT FOR PROSTATE CANCER	Nicolas A Soputro
43	**BEST ABSTRACT AWARD** ROBOTIC TRANSURETHRAL BLADDER TUMOR RESECTION: A NEW ERA OF NATURAL ORIFICE TRANSLUMINAL ENDOSCOPIC SURGERY (NOTES)	Nicolas A Soputro
44	**TOP 10 ABSTRACT** PROSTATE DUCTAL ANATOMY AS A CANCER CONTRAST MECHANISM FOR ULTRASOUND	Dan Luca
45	ASSESSING PERSONAL STATEMENTS FOR UROLOGY RESIDENCY APPLICANTS GENERATED BY ARTIFICIAL INTELLIGENCE COMPARED TO APPLICANT WRITTEN PERSONAL STATEMENTS	Iyla Bagheri
46	THE FIRST EXPERIENCE USING 5.1 FR. WORKING CHANNEL WITH SUCTION (SINGLE-USE FLEXIBLE URETEROSCOPES PU 400A) AND BENDABLE ACCESS SHEATH 12/14 FR. IN COMPLETE 2-3 CM RENAL STONE REMOVAL	Bogdan Geavlete
47	A COMPARATIVE *IN VITRO* STUDY OF STANDARD VERSUS FLEXIBLE SUCTION URETERIC ACCESS SHEATH	Mario Basulto-Martínes
48	**TOP 10 ABSTRACT** IMPROVED CONTROL OF RENAL PELVIS PRESSURE USING A PROTOTYPE FLUID MANAGEMENT SYSTEM INCORPORATING URETEROSCOPE PRESSURE FEEDBACK	Leilane Glienke
49	LASER LITHOTRIPSY OF A BRUSHITE CRYSTALLINE AGGREGATE STONE MODEL: FRAGMENT DISTRIBUTION VS. BEGOSTONE AND HUMAN STONES	Leilane Glienke
50	AUGMENTED REALITY ASSISTED MRI-ULTRASOUND FUSION FOR NON-RECTAL FULLY-TRANSPERINEAL PROSTATE BIOPSY	Braden Millan

Sharpen Your Skills:
Interactive Robotic Urology at the AUA SURS Program!

Dear Friends and Colleagues,

Get ready for the SURS program during the AUA Annual Meeting in Las Vegas on **Monday, April 28th, from 1:00 PM to 5:30 PM**. We're offering a deep dive into five key areas of robotic urology, with a strong emphasis on interactive case presentations that let you apply your knowledge in real time:

- **AI and Simulation in Robotic Surgery:** Explore the future of surgical training and AI integration.
- **Robotic Urinary Tract Reconstruction:** Test your skills with complex case presentations covering fistula repair, ureteral strictures, and more.
- **Robotic Cystectomy and Urinary Diversion:** Analyze challenging cases and refine your approach to optimizing functional outcomes and complex dissections.
- **Robotic Kidney Transplantation:** Sharpen your decision-making with case studies highlighting the latest techniques in robotic kidney transplantation.
- **Robotic Prostatectomy:** Apply your knowledge to diverse prostatectomy cases, exploring different approaches and troubleshooting challenging scenarios.

This program features a collaborative learning experience led by both established leaders and rising stars in the field. Beyond interactive case presentations, you'll have the opportunity to engage in dynamic discussions, explore cutting-edge techniques, and refine your surgical approach. Don't miss this unique opportunity!
We look forward to seeing you in Las Vegas.

Sincerely,

Michael D. Stifelman, MD
President and Program Chair
Society of Urologic Robotic Surgeons

SOCIETY OF UROLOGIC ROBOTIC SURGEONS MEETING
Program Chair: Michael Stifelman, MD

1:00pm- 1:05pm Welcome
Michael Stifelman, MD
President, Society of Urologic Robotic Surgeons

1:05pm – 1:20pm AI in Robotic Surgery – Where are we Heading?
Andrew Hung, MD

1:20pm – 1:35pm Simulation in Robotic Surgery
Thomas Osinski, MD

1:35pm – 2:35pm Module I: Robotic Urinary Tract Reconstruction
Moderators: *Sammy Elsamra, MD*
Ziho Lee, MD

1:35pm – 1:45pm Robotic Fistula Repair: Optimizing Outcomes
(Key Points: Types of fistulas, surgical approaches, tips for successful repair, long-term outcomes)
Ziho Lee, MD

1:45pm – 1:55pm Managing Distal Ureteral Strictures: A Tailored Approach
(Key Points: Reflux vs. side2side vs. nonrefluxing vs. UU, Ureteroenteric Anastomosis: Techniques and Pearls)
Judith Hagedorn, MD

1:55pm – 2:05pm Buccal Mucosa Ureteroscopy: A Decade of Success
(Key Points: Standard Technique, adjuncts to help with success, versatility, data)
Daniel Eun, MD

2:05pm – 2:15pm Vascular Reconstruction – What Are We Being Asked to Do, What Could We Do or Teach?
(Nutcracker Syndrome, Aneurysm repair, exposure)
Sammy Elsamra, MD

2:15pm – 2:35pm Case Presentations and Panel Discussion
- Four Complex Urinary Tract Reconstruction Cases will be Presented
- A Panel of Experts will Provide Their Recommended Approach in 2 Minutes
- The Audience will Vote on the Preferred Technique Based on the Presentation

Panelists: *Daniel Eun, MD*
Sammy Elsamra, MD
Judith Hagedorn, MD
Ziho Lee, MD

2:35pm – 3:15pm SURS Session: Rising Stars in Robotic Urology
Presentation of Videos from Rising Stars in Robotic Urology
- Award Ceremony Recognizing Their Contributions

3:15pm – 3:45pm **Module 2: Robotic Cystectomy and Urinary Diversion**
Moderators: *Alvin Goh, MD*
Mutahar Ahmed, MD

3:15pm – 3:25pm Improving Functional Outcomes in Men and Women
(Key Points: Nerve-sparing techniques, optimizing continence, sexual function preservation
Janet Kukreja, MD

3:25pm – 3:35pm The Extended Node Dissection: How, When and Why
(Key Points: Indications, surgical technique, impact on oncological outcomes, potential complications)
Mihir Desai, MD

3:35pm – 3:45pm 10 Tricks to Improve Your Conduit and Neobladder Efficiency and Success
(Technical pearls for conduit and neobladder creation, minimizing complications, optimizing outcomes)
Mutahar Ahmed, MD and Alvin Goh, MD

3:45pm – 4:00pm Case Presentations and Q&A
- Two Complex Robotic Cystectomy Cases will be presented
- Open Discussion and Q&A with the Audience

Panelists: *Janet Kukreja, MD*
Mihir Desai, MD
Mutahar Ahmed, MD
Alvin Goh, MD

4:00pm – 4:30pm **Module 3: Robotic Kidney Transplantation**
Moderators: *Michael Palese, MD*
Albert Breda, MD

4:00pm – 4:15pm Robotic Kidney Transplantation: The European Experience
(Key Points: Advantages of Robotic Approach, Surgical Technique, Outcomes Compared to open surgery)
Alberto Breda, MD, Karel Decaestecker, MD

4:15pm – 4:30pm Donor Nephrectomy: Is Single Port the Answer?
(Key Points: Benefits and Challenges of Single-Port Donor Nephrectomy, Patient Selection, Surgical Technique)
Simone Crivellaro, MD
Michael Palese, MD

4:30pm – 4:45pm Case Presentations and Panel Discussion
- Three Complex Robotic Kidney Transplant Cases will be Presented.
- A Panel of Experts will discuss the cases and answer audience questions

Panelists: *Obi Ekwenna, MD*
Alvin Wee, MD
Mohamed Eltemamy, MD
Simone Crivellaro, MD
Karel Decaestecker, MD
Michael Palese, MD
Alberto Breda, MD

4:45pm – 5:15pm **Module 4: Robotic Prostatectomy**
Moderators: *John Davis, MD*
Vipul Patel, MD

4:45pm – 4:55pm Robotic Prostatectomy: Retzius Approach
(Key Points: Surgical technique, advantages and disadvantages, oncological and functional outcomes)
Kirsten Greene, MD

4:55pm – 5:05pm Transvesical Single-Port Robotic Prostatectomy
(Key Points: Patient selection, surgical technique, benefits and limitations compared to multiport approach)
Jihad Kaouk, MD

5:05pm – 5:15pm Extraperitoneal Single-Port Robotic Prostatectomy
(Key Points: Surgical technique, advantages and disadvantages, comparison with other approaches)
Jean Joseph, MD

5:15pm – 5:30pm Case Presentations and Q&A
- Three Complex Robotic Prostatectomy Cases will be presented
- Open Discussion and Q&A with the Audience

Panelists: *Vipul Patel, MD*
John Davis, MD
Jean Joseph, MD
Kirsten Greene, MD
Jihad Kaouk, MD

ABSTRACTS:

ABSTRACT 1

SPONTANEOUS URETERAL RUPTURE MANAGED WITH NOVEL NON-REFLUXING RELIEF STENT

George Gheordunescu[1], Michael Zell[1]
[1] Urology Institute, University Hospitals Cleveland Medical Center, Cleveland, OH

Introduction: Spontaneous ureteral rupture is a rare urological condition, usually secondary to an obstructing ureteral stone, and typically managed with double J ureteral stent insertion [24768334]. The RELIEF stent is a novel ureteral stent that eliminates the vesicoureteral reflux of traditional double J stents due to substitution of the attached semirigid distal coil with a floating monofilament [38408491]. This allows for coaptation of the ureteral orifice and avoids constant contact with the bladder trigone, minimizing the flank pain due to reflux and bladder spasms caused by traditional ureteral stents. The RELIEF stent is FDA approved for temporary drainage of the ureter and prevention of vesicoureteral reflux. The initial clinical trial was conducted in patients with renal and ureteral calculi. To our knowledge, this is the first published report using the RELIEF stent for management of a ureteral injury.

Methods: Case Presentation: A 73-year-old male with a history of benign prostatic hyperplasia and nephrolithiasis presented to the emergency department with abdominal pain and left flank pain. Initial evaluation revealed stable renal function (creatinine 0.96) and no signs of infection. Contrast-enhanced Computed Tomography (CT) with delayed phase imaging demonstrated contrast extravasation likely from the left proximal ureter/ureteropelvic junction with an extensive left-sided retroperitoneal urinoma. He was taken to the operating room for cystoscopy, retrograde pyelogram, and ureteral stent placement.

Results: Cystoscopy was unremarkable other than an enlarged prostate. Interestingly, retrograde pyelogram did not demonstrate any contrast extravasation. A 6 French by 26-centimeter RELIEF stent was placed in the left ureter. After stent placement an intraoperative cystogram was performed and there was no vesicoureteral reflux noted. He was discharged on post-operative day 1. On post-operative day 23 a repeat CT Urogram revealed resolution of previously seen urinoma, no contrast extravasation, and the ureteral stent in the correct position. Stent was then removed in the office on post-operative day 30 and repeat CT Urogram on post-operative day 45 again showed no contrast extravasation.

Conclusion: The RELIEF stent has not previously been reported in the setting of ureteral rupture. However, it should be considered in future cases of proximal ureter or renal pelvis injuries as it has demonstrated success while eliminating vesicoureteral reflux that may prolong or impede healing. Additonally, compared to standard ureteral stents, the RELIEF stent has been shown to reduce patient discomfort, potentially improving tolerance. This case supports exploring the use of the RELIEF stent in other settings of upper tract injury or iatrogenic trauma that require double J stent placement such as after percutaneous nephrolithotomy, ureteropelvic junction repair, urine leak after partial nephrectomy, or other collecting system injuries. Future studies are needed to determine the full scope of its usage and long-term efficacy in these settings.

Figure 1: Left: large urinoma and contrast extravasation from left ureteropelvic junction.
Middle: follow-up CT Urogram two weeks after stent removal. Right: RELIEF stent

ABSTRACT 2 **BEST ABSTRACT AWARD**

BIOPSY NEEDLE DESIGN MATTERS: 96% REDUCED BACTERIAL TRANSFER AND SIGNIFICANTLY IMPROVED TARGETING MAY CHALLENGE TR vs TP PROSTATE BIOPSY PARADIGMS

Andreas Forsvall [1,2,3] for the Lund/Xaga study group
[1] Faculty of Medicine, Department of Clinical Sciences, Infection Medicine, Lund University, Lund, Sweden [2] Department of Urology, Helsingborg Hospital, Helsingborg, Sweden [3] Xaga Surgical AB, Eslov, Sweden

Introduction: The Tru-cut biopsy needle was patented in 1969. A vast improvement at the time, but not designed for modern MRI first target biopsy or infection control in times of antibiotic resistance.

The root cause of infection in transrectal biopsy (TR) is the transfer of colonic bacteria from the rectum into sterile tissue. Efforts to address infections have reintroduced the transperineal biopsy (TP) approach and for example target antibiotics and rectal cleansing in TR. However, the actual cause of infection - the bacterial transfer by the biopsy needle has remained unaddressed. At the same time prostate cancers are heterogenous, very precise sampling of lesions is critical, yet the Tru-cut needle deviates in tissue. The Forsvall biopsy needle aims reduce infection risk and improve target biopsy.

Methods: The physical mechanism of bacterial transfer and needle deviation was evaluated, and the Forsvall needle was developed based on these findings. The current Tru-cut and the Forsvall needle designs were compared in three studies: an ex-vivo study measuring bacterial transfer across the human colon wall (1). An in-vitro, gel-based study comparing target tissue collection in simulated distal (30 mm from needle point of entry) basal, anterior 8 mm PI-RADS 4 lesions in 50 biopsies, both TP and TR (2). And a clinical TR trial evaluating 249 biopsy results in 20 patients (3).

Results: We found that the bacteria causing infection in transrectal prostate biopsy is transported across the colon wall trapped **inside** the tru-cut needle, while tissue friction almost eliminates bacteria from the outside of the needle (right image, large red arrow indicates location of bacterial transfer in tru-cut, small image shows fecal matter collected inside tru-cut after simulated colon puncture). Deviation in tissue was related to three things: the wedge-shaped grinding of the inner needle, the angled outer needle sheath and tolerances between the needle parts (3 red arrows in left image). The Forsvall needle basic feature aligning the needle head with the needle sheath, creating a **closed, completely smooth needle**. In combination with a new biopsy gun mechanism and grinding of the needle head, it addresses the flaws (red arrows) of the current tru-cut needle. The study results are a **96% reduction** [95% CI 93.0–97.7%] ($p<0.001$) in the infection causing bacterial transfer across the colon wall (1). A significantly improved on target tissue collection; where the Tru-cut needle sampled the target in only 4% of biopsies due to deviation, The Forsvall needle hit and sampled the target in **100% of biopsies** ($p<0.001$) (2). Patient experience and biopsy length were **non-inferior** to the Tru-cut needle (3).

Conclusion: Prostate biopsy remains pivotal in prostate cancer diagnosis. Deviation and infection are needle caused complications. By redesigning the Tru-cut needle to eliminate bacterial reservoirs and improve targeting, this technology addresses current limitations. Future clinical trials validating infection reduction and cancer detection accuracy may necessitate re-evaluation of prior TR/TP studies, all conducted with suboptimal (1969) needle designs. The Forsvall biopsy system's FDA clearance in March 2025 marks a critical step toward translating engineered needle solutions into clinical practice.

ABSTRACT 3 **TOP 10 ABSTRACT**

A STEERABLE KIDNEY STONE BASKET

Peter Connor[1], Joshua Gafford[2], Scott Webster[2], S. Duke Herrell[1,2,3], Nick Kavoussi[3], Kim Maciolek[3], Amy Reed[3], Kent Chevli[4], Jake Childs[2], Tyler Efird[2], and Robert J. Webster III[1,2,3]
[1] Vanderbilt University, [2] EndoTheia Inc.
[3] Vanderbilt University Medical Center, [4] WNY Urology Associates

Introduction: While kidney stone removal is a standard clinical procedure, surgeons can encounter stones which lie in recessed areas that are challenging to reach. Particularly, stones which are present in the lower pole (accounting for 25-35% of all kidney stones [PMC10039418]) can be difficult due to anatomical constraints and the limited maneuverability of existing ureteroscopes and ureteroscopic tools. We hypothesize that an independently steerable stone retrieval basket will provide improved access to difficult-to-reach kidney regions, enabling quicker stone removals compared to standard techniques.

Methods: We designed, manufactured, and evaluated a stone retrieval device with an independently steerable tip based on recently invented concentric push-pull technology [PMC10871709]. To demonstrate access, we performed an experiment where a user navigated the device through a porcine kidney to demonstrate reachability of all calyces and found that complete access was possible. To demonstrate usability and the potential to improve procedure times, a cohort of users (N=11, experience level ranging from novice to expert) used the device to remove as many stones as possible from the lower pole of a synthetic kidney simulator, both with and without our device. The stone capture rate for each trial was recorded.

Results: We found that a user was able to deploy our basket into all calyces of the kidney without adverse effects (as confirmed by a post-operative inspection), even those in the lower pole. Users in the stone removal trials were able to remove lower pole stones significantly more rapidly using our device compared to standard techniques (2.7 ± 1.8 stones/min with our basket compared to 0.9 ± 0.10 stones/min with a standard basket).

Conclusion: Our device not only provides increased reachability within the kidney to remove challenging stones but also enables faster retrieval of more typical stones. These results demonstrate that a steerable basket retrieval device can improve the process of stone retrieval.

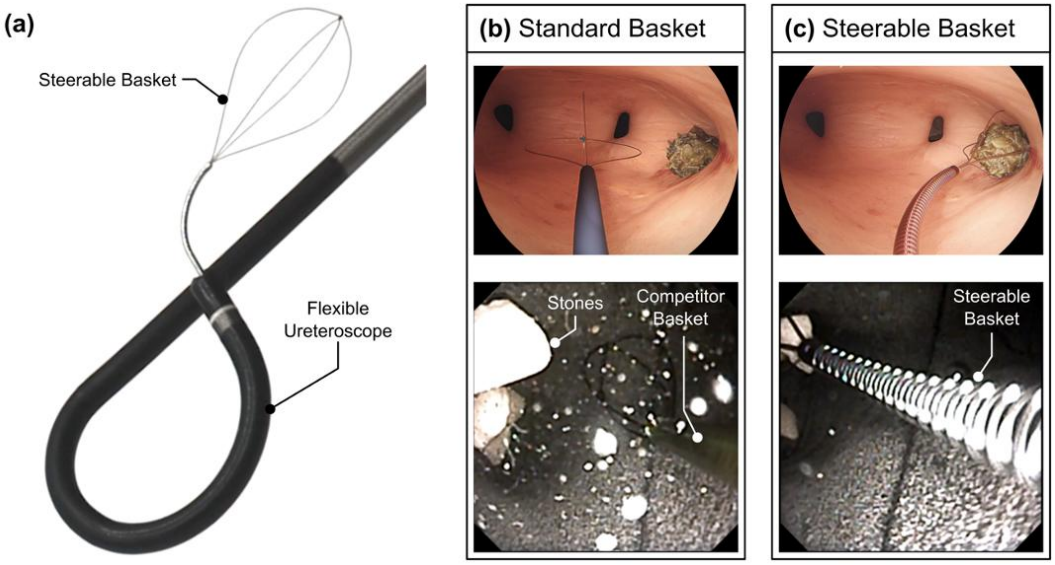

Figure 1: (a) Image of our steerable basket deployed through a flexible ureteroscope, (b) a standard basket unable to reach a challenging stone due to anatomical constraints, and (c) the steerable basket capturing a challenging stone

ABSTRACT 4 **TOP 10 ABSTRACT**

OPTIMIZATION OF GOLD-SILVER NANOPARTICLE COATINGS WITH ANTIMICROBIAL AND ANTIBIOFILM PROPERTIES

Alejandro Bautista-Perez-Gavilan[1]; Jorge Gutierrez-Aceves[1]; Smita De[1]; Aaron W. Miller[1,2]; Vijay Krishna[3]

[1] Urology Department, Cleveland Clinic Glickman Urological Institute, Cleveland, OH, USA
[2] Cardiovascular and Metabolic Sciences Department, Cleveland Clinic Lerner Research Institute, Cleveland, OH, USA. [3] Biomedical Engineering, Cleveland Clinic Lerner Research Institute, Cleveland, OH, USA

Introduction: Biofilms on devices such as urethral catheters and ureteral stents are associated with infections that ultimately require device exchange or removal**.** Our group has previously developed novel gold-silver nanoparticles (GSNP), which on polyurethane discs achieved 100% reduction in bacterial loads, at physiologically relevant densities, for diverse Gram positive and negative uropathogens. GSNPs are non-toxic at minimum inhibitory concentrations for all tested human uropathogens. Here, we evaluate synthesis conditions and polymer matrix for GSNP coating on its antimicrobial activity over several days.

Methods: GSNP synthesis conditions were varied by changing the stirring speed (200 and 600 rpm) and samples taken at 1, 3, 7, 10 and 14 days were characterized for nanoparticle size with dynamic light scattering and concentration using UV-Vis spectrophotometry. Next, GSNP coatings with polydopamine (PDA) as a polymer matrix were evaluated. Four replicates were prepared on polyurethane coupons with GSNP only, PDA only, a layered GSNP coating followed by a PDA coating, and a mixed GSNP-PDA coating. Antimicrobial activity was tested in a static model, a semi-static model, and a dynamic model with commercially available *E. coli*. Efficacy of coating strategies was quantified through the abundance of colony-forming units (CFU)/mL derived from each model.

Results: The concentration of GSNP obtained was higher 600 rpm stirring speed and the concentration increased with time for both stirring speed (Fig 1A). In the static model, all GSNP coatings showed 100% reduction in *E. coli* concentration across the first 4 days (data not shown). In the semi-static model, all three GSNP-containing coatings showed 100% bacterial load reduction in the first 24 hours (Fig 1B). Only the GSNP-PDA coating was able to maintain strong antimicrobial activity for 3 days. In the dynamic model, the GSNP-PDA coating showed significant reduction of biofilm activity after 48 hours of exposure, however, did not achieve 100% reduction as observed in semi-static and static models (Fig 1C).

Conclusion: PDA is a suitable matrix for coating GSNP however, further optimization of coating parameters is needed. A limitation of this study is use of bacterial concentrations that are substantially higher than that seen in the human urinary tract.

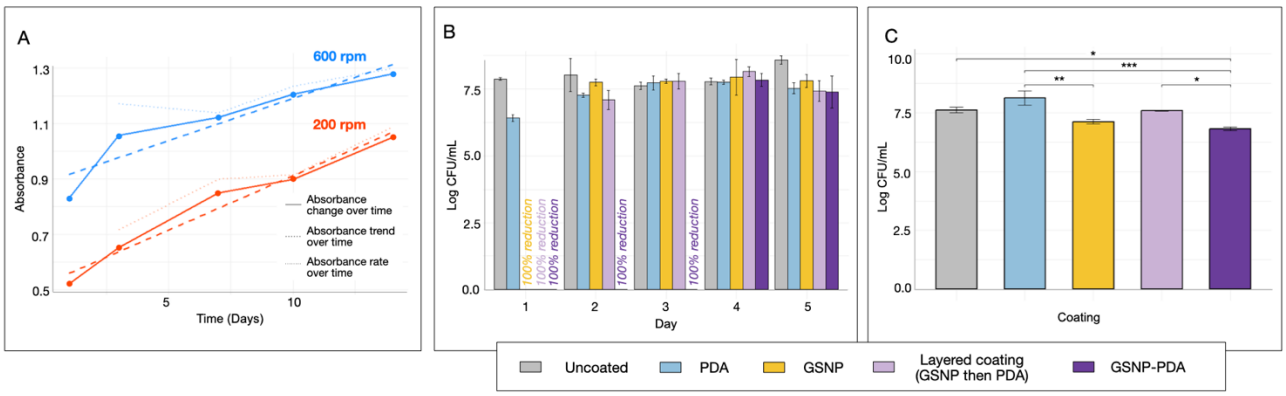

Figure 1. (A) Absorbance over time for different stirring speeds. **(B)** log CFU/mL across coatings over time. All replicates were serially exposed to a working stock containing *E coli* every 24 hours over 5 days. (**C)** Significant differences in biofilm activity across coatings when exposed to a dynamic environment simulating the urinary tract with supraphysiological levels of *E coli* for 48 hours.

ABSTRACT 5 **TOP 10 ABSTRACT**

A NEW ULTRASOUND PROBE AND ROBOT FOR PROSTATE BIOPSY

Dan Stoianovici[1,2], Katarzyna J. Macura[3], Doru Petrisor[1,2], Arvin K. George[1], Misop Han[1]
[1]Brady Urological Institute [2]Robotics Laboratory, [3]Department of Radiology, Johns Hopkins University

Introduction: MRI-ultrasound fusion has become the standard procedure for prostate biopsy, on the transrectal (TR) and more recently on the transperineal (TP) needle path approach [PMC38212178]. Fusion biopsy was enabled by commercial devices typically with a handheld end- or side-fire ultrasound probe. Robotic probe handling was enabled by the TP biopsy Mona Lisa (BioBot Surgical, Ltd.) robot and our TR biopsy TRUS-Robot [EUS2017 Abs.34, EUS2023 Abs.11]. All manual and robotic devices use off-the-shelf ultrasound probes. We report a novel probe purposely designed for the prostate and robotic operation. Moreover, the probe-robot (ProBot) uniquely applies to either TR or TP biopsies.

Methods: Biopsy needle-guides are typically fixed to the ultrasound probe. As such, the probe must be moved to orient the guide on each biopsy target. These movements deform the gland while complicating the fusion to MRI, and make needle targeting prone to errors. Instead, we invented a side-fire probe (US Patent 10,159,469 B2) that allows a variable angulation of the needle relative to the probe. The angulation together with a rotation of the probe about its axis allows to target any prostate location. None of these 2 motions can change the compression of the prostate, potentially improving needle targeting. The 2 degrees of freedom (DoF) are actuated robotically with a simple and small 2-DoF robot. A TR or TP procedure is done by simply changing a needle-guide adapter. We designed and built the probe (with a Hitachi EUP-U533 linear array) and robot, and wrote the fusion and ultrasound-guided robot biopsy control.

Results: The robot has a small size and together with the probe weighs only 1.3Kg. Preclinical tests showed needle targeting errors bound to 0.79mm in a water tank. In prostate mockups at TR and TP simulated biopsies over 27 and 30 targets, average errors were 0.30mm (SD 0.19mm) and 0.41mm (SD 0.22mm), and maximum errors were 0.67 and 0.92mm, respectively. With FDA and IRB approval, two patients had TR biopsy with ProBot. The robot scanned and targeted for biopsy hands-free. The urologist inserted the needle through the needle-guide and sampled the biopsies (Figure 1). Prostate volumes were 45.7 and 55.1cm^3, the total duration of the cases were 20.07 & 15.68min of which 0.47 & 0.57min for the 3D scan, 4.35 & 6.13min for biopsy planning, and 8.9 & 5.85min for the actual biopsies. All biopsy samples were collected successfully with the robot and no complications occurred. No prostate deformations or interference of ProBot with the patients were observed.

Conclusions: Substantial work was needed to take the invention through prototype building, software developments, and regulatory approvals to the clinical trial. Through experiments and biopsies, we showed that 3D ultrasound scanning and needle targeting can be performed with only 2 DoF, a minimum number never used before. This translates into a remarkably simple and small robot. Reducing DoF also improves accuracy. Hands-free probe operation also has the potential to improve targeting accuracy and reduce the skill required and variability of outcomes among physicians. Additional cases are planned to determine if this new approach improves clinical outcomes, and to test the ProBot using the TP approach. If successful, ProBot will be the only robotic prostate biopsy device for both TR and TP biopsies. This is our first report of ProBot.

Figure 1: ProBot robot at TR biopsy procedure

Acknowledgment: Research reported in this publication was supported in part by the National Cancer Institute of the National Institutes of Health under award number R01CA247959, PI Stoianovici.

ABSTRACT 6 **TOP 10 ABSTRACT**

THE EFFECT OF PROSTATE SIZE AND NUMBER OF CORES AT SYSTEMATIC PROSTATE BIOPSY – STUDY UPDATE

Dan Stoianovici[1,2], Katarzyna J. Macura[3], Bruce Trock[1],
Amin Herati[1], Christian Pavlovich[1], Arvin George[1], Misop Han[1]
[1]Brady Urological Institute [2]Robotics Laboratory, [3]Department of Radiology, Johns Hopkins University

Introduction: At fusion MRI-targeted biopsy (TB), systematic biopsy (SB) may detect clinically significant prostate cancer (csPCa) that is missed by the TB cores [PCM35507051]. The number of SB cores to use is uncertain. Last year, we reported the effect of the number of SB cores on sampling csPCa (> 0.5cm^3 [PCM7506797]) as a function of prostate volume [EUS2024 Abs.19][PMC38184758]. Here we update the results with additional patients from the underlying clinical trial [EUS2023 Abs.11].

Methods: The update is from 42 to 56 patients enrolled in the robot-assisted biopsy trial [EUS2017 Abs.34]. SB plans with 1 to 24 cores were simulated for each patient, resulting in 1,128 biopsy procedures and 16,800 cores. Each plan was optimized to increase csPCa detection probability (csCDP) [EUS2022 Abs.36] ("capsules" / gland volumes). The aims of the simulation were to evaluate the joint influence of the number of SB cores and prostate volume on 1) csCDP and 2) percentage of MRI depicted regions of interest (ROI) successfully sampled by SB alone.

Results: Figure 1 shows results of SB simulations regardless of MRI findings. In Figure 1a, each dot represents a patient, with colors matched to Figure 1b where each curve simulates 1 to 24 biopsies of that patient. It shows that the prostate volume plays a significant role in detecting csPCa.

Then, we investigated how many cores it would take an SB plan to sample a ROI, even if blinded to the MRI. In Figure 2a and b, patients were placed in groups with prostate volumes delimited by a) 60cm^3, and b) 30cm^3 and 60cm^3. Each curve is derived from all patients within the group. Each dot gives the likelihood of sampling a ROI at SB with the selected number of cores. Figure 2b was enabled by the update. The likelihood of sampling ROIs increases with the number of SB cores and is substantially better for smaller glands. For example, in small <30 cm^3 glands, an optimized SB plan of only 12 cores would sample nearly 90% of the ROI, even without MRI.

Conclusions: In small prostates, SB can achieve adequate cancer detection even without pre-biopsy MRI, fusion, and TB. In large prostates, however, SB alone is likely to result in under-sampling and under-detection of csPCa.

Disclosure: Under a license agreement between Eigen Health Services and the Johns Hopkins University, author DS, and the University are entitled to royalty distributions related to technology described in this article. This arrangement has been reviewed and approved by the Johns Hopkins University in accordance with its conflict-of-interest policies.

Acknowledgment: Research reported in this publication is supported by the National Cancer Institute of the National Institutes of Health under award number R01CA247959, PI Stoianovici.

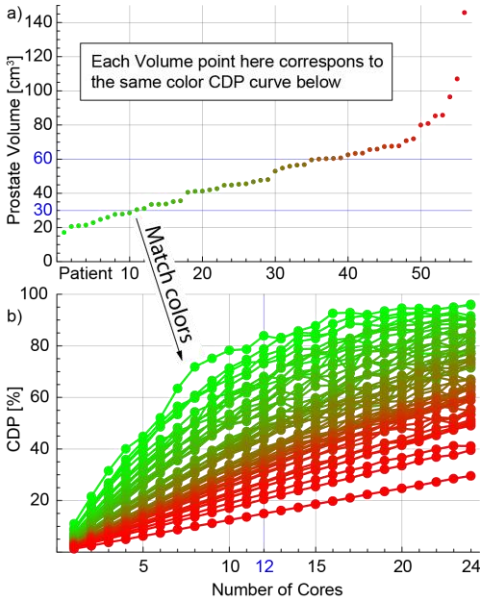

Figure 1: a) Sorted prostate volumes of the patients and b) csCDP vs. number of cores for each volume.

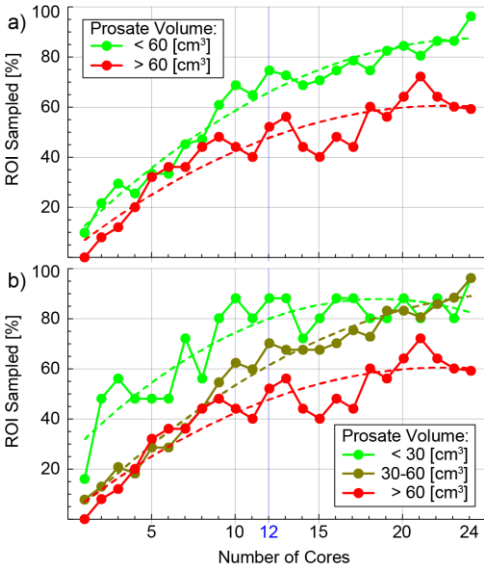

Figure 2: ROI sampling rate vs. number of SB cores for prostate volumes within a) two and b) three groups. Dotted curves are quadratic fits.

ABSTRACT 7

A FIBER-STEERING DEVICE TO REDUCE LASER LITHOTRIPSY PROCEDURE TIME

Peter Connor[1], Joshua Gafford[2], Scott Webster[2], S. Duke Herrell[1,2,3], Nick Kavoussi[3], Kim Maciolek[3], Amy Reed[3], Kent Chevli[4], Chris Schlichter[2], Patrick Anderson[2], Mina Schaafsma[2], and Robert J. Webster III[1,2,3]

[1] Vanderbilt University, [2] EndoTheia Inc.. [3] Vanderbilt University Medical Center, [4] WNY Urology Associates

Introduction: During laser lithotripsy, it is important for surgeons to maintain consistent and controlled motions of the laser across the surface of the stone, to ensure that all fragments are reduced to an acceptable size expeditiously. Existing ureteroscopes can be challenging to consistently sweep across the stone. We hypothesize that an independently steerable laser guide device can help the physician aim the laser as desired and thereby reduce procedure time.

Methods: We designed and manufactured a steerable sheath based on recently invented concentric push-pull technology [PMC10871709] which has an open central lumen to carry a laser fiber. The device is shown in Figure 1. It passes through the working channel of the ureteroscope and enables users to independently aim and steer laser fibers, instead of relying solely on the ureteroscope's motion when performing laser lithotripsy. To demonstrate the potential of the device to improve lithotripsy procedure times, we performed a series of stone lithotripsy experiments in a synthetic kidney phantom using a Karl Storz flexible ureteroscope outfitted with (a) our device, and (b) a standard laser fiber. A range of novice to expert users (N=11) fragmented and removed a 12 mm artificial stone (BegoStone [PMID: 12398432]) using both a standard ureteroscope and our new device. We recorded the stone lithotripsy rates (stone volume removed per minute) for each procedure to compare the rates with and without our device.

Results: Users performed stone fragmentation faster with our steerable device than with standard techniques. Users removed stones at a rate of $14.4 \pm 3.74\ mm^3/min$ using the steerable device compared to a rate of $11.0 \pm 1.99\ mm^3/min$ using standard endoscopic techniques. Thus, there is a 23% reduction in procedure time ($p<0.05$) when using our device.

Conclusion: Our fiber-steering device enhances laser precision, enabling the surgeon to perform the desired laser sweeping technique more rapidly and consistently - resulting in a 23% reduction in procedure time. This benefit holds true regardless of surgeon experience level, demonstrating that the device offers advantages for surgeons of all skill levels.

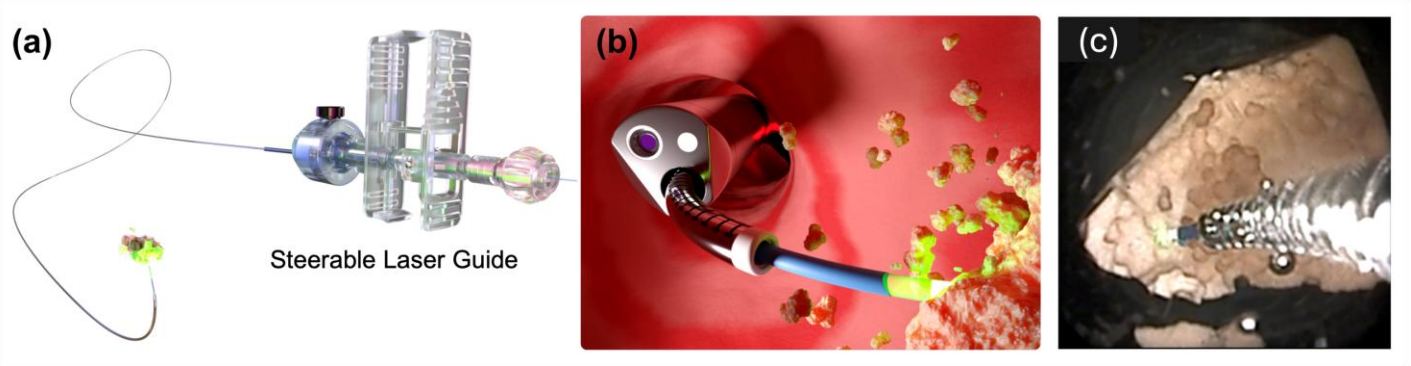

Figure 1: (a) Overview of our fiber laser steering and its user interface, (b) the device aiming a laser at a stone during lithotripsy, and (c) endoscopic image from one laser lithotripsy experiment using our device.

ABSTRACT 8

A 3D-PRINTED DUAL-MODEL TRAINING PLATFORM FOR PEDIATRIC HYPOSPADIAS REPAIR: ENHANCING SURGICAL SKILL DEVELOPMENT

Akash Chauhan[1], Felix Yiu[1], Irene Choi[2], Maral Demirjian[1], Lorna Kwan[1], Kristin Ebert[2], Vinaya Bhatia[2], Walid Farhat[2], Renea Sturm[1]

[1] UCLA David Geffen School of Medicine Department of Urology. [2] UW Madison Department of Urology

Introduction: Hypospadias repair is technically challenging, with a steep learning curve and limited opportunities for hands-on practice. Existing bench models lack realistic anatomic features and tissue fidelity. We developed two complementary 3D models to provide an anatomically accurate, layered training platform for hypospadias repair.

Methods: Two models were designed from pediatric hypospadic penile geometry using Autodesk Fusion 360 and Meshmixer, derived from de-identified 3D surface scans in the operating room (IRB#20-000143). (1) Urethroplasty Model: thermoplastic polyurethane (TPU) shaft with a removable slider attached to a tri-layered silicone (00-20, Gel 2, 00-30 with mesh) urethral plate. (2) Urethroplasty + Glansplasty Model: TPU shaft with corpus cavernosum-like rods with a removable urethral plate attached to a silicone glans (00-30) (**Figure**). Urology residents (PGY1-5) were randomly assigned into two groups, based on order of participation in low-fidelity versus high-fidelity exercises. Pediatric urologists rated each resident's suturing technique, tissue handling, and final construct integrity. A resident questionnaire assessed ease of tissue manipulation, suture handling, and overall satisfaction. Responses were provided on a 1-5 Likert scale (5 = most favorable).

Results: 14 residents and 6 raters participated. Overall performance scores for model 1 was 3.7 ± 1.0 and model 2 was 3.4 ± 1.0 (mean±SEM). Group 1 (low-fidelity tasks first) scored 3.9 ± 1.0 and 3.3 ± 0.9, for models 1 and 2 respectively, while Group 2 (model tasks first) scored 3.6 ± 1.0 and 3.6 ± 1.0. Interrater agreement for models 1 and 2 were κ = 0.23 and κ = 0.69, respectively. Resident ratings included tissue manipulation (3.3 ± 0.7), suture handling (4.0 ± 0.6), and overall satisfaction (4.1 ± 0.5).

Conclusion: Our models demonstrated high user acceptance, realistic anatomical representation, and applicability to surgical training among residents of varied training levels. Future longitudinal studies will track skill acquisition when these models are integrated intro surgical education.

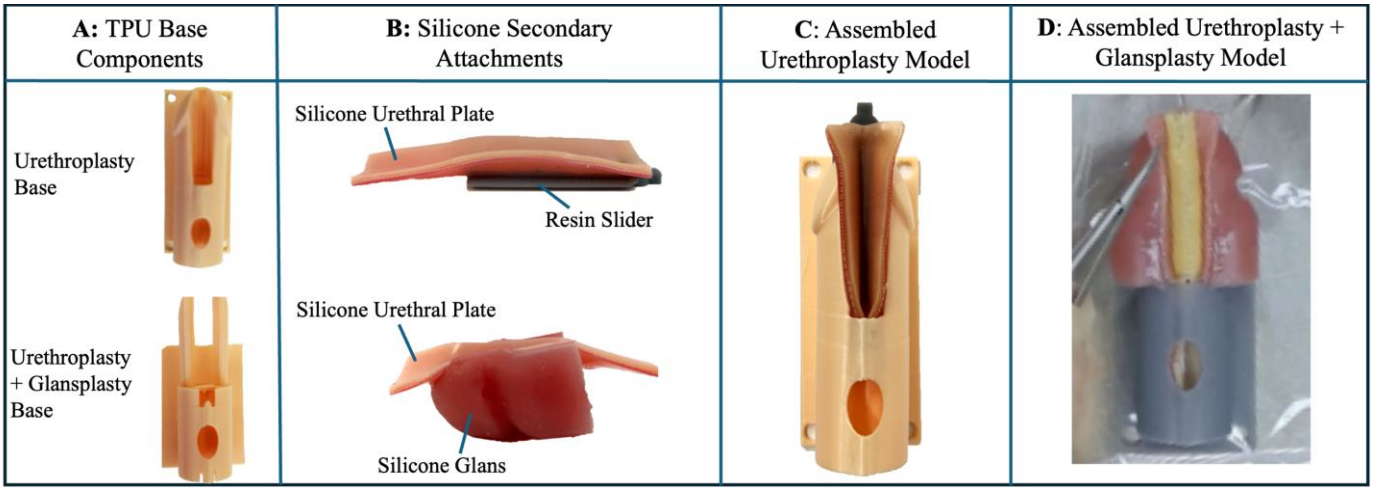

Figure: Hypospadias Training Model Components A) Dorsal view of TPU base model designs. B) Operable multi-layered silicone replaceable attachments for each model type. C) Fully assembled Rigid Model with slider inserted within penile shaft. D) Operable fully assembled Glans Model illustrating tubularization step of glansplasty.

ABSTRACT 9

PROSTATE CANCER EXTRACAPSULAR INVASION DETECTION VIA NON-CONTACT LASER INDUCED FLUORESCENCE SPECTROSCOPY

Tanner J. Zachem[1], Michael Ivey[2], Michael B. Rothberg[2], C. Rory Goodwin[3], Patrick J. Codd[1,3], Michael Abern[2]
[1]Mechanical Engineering, Duke University [2]Urology, Duke University, [3]Neurosurgery, Duke University

Introduction: The most common mode of Prostate cancer (PCa) relapse after surgery is locally in the pelvis, with which positive surgical margins are strongly associated. Pre-operative 3 Tesla multiparametric MRI (mpMRI) is the standard of care for pre-surgical tumor mapping however, its accuracy of predicting extracapsular tumor extension is modest at 65%. Robotic assisted surgery (RAS) has gained prominence; however, the oncologic outcomes have essentially remained unchanged. A limitation of surgical efficacy is the inability for the surgeon to determine the completeness of resection without histopathology. We have developed a non-contact dye-free laser induced fluorescence spectroscopy device called the "TumorID" which interrogates a 0.75mm diameter of tissue. Metabolic differences in normal and tumorous tissues lead to differing concentrations of endogenous co-factors such as NAD(P)H and FADH which are used for tissue identification. We present the findings of the first patients in an ongoing study.

Methods: Patients undergoing RAS prostatectomies with attending surgeons on the study were included. The ex-vivo prostate was scanned in the operating room, first with its anterior side up on the system's robotic platform. The sample is imaged by a color camera, after which the urologist and study team place desired scan points on the prostate. A laser sensor calculates the height of each point, before moving the prostate in 3-dimensions to scan the points with a 100mW 405nm laser for 0.5s and recording the resulting endogenous spectra with a CCD spectrometer from 200-1000nm. Only data from 450-750nm are included and for each signal, max normalization followed by Savitzky-Golay filtering is conducted. Each scan is then labeled as being from one of 12 prostate zones for correlation with preoperative mpMRI and final histology. The 12 zones split the prostate into right/left, anterior/posterior, and apex/mid/base. These data are then used to train and validate three machine learning models: a support vector machine, a sparse mixture of learned kernels, and multi-layer perceptron for comparison prior to a final prospective test.

Results: 8 patients have been included in the study to date resulting in 320-point scans of prostate tissue, with each prostate taking approximately 2 minutes to scan. To date, one patient has had focal extracapsular invasion of the left anterior and posterior quadrants from apex to base, showing initial differences in spectra. These patients will be used for training and validation, with a final testing cohort to initiate at 20 patients to predict extracapsular invasion in each of the 12 zones.

Conclusion: This ongoing study represents a first step in needed innovation for intraoperative real-time identification of PCa. Next steps include adding additional patients to this ex vivo study cohort, while simultaneously scanning biopsy cores, to see if it is possible to identify tumor immediately during biopsy. Finally, the device is being altered to allow for *in vivo* endoscopic use in the future.

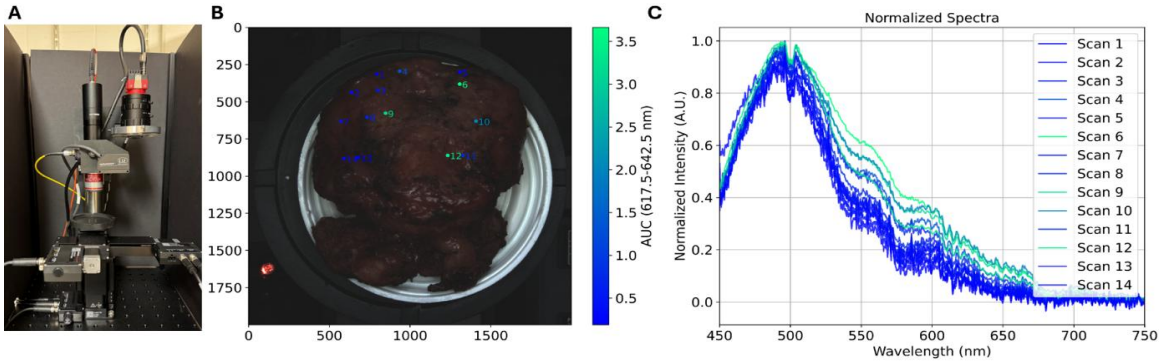

Figure: A) Overview of Tumor ID, B) Anterior Prostate with extracapsular invasion, C) Spectra of Points labeled in B

ABSTRACT 10

SIMULATION OF DIAPHRAGMATIC DISPLACEMENT DURING PERCUTANEOUS NEPHROLITHOTOMY: A COMPUTATIONAL APPROACH FOR OPTIMIZING AIRWAY MANAGEMENT

Atieh Ashkezari[1, 3], Gazi Husain[2], Tareq Aro[1], Milan Toma[3]
[1] The Smith Institute for Urology, Northwell Health, NY [2] Department of Anatomy, New York Institute of Technology College of Osteopathic Medicine, NY [3] Department of Osteopathic Manipulative Medicine, New York Institute of Technology College of Osteopathic Medicine, NY

INTRODUCTION:
Prone positioning during percutaneous nephrolithotomy (PCNL) in morbidly obese patients can cause cranial diaphragmatic displacement due to increased intra-abdominal pressure (IAP), potentially altering airway anatomy and endotracheal tube (ET) depth. Previously, Cone Beam Computed Tomography (CBCT) was used to quantify diaphragmatic displacement between supine and prone positions in clinical cases. This study aims to build upon that data by developing a computational simulation model capable of predicting diaphragmatic displacement under various body mass index (BMI) and intra-abdominal pressure (IAP) conditions, with the goal of optimizing airway management.

METHODS:
A three-dimensional (3D) diaphragm model was generated from CAD-based stereolithography (STL) files, customized for varying BMI and IAP parameters. Model surfaces were refined and mesh integrity verified using Netfabb. Optimized volume mesh generation was performed using GMSH. Custom MATLAB scripts were developed and employed to prepare the model for finite element analysis (FEA), which was executed using Impetus Afea Solver. Biomechanical accuracy was validated against previously obtained Cone Beam Computed Tomography (CBCT) data.

RESULTS:
Preliminary geometric modeling indicates potential increases in diaphragmatic displacement with rising IAP and higher BMI categories, especially in prone positions. The computational model offers precise quantification potential, allowing for an in-depth understanding of diaphragm height changes and their implications on airway management. The diaphragm model was visually represented with color-coded displacement areas for enhanced interpretation of results (Figure 1).

CONCLUSIONS:
This computational approach offers a non-invasive preoperative tool for predicting diaphragmatic displacement during PCNL in morbidly obese patients. These findings will support improved ET tube positioning, potentially reducing airway-related complications during prone positioning. Future work will focus on further refining the model and incorporating additional clinical validation.

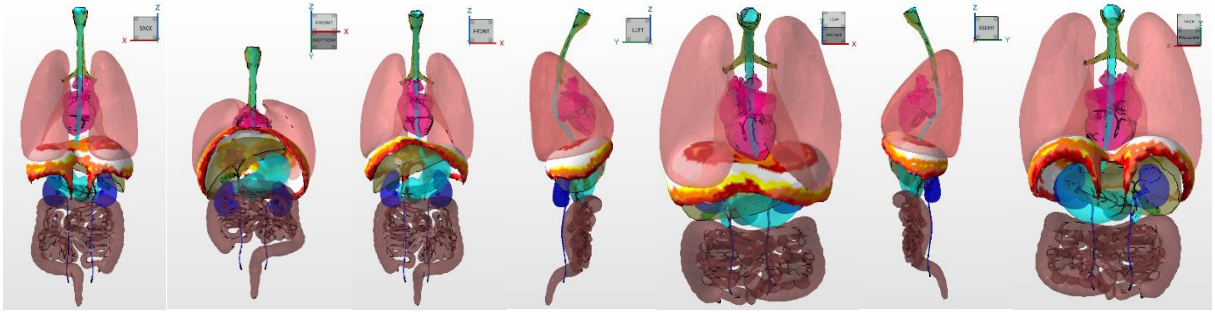

Figure 1: Three-dimensional computational diaphragm model illustrating areas of anticipated maximal displacement (highlighted in red) under elevated intra-abdominal pressures in the prone position, generated using Netfabb, GMSH, MATLAB, and Impetus Afea Solver.

ABSTRACT 11

HIGH-FIDELITY PHYSICAL SIMULATOR MODEL FOR TRAINING MALE INFANT FOLEY CATHETERIZATION WITH INTEGRATION INTO OPERATING ROOM NURSING TECHNICAL SKILLS CURRICULUM

Lauren Poniatowski[1,2,3], Robert Sweet[2,3], Maegan Chua[3], Kathleen Kieran[1,2], Margarett Shnorhavorian[1,2], Paul Merguerian[1,2]

[1]Department of Pediatric Urology, Seattle Children's Hospital, Seattle, WA; [2]Department of Urology, University of Washington, Seattle, WA; [3]Center for Research in Education and Simulation Technologies (CREST), University of Washington, Seattle, WA

Introduction: Pediatric foley catheter placement is a commonly performed procedure in the operating room (OR). Placement is most often completed by nursing staff with assistance from urology in the context of a difficult foley. Foley catheterization can result in iatrogenic injury when performed improperly with multiple associated complications including hematuria, false passage, bladder injury, foreskin injury and/or urethral stricture in the long term. Our institution set out to reduce iatrogenic foley catheter injuries for catheters placed in the OR by nursing through a simulation curriculum including technical skills training. Our objective was to develop a high-fidelity male infant foley catheterization model for integration into a didactic and technical skills curriculum for training male infant foley catheter insertion and evaluate the model and clinical outcomes.

Methods: The male infant foley simulator model was created using silicone-based materials. The material was cast over a 3D-printed mold of a male infant lower urinary tract. An infant bony pelvis was also 3D-printed to provide structure around the simulated bladder/urethra. A simulated suprapubic fat pad was integrated to allow for Crede maneuver. The bladder was filled with simulated urine. Starting January 2024, simulation sessions utilizing didactic and technical skills segments were incorporated into educational time for OR nursing staff and taught by the pediatric urology fellow. The didactic and technical skills portions emphasized "red flags" to stop the procedure including resistance with insertion, visualization of blood or no urine return. Additionally, the balloon should only be inflated if the catheter was hubbed and there was urine return present. Participants completed surveys to evaluate the simulator model. Our institution's incident reporting system was used to determine incidents of difficult foley placement from 2018 to 2025.

Results: A total of 19 participants filled out post-task surveys using a Likert scale (minimum score of 1 is unfavorable, maximum score of 5 is favorable) for model evaluation in multiple domains. The average scores for evaluation were greater than 4.1 in all areas. Importantly, participants felt the model allowed them to demonstrate the technical skills required for foley catheter placement with average scores greater than 4.5. All participants answered yes when asked if participating in didactics or simulation training should be completed prior to performing foley catheter insertion on a patient. Clinical foley events in the operating room were evaluated from 2018 to 2025 and compared pre and post-implementation of simulation curriculum in January 2024. Pre-implementation there were 3 difficult foley events in 2018 resulting in 3 urethral injuries and 3 difficult foley events in 2023 resulting in 2 urethral injuries. Post-implementation there were 2 difficult foley events in 2024 with no urethral injuries.

Conclusion: Development of a high-fidelity simulator model for training pediatric foley catheter insertion with integration into a curriculum showed favorable outcomes in participant ability to demonstrate required technical skills. Following curriculum implementation, there has not been an iatrogenic catheterization injury in the OR setting. Urology is often involved in difficult foley events and collaboration between urology and nursing in the simulation setting may play an important role in improving patient safety.

ABSTRACT 12

ELUCIDATING THE PHYSICAL PROPERTIES OF URETERAL STENTS

Felix Yiu[1], Eleanor Casey[1], Ishant Goel[1], Akash Chauhan[1], Neha Iyer[2], Jonathan Balderrama[1], Jiayue Chen[1], Lorna Kwan[1], Kymora Scotland[1], Renea Sturm[1]

[1] University of California Los Angeles Dept of Urology, [2]University of California San Diego Dept of Bioengineering

*Stent selection guided by common stents employed in the Pediatric Kidney Stone (PKIDS) Care Improvement Network Trial led by PI Gregory Tasian at Children's Hospital of Philadelphia

Introduction: Physical factors of ureteral stents such as their unique materials, tensile, and flow properties can impact their effectiveness and patient symptoms following placement. Our aim was to elucidate the benchtop flow and tensile properties of commonly employed commercial ureteral stents.

Methods: First, we identified common ureteral stents used across a large multi-institutional network (PKIDS) and selected six for benchtop testing. Stent variables included: manufacturer, subtype of stent, binary diameter, and length. Benchtop flow evaluation was completed by submerging the proximal coil of a suspended stent in artificial urine maintained at 5cm-H_2O. After a 60 second equilibration period, 60 seconds of flow volume was recorded (Fig. 1a), with 3 repetitions per stent. Tensile tests were performed on each coil and the mid-section independently after equilibration to 37°C within a saline bath at a rate of 50cm/min using an Instron 34SC-1 mechanical tester equipped with a 100 N load cell (ASTM F1828-22) The mean and SEM of each stent subtype and result was calculated; ANOVA was used to evaluate between group differences.

Results: 24 stents in total, including 6 stent subtypes from 3 manufacturers ranging from 4.7-6F and 14-30cm in length were evaluated. As anticipated, there was a significantly higher flow in larger versus smaller diameter stents (Fig. 1b). However, although longer stents were hypothesized to have slower flow rates, the finding was inconsistent across stent types (Fig. 1c). Tensile properties between stent types varied widely (Fig. 1d-e provide mid-stent modulus results as an example), with one manufacturer's stents (type 1, 2) demonstrating the highest modulus, particularly among those categorized as having small diameters.

Conclusion: Wide variability in flow and tensile properties exists across commonly employed commercial ureteral stents. Further studies in conjunction are planned to apply this benchtop data to evaluate clinical correlation with stent symptoms. Additionally, we are evaluating parameters such as drainage hole distribution with computational modeling to determine their role in the benchtop findings that are not readily explained by fluid mechanics.

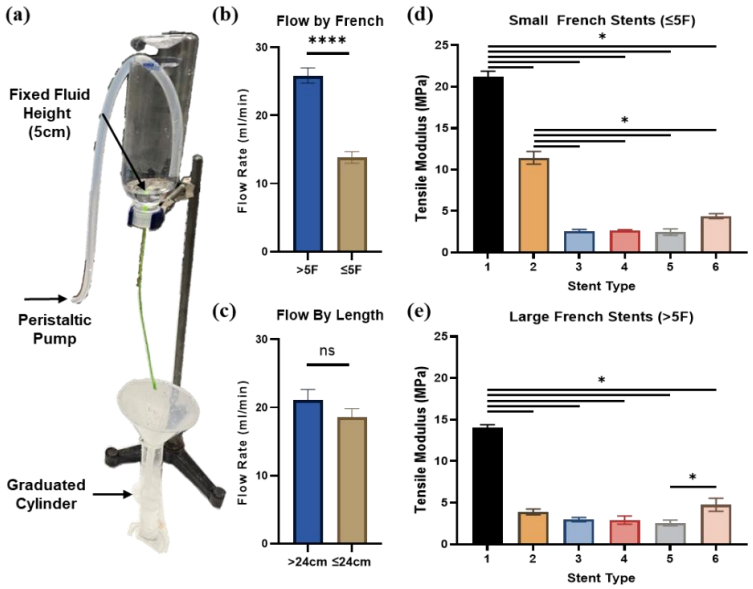

Figure 1. Benchtop Evaluation of Stent Properties a) Experimental setup for flow rate, b) Flow rate by French diameter, c) Flow rate by stent length, d) Tensile modulus of stents ≤5F, e) Tensile modulus of stents >5F.

ABSTRACT 13

NOVEL FOLEY CATHETER WITH TOROIDAL BALLOON SHEATH REDUCES URETHRAL TRAUMA

Grant Steele[1], Mathieu J. Massicotte[1], Troy J. Ziegler[2]
[1] Massachusetts General Hospital. [2] Proluma Medical, Inc.

Introduction: There is great interest in reducing discomfort and pain from Foley catheters. Additionally, long-term exposure to friction from Foley catheters in the urethra is associated with trauma, including urethritis, urethral erosion, and urethral strictures. Thus, any catheter that significantly reduces friction in the urethra would be an improvement for patients using Foley catheters.

Methods: The prototype Proluma Foley catheter uses a proprietary toroidal balloon sheath covering the catheter shaft. The balloon sheath allows the underlying catheter shaft to move back and forth along the length of the urethra while the outside sheath remains stationary to reduce friction. When inflated, the Proluma catheter diameter is approximately 18 Fr.

Two live female pigs were chosen for control and experimental models. General anesthesia was administered. In both models, a Foley catheter was inserted into the urethra extending into the bladder. The control case used a Bard Bardex 18 Fr. Lubricious Coated Foley catheter, and the experimental case used a prototype Proluma Medical Foley catheter. A linear actuator modeled catheter motion associated with daily activity by cycling the catheters in and out by 1 cm at a rate of 1 cycle/second. The actuator was active in both cases for 2 hours and 9 minutes. Endpoints included post-mortem visual observations of dissected urethra for discoloration, abrasion, erosion, hemorrhaging, and other observable markers of trauma.

Results: Trauma was observed in the control model, including streaks of reddening and inflammation of the urethral mucosa. Hematoma and hemorrhaging were also observed in the control model on and around the Skene's gland (Figure 1). Far less trauma was observed in the experimental model using the Proluma catheter, with only slight reddening on and around the Skene's gland (see Figure 2).

Conclusion: Urethral trauma associated with motion and friction of Foley catheters was substantially reduced by the Proluma Medical catheter.

Figure 1: Bard Catheter

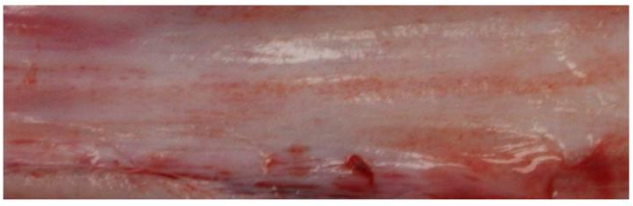

Figure 2: Proluima Medical Catheter

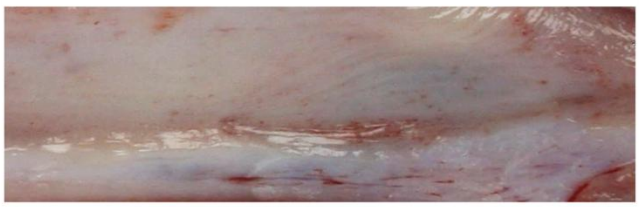

ABSTRACT 14

A NOVEL PLATFORM FOR REMOTE MICROSCOPIC URINALYSIS: THE U-CHECK SYSTEM

André F Santos[1], Eric C Becman[1], Oscar E H Fugita[2,3], Daniel F Castro[3], Oswaldo Horikawa[4], Fábio C Carvalho[4], Gabriela T P Agostini[4], Isadora R Bisognin[4], João P Cypriano[4], Marina M Bisordi[4], Pedro S Calvo[4], Arturo Forner-Cordero[1]

[1] Biomechatronics Laboratory. Department of Mechatronics and Mechanical Systems - Escola Politecnica, Universidade de Sao Paulo, Sao Paulo, Brazil. [2] Innovation & Technology Centre (INTEC) - Hospital Universitario, Universidade de Sao Paulo, Brazil. [3]Department of Urology - Faculdade de Medicina de Botucatu, Universidade Estadual Paulista, Brazil. [4]Escola Politecnica, Universidade de Sao Paulo, Sao Paulo, Brazil.

Introduction: Urinalysis is an essential diagnostic procedure to detect urinary infections. Urine is usually collected at clinical facilities, requiring patients to travel. This can be difficult for patients with reduced mobility or from remote areas, particularly in underdeveloped countries. Herein, we present the U-Check, a prototype developed at Universidade de Sao Paulo, to address these challenges by offering an automated device to capture high-resolution images of urine samples for remote analysis. As a first step for developing interventions to reduce errors (by redesigning the device), we performed a heuristic evaluation for identification of usability problems and their severities.

Methods: We used the Neilsen-Shneiderman [PMID 14552844] heuristics principles for identification of U-Check usability and design problems. Six evaluators (3 healthcare and 3 non-healthcare volunteers) were asked to use and evaluate the U-Check. If a heuristic was violated, the volunteers were asked to fill a problem form and give a severity rating. They assigned a value based on a 0-4 points scale (0=not a usability problem; 1=cosmetic problem; 2=minor problem; 3=major problem; 4=usability catastrophe) to a set of designated features to the usability expectations (user guide, device design, device handling, assembly instructions, urine sample handling, microscope and camera handling). The severity ratings were divided into 4 regions: >3.5 (catastrophic); < 3.5>2.5 (major); <2.5>1.5 (minor); < 1.5 (cosmetic)

Results: Chart 1 shows the number of heuristic violations for U-Check. Heuristics were violated a total of 40 times into 6 different categories: 1.*Consistency* (“confusion with similar words”); 2.*Match* (“hard to identify some parts of the device”); 3.*Minimalist* (“too many parts”); 4.*Memory* (“too many information”) 5.*Message* (“I don’t know what is wrong”); 6.*Document* (“need for a more detailed tutorial”). Chart 2 summarizes the severity of the problems found in the U-Check. Severity ratings were divided into 4 regions: catastrophic (4), major (23), minor (11) and cosmetic (2).

Conclusions: The U-Check was well evaluated by healthcare professionals (data not shown) but the heuristic evaluation showed that improvements are mandatory before additional testing in real-world scenarios.

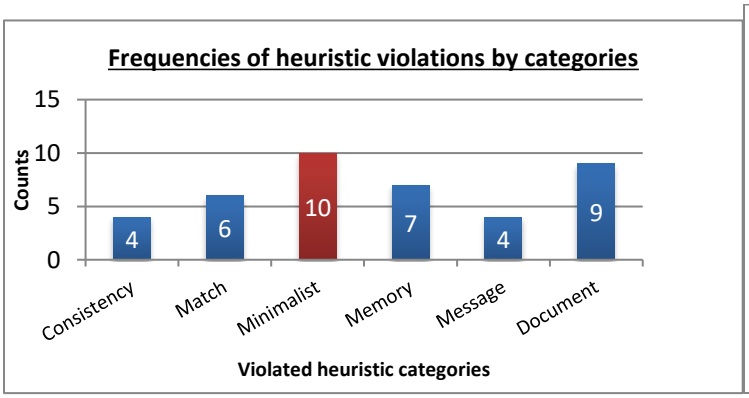

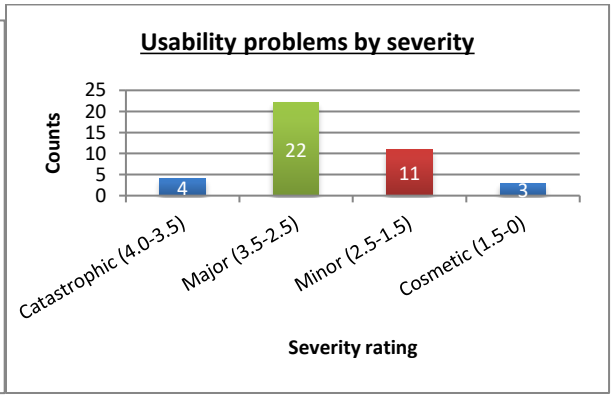

ABSTRACT 15

VISUAL EXPLANATION OF DEEP LEARNING MODELS FOR AUTOMATIC KIDNEY STONE DETECTION USING MULTIPLE CT SOURCES DATASET

Gabriel Nunes Missima[1], Murillo Freitas Bouzon[2], Fernando Pujaico Rivera[3], Gilson Antonio Giraldi[4], Oscar Eduardo Hidetoshi Fugita[5], Paulo Sergio Silva Rodrigues[6]
[1,2,3,6] Centro Universitário da FEI, Electrical and Computer Science Department, São Bernardo do Campo, São Paulo, Brazil
[4] National Laboratory for Scientific Computing, Petrópolis, Rio de Janeiro, Brazil
[5] Hospital Universitário – Universidade de São Paulo, São Paulo, Brazil

Introduction: Diagnosing kidney stones using computed tomography (CT) scans may be time-consuming due to the limited availability of radiologists and the increasing demand for imaging examinations. Deep learning offers a promising option to speed up this process, However, the lack of interpretability reduces clinical confidence, as clinicians require explanations to trust automated decisions. Additionally, the existing approaches rely on single-source datasets, limiting their generalizability. To address these challenges, we propose a deep learning-based method using multiple datasets to improve generalization and applied visualization techniques to enhance interpretability.

Methods: Two CT scan datasets were used, Dataset A [1] and Dataset B [2], totaling 3383 images (1304 with kidney stones and 2079 without kidney stones). We employ an ensemble of two Convolutional Neural Networks (CNNs) pre-trained on both datasets as feature extractors.

The outputs of both CNNs are concatenated and used as input to train the dense layers of a Multi-Layer Perceptron (MLP). To improve interpretability, we applied Grad-CAM to highlight key regions in CT images that influenced the model's decisions, making it easier for clinicians to assess its reliability. Figure 1 illustrates the workflow of the proposed method.

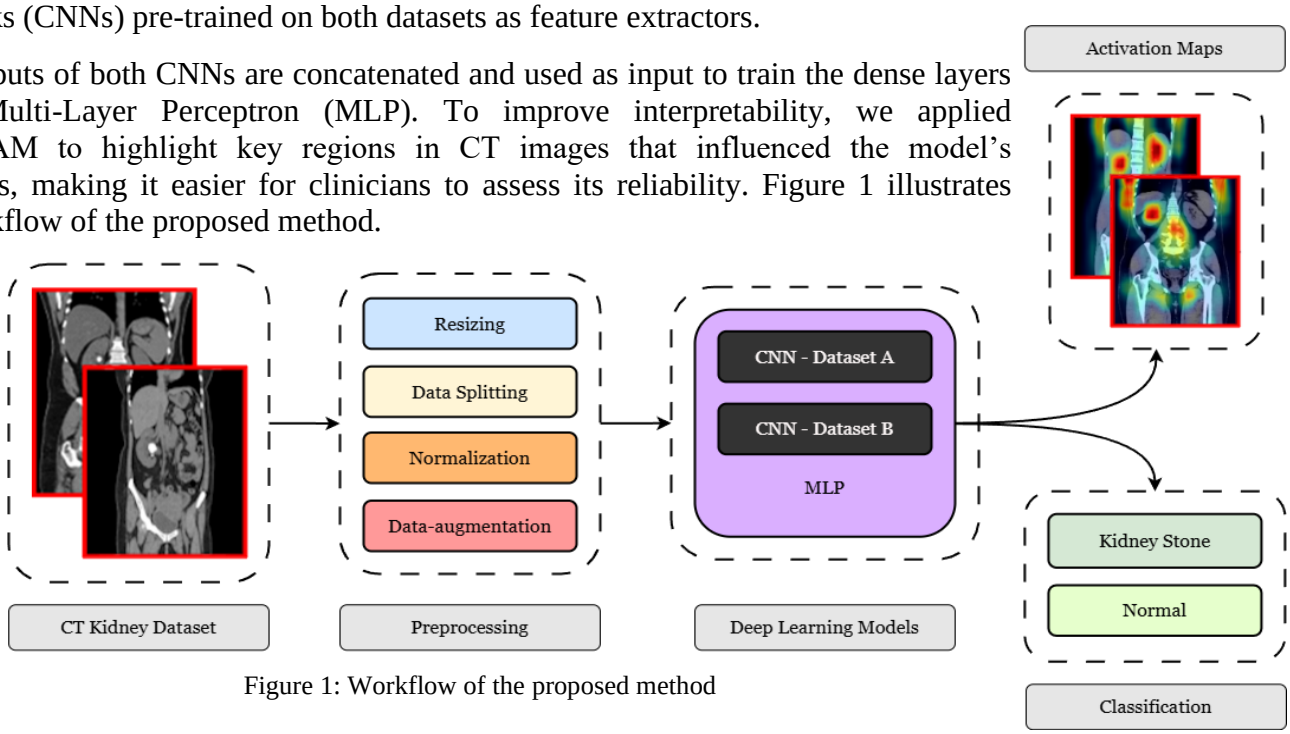

Figure 1: Workflow of the proposed method

Results: The proposed model achieved **99.6 ± 0.49%** accuracy, **99.0 ± 0.45%** precision, **99.4 ± 1.02%**, and **99.5 ± 0.67** F1-score. The Grad-CAM visualizations successfully highlighted key regions in CT images, providing insights into the model's decision. Figure 2 presents the visual results of the Grad-CAM.

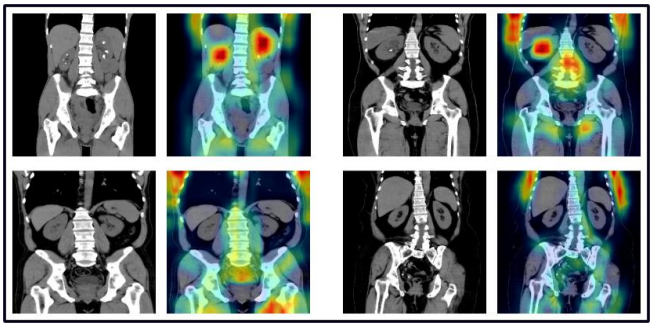

Figure 2: Examples of Grad-CAM activation maps

Conclusion: Our method demonstrates high accuracy and interpretability, making it a promising approach for automated kidney stone detection. By combining multiple datasets and applying visualization techniques, this work may improve the reliability and clinical applicability of deep learning-based diagnostic tools.

ABSTRACT 16

A TALE OF TWO PERCS: A CAUSAL ANALYSIS OF PAPILLARY PERCUTANEOUS ACCESS USING THE MONARCH™ PLATFORM, UROLOGY

Lauren Friend[1], Nancy L. Sehgel[1], Jacob Caldwell [1], Carl Sarkissian [1], Hedyeh Rafii-Tari[1]
[1] Research & Development, Johnson & Johnson MedTech Surgery, Santa Clara, CA

Introduction: The MONARCH™ Platform, Urology is a robotically-assisted surgical system designed for use in urology diagnostic and therapeutic procedures, including percutaneous renal access. In prior work (Friend, 2024), causal discovery was used to algorithmically derive a Directed Acyclic Graph (DAG) revealing the causal relationships within the workflow. One use of this technology is root-cause analysis. Here we use that DAG alongside robotically produced data to compare two clinical procedures.

Methods: The MONARCH™ ureteroscope camera was used to visualize the position and orientation of tools at the time percutaneous access was gained, as shown in Figure 1. In percutaneous access A ("Perc A"), the needle punctured at the papilla; in percutaneous access B ("Perc B"), the needle punctured outside the papilla. A root cause analysis of this difference in outcome was completed by tracing the causal path in the DAG (Figure 2) from the final node, Access Quality, upstream to its causal parents. At each step, the metric value of each node was compared.

Results: According to the DAG (Figure 2), there are multiple causal ancestors of Access Quality: tract length, distance to target, targeting quality, and coaxiality. Between these nodes, coaxiality (defined as the difference in orientation between the ureteroscope and needle insertion trajectory) had by far the largest difference in value between Perc A (8°) and Perc B (36°) (Figure 3). This data suggests that to improve the quality of puncture in Perc B, the user could aim to reduce the angular delta between the needle and ureteroscope.

Conclusion: The MONARCH™ DAG allows for quick, precise, and transparent investigation and comparison of percutaneous access attempts. In this work, we demonstrate this by comparing two clinical percutaneous access examples and identify how the needle and scope positioning technique could have been improved in Perc B to increase Access Quality. This suggests a future where the MONARCH™ Platform can provide insights for optimizing percutaneous access, ultimately elevating surgical technique from good to exceptional.

Figure 1: Visualization of percutaneous access gained through the papilla (A) and outside of the papilla (B)

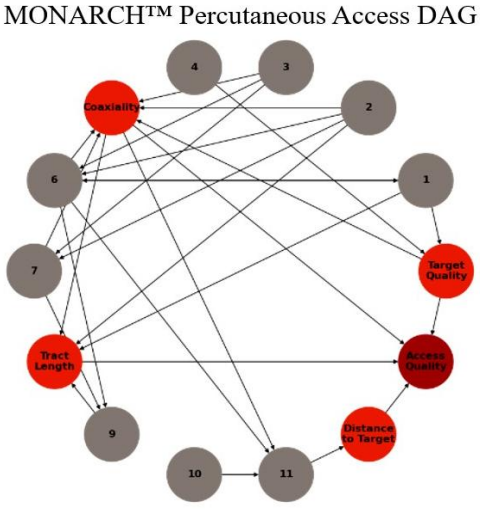

Figure 2: The MONARCH™ percutaneous access DAG. The sink node (Access Quality) in maroon and its causal parents in red. Non-parent nodes are in grey.

Coaxiality (deg)	
Angular delta between needle trajectory and scope orientation	
Perc A	8
Perc B	36

Distance to Target (mm)	
Minimum distance between needle tip and the EM target	
Perc A	0.2
Perc B	0.8

Target Quality (deg)	
Angular delta between scope orientation at TAG and PARK	
Perc A	10
Perc B	12

Tract Length (mm)	
Distance between target and needle tip at skin puncture	
Perc A	98
Perc B	90

Figure 3: Values of the parent nodes of Access Quality automatically generated from robotic data, machine learning, and feature engineering.

ABSTRACT 17

A BENCHTOP KIDNEY MODEL FOR MEASURING SPATIAL VARIATION IN TEMPERATURE DURING SIMULATED LITHOTRIPSY

Alycia Abbott, Jessica Williams, Thomas Zappia, Aditi Ray
Boston Scientific, Inc

Introduction: Increased temperature in the urinary tract due to laser usage during endourological procedures presents a risk of thermal injury to adjacent tissue. Previously, we presented a benchtop model that enables study of intrarenal pressure (IRP) throughout periods of fluid irrigation during simulated ureteroscopy [1, 2]. Here we present the ability of the bench model to enable study of spatial variations in temperature during simulated lithotripsy with or without irrigation. This extends the ability of the model to further understand interactions between flowrates, intrarenal pressures and temperatures.

Methods: The Boston Scientific Bench (BSB) kidney model consists of a chamber (with a 3-D printed "kidney" insert) ringed by sensors with outflow paths available through use of a ureteral access sheath (UAS) and/or through use of valves. Experiments were conducted with an 11/13F Navigator™ HD UAS placed for outflow. The IRP was monitored through use of the LithoVue™ Elite Single-Use Digital Flexible Ureteroscope System with intrarenal pressure monitoring. Laser power was provided by a Moses™ 200 D/F/L laser fiber connected to a Lumenis Pulse™ 120H Laser System. Three thermocouples Sensors 1,2 and 3, were used and placed 0.4, 0.5, and 0.9 cm from the tip of the laser fiber, respectively. Laser settings used were 1 J and 40 Hz (40 W) and 0.5 J and 20 Hz (10 W). Irrigation was provided by a prototype fluid management system at the following pump pressures settings: no flow, 40, 75, 200, and 300 mmHg. For all runs 80 s of data was collected: 20 s of irrigation, 40 s of laser activation, and 20 s of irrigation.

Results: As a first step in model development, the temperatures produced during no flow laser scenarios were compared to a previously established bench model and volume averaged mathematical model [3]. The BSB temperature sensors aligned with the model predictions and required no additional parameter fitting. Overall, the BSB model displayed the expected behavior of larger temperature increases with 1) higher laser energy and/or 2) lower flow rates. Spatial variation was demonstrated by the thermocouples with a largest difference of 2.3°C between Sensors 1 and 3. Overall, as flow rate increased, the difference in thermocouple values decreased (Table 1). This effect was more pronounced from trials with higher laser energy.

Laser Energy (W)	Pump Pressure (mmHg)	Temperature Difference (°C)	
		Sensor 2	Sensor 3
40	40	0.7	2.0
40	75	0.4	1.7
40	300	0.0	0.3
10	75	0.1	0.2
10	300	0.1	0.1

Table 1: Average temperature differences with respect to Sensor 1 from thermocouples in the BSB model by Laser Energy and Flowrate Setting. Sensor 1 was 0.4 cm behind and below the laser fiber and set as the reference, sensor 2 was 0.5 cm in front of and below the laser fiber, sensor 3 was 0.9 cm behind and above the laser fiber. Data presented as mean from $n \geq 3$ trials.

Conclusion: The BSB temperature data aligned with a previously established bench and mathematical model of lithotripsy. The BSB model displayed the expected behaviors of greater temperature increases with higher laser energy and lower flowrates as well as spatial variation in these temperature increases. Although temperature is the focus of this abstract, the additional sensors in the BSB can help characterize the relationships between pressure, flow rate, and temperature during simulated ureteroscopy scenarios.

Disclaimers: Prototype fluid management system used in this study was a concept device/technology, which was not available for sale at the time the study was conducted. Bench testing results may not necessarily be indicative of clinical performance. Testing was performed by Boston Scientific. Data on file.

ABSTRACT 18

MATHEMATICAL MODELING OF INTRA-RENAL PRESSURE DURING SCOPE WITHDRAWAL THROUGH A FANS

Jessica Williams, Alycia Abbott, Anya Chase, Aditi Ray
Boston Scientific, Inc

Introduction: Resistance to fluid flowing back out of the kidney during ureteroscopy – outflow resistance – governs the relationship between intra-renal pressure (IRP) and flow rate [1]. Typically, outflow resistance is controlled by the size of the ureteroscope and the presence and/or size of a ureteral access sheath (UAS) or ureter. While the scope is within the renal pelvis, the outflow resistance is consistent. With the advent of suction through a flexible and navigable suction UAS (FANS), a common technique is to withdraw the scope to the FANS hub to allow for stone fragments to aspirate more freely through the FANS [2]. When the scope is withdrawn, the outflow resistance drops significantly, and during withdrawal, it changes dynamically, impacting the relationships between pump pressure, flowrate, and IRP.

Methods: We use physics-based mathematical modeling to model outflow resistance as a function of how far the scope is withdrawn in the sheath. As flow resistance is linearly dependent on the length of the flow channel [3], outflow resistance through a sheath with a partially withdrawn scope can be modeled piecewise, connecting flow through an empty sheath (the portion proximal to the kidney) with flow through a sheath with a scope inside (the portion distal to the kidney). The ratio between these two lengths changes dynamically as the scope is withdrawn.

Results: Outflow resistance decreases linearly with withdrawal length. Assuming the scope is withdrawn steadily over a five-second period (between seconds 20-25) and re-inserted with the same speed (between seconds (35-40), we simulate IRP over a 60-second interval in Figure 1. We assume 50 mmHg suction, a 9.5 Fr OD scope with a 3.6 Fr working channel (containing a 200 µm laser fiber), an 11/13 Fr FANS (with vent fully closed), and three different irrigation pressures (200, 250, and 300 mmHg). IRP dips as the scope is withdrawn due to the sudden decrease in outflow resistance. When the scope is fully inserted, the resting IRP is 28, 43, and 59 mmHg, respectively for 200, 250, and 300 mmHg irrigation pressures. With the scope fully removed, IRP is between -37 and -32 mmHg for all cases, indicating a full loss of kidney distention (i.e. a "collapsed kidney").

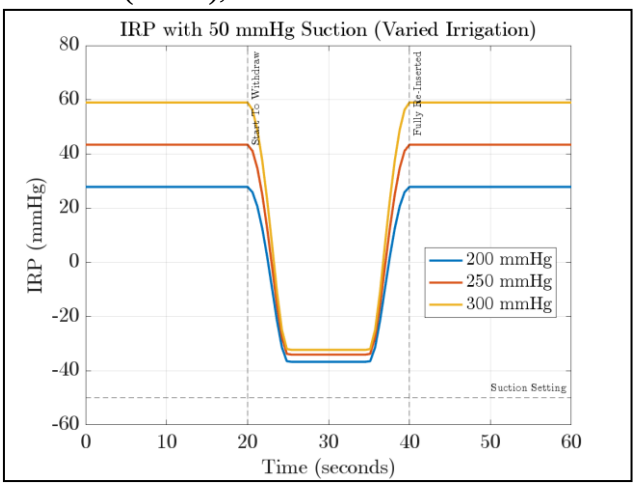

Figure 1: IRP over a 60-second window, assuming the scope is withdrawn at a fixed speed between seconds 20-25 and is re-inserted between seconds 35-40. The different lines assume different irrigation settings (labeled in legend). All simulations assume a laser fiber in the channel, a 9.5 Fr OD scope, and an 11/13 FANS.

Conclusion: With the configurations modeled here, IRP is expected to drop to negative values – leading to loss of kidney distention/kidney collapse – as the scope is withdrawn while using a FANS. Important to note that as the scope is withdrawn when this collapse happens, it's not visible to the operating surgeon. As the outflow resistance is so low when the sheath is empty, the IRP drops close to the setting on the suction sheath (assuming the FANS vent is closed, i.e. suction is fully effective). Increasing the irrigation pressure (here between 200 and 300 mmHg) leads to higher IRPs when the scope is inserted but has less of an impact on IRP when the scope is removed. Therefore, careful consideration of flow and IRP management is needed to keep IRPs from becoming too high when the scope is inserted within a FANS yet preventing collapse when the scope is withdrawn.

Disclaimer: Mathematical modeling results may not be indicative of clinical results.

ABSTRACT 19

USE OF ARTIFICIAL INTELLIGENCE AND NOVEL ELECTROMAGNETIC DEVICE IN PROSTATE CANCER DETECTION: DEVELOPMENT OF A MODEL OF PCA RISK ASSESSMENT

Carlo Bellorofonte[1], Tommaso Calcagnile[2], Davide Perri[2], Andrea Pacchetti[2], Daniele Bianchi[2], Matteo Maltagliati[2], Mauro Frongia[2], Giorgio Bozzini[2]

[1] Columbus Clinic Center, Milan, Italy. [2] ASST Lariana, Como, Italy

Introduction: Despite its prevalence, no validated screening methods for prostate cancer (PCa) are currently available and risk-based strategies for its detection still require refinement. Scanget (TXT HealthProbe) is a non-invasive electromagnetic device that detects differences in electrical properties between healthy and malignant cells, facilitating the risk of PCa assessment. The present study aims to propose a software that uses machine learning models to correlate patient-specific characteristics with Scanget results, with the goal of evaluating a patient's risk of presenting with PCa at the first clinical encounter.

Methods: Data from 500 patients undergoing prostate biopsy in a single center (Columbus Clinic, Milan, Italy) between 2021 and 2024 were retrospectively collected and analyzed. Inclusion criteria were: age >18 years, information on family history of PCa, prostate volume (assessed through mpMRI or TRUS), PSA testing, digital rectal examination and Scanget results (the last two carried out by a single expert operator). At the end, a transperineal fusion prostate biopsy was performed in all cases.

Data were cleaned and transformed to enable machine learning compatibility.

The entire experimental dataset including clinical data and Scanget test were used to train machine learning models based on XGBoost, optimized through RandomizedSearchCV. Training focused on maximizing diagnostic metrics crucial to PCa detection: sensitivity, specificity and positive predictive value (PPV). Incorporating all the available records allowed to enhance the predictive capability and thus provided more accurate inferences in the practical application of the software.

Results: A total of 321 patients met the inclusion criteria and their data were therefore used for model training, with PCa detection through biopsy used as the diagnostic reference.

Scanget test showed a sensitivity of 95.8% and specificity of 88.3%. PPV was 86.16%.

A model including all the available data was created and incorporated in a risk-calculator software, able to predict the probability of obtaining a positive biopsy. The risk assessment of the software is expressed in a five-class PI-RADS-like method, from "Highly Unlikely" (1) to "Highly Likely" (5).

Conclusion: The combination of Scanget test and clinical variables through artificial intelligence provides a risk-assessment of PCa in the early clinical setting. Even if the machine learning method here presented may expose the model to risks of overfitting, it seems to be a promising tool to assist physicians determine whether further examinations are warranted for the patient and to allow for a better allocation of healthcare resources.

ABSTRACT 20

INITIAL EXPERIENCE OF ARTIFICIAL INTELLIGENCE-GUIDED CORRELATION BETWEEN MPMRI AND ELECTROMAGNETIC DIAGNOSTIC TOOL IN MANAGEMENT OF PI-RADS 3 LESIONS

Carlo Bellorofonte[1], Tommaso Calcagnile[2], Davide Perri[2], Andrea Pacchetti[2], Daniele Bianchi[2], Matteo Maltagliati[2], Mauro Frongia[2], Giorgio Bozzini[2]

[1] Columbus Clinic Center, Milan, Italy. [2] ASST Lariana, Como, Italy

Introduction: Despite the increasingly important role of multiparametric magnetic resonance (mpMRI) in identifying clinically significant prostate cancer (PCa), the debate over the necessity of biopsies for PI-RADS 3 lesions remains active, and more refined and comprehensive tools than its correlation with PSA density still need to be explored.

The present study introduces an artificial intelligence-based software that integrates clinical variables, mpMRI findings and results from a new electromagnetic diagnostic test (Scanget, TXT HealthProbe) to assist physicians in decision-making in case of PI-RADS 3 lesions detection.

Methods: Retrospective data were gathered and analyzed from 500 patients who underwent prostate biopsy at a single center (Columbus Clinic, Milan, Italy) between 2021 and 2024. Inclusion criteria included: age > 18 years old, information about family history, PSA testing, mpMRI findings ≥ 3, results from digital rectal examination and Scanget test, the last two performed by an expert operator. A transperineal fusion prostate biopsy was conducted for each patient.

Information about clinical variables, mpMRI and Scanget test were used to train machine learning models based on XGBoost, optimized through RandomizedSearchCV. The model was evaluated using cross-validation on a dataset divided into training and test sets, to ensure the model's robustness on unseen data. Training focused on maximizing diagnostic metrics crucial to PCa detection: sensitivity, specificity, and positive predictive value. After incorporating all the available data in a model, a software providing the risk of obtaining a positive result in prostate biopsy was created.

Results: Data from 268 patients who met the inclusion criteria were inserted in the model training. Scanget test showed a sensitivity of 0.93 and a specificity of 0.87; mpMRI had a sensitivity of 0.72 and a specificity of 0.87. The lower sensitivity of mpMRI is believed to be due to the low PCa detection rate in PI-RADS 3 lesions (22.4%).

A single model including clinical variables, mpMRI results and Scanget findings was therefore created and uploaded to a software capable of providing 4 PCa risk classes: "Highly Unlikely", "Unlikely", "Likely", "Highly Likely".

Conclusion: Integrating Scanget test, clinical data, and mpMRI findings through artificial intelligence may offer a valuable approach for clarifying uncertain cases, such as those involving PI-RADS 3 lesions. Although the rate of positive Scanget test results linked to insignificant PCa is yet to be fully understood, we believe that machine learning models, like the one proposed here, could soon help reduce the number of unnecessary prostate biopsies.

ABSTRACT 21

COMPARATIVE EVALUATION OF THE PHYSICOCHEMICAL PROPERTIES OF ADHESIVE AGENTS FOR THE ENHANCEMENT OF POST-LITHOTRIPSY STONE CLEARANCE

Harel Sims, Aymon Ali, Bruce Gao, Seyedamirvala Saadat, Mahbod Fattahi, Candices Tran, Yezan Hadidi, Eman Chaudhri, Sohrab Ali, Pengbo Jiang, Roshan Patel, Jaime Landman, Ralph V. Clayman.
University of California, Irvine Department of Urology

Introduction: Residual stone fragments (RSFs) following laser lithotripsy can act as nidi for future stone formation. To improve stone-free rates, biologic and synthetic aggregation agents have been explored as a means of efficiently collecting and consolidating "too small to basket" fragments for efficient removal. In this study, we evaluate the physicochemical properties of two adhesive agents: MediNiK® Hydrogel (Purenum) and TISSEEL Fibrin Sealant (Baxter) with regard to tensile strength, adhesive strength, transparency, and solubility.

Methods: Tensile strength of the adhesive was evaluated using a tray with two aligned holes allowing positioning of two diametrically opposed 1.7 F NGage® stone baskets (Cook Medical Inc., Bloomington, IN) (Figure 1). One basket was tethered to the novel UCI Force Sensor capable of measuring force in hundredths of a Newton. A 1 cm segment of either MediNiK® or TISSEEL was grasped between the baskets and pulled linearly via the force sensor until the adhesive ruptured; this was repeated four times for each substance. The force at which rupture of the adhesive occurred was recorded as the tensile strength.

Adhesive strength to an entrapped 3 x 6 mm calcium oxalate stone was also evaluated. The stone was held within one basket and then encapsulated with adhesive for the recommended "curing" time. Next, the stone-containing basket was pulled from the adhesive. The force of separation was recorded. This was repeated four times. Transparency of each adhesive was assessed using a Lux meter (Mashtech); saline was used as a control. Solubility was evaluated by immersing pre-weighed adhesive samples in 37°C saline with continuous circulation for 48 hours. Residual adhesive was filtered (210-micron mesh) and weighed in triplicate.

Results: Tensile strength was not statistically different between MediNiK® (0.97 ± 0.18 N) and TISSEEL (1.08 ± 0.30 N) ($p = 0.547$) (Figure 2A). Adhesive strength was far greater with TISSEEL (1.55 ± 0.04 N) compared to MediNiK® (0.61 ± 0.16 N) ($p < 0.0001$) (Figure 2B). MediNiK® was more transparent (17.49 ± 0.13 Lux) than TISSEEL (14.01 ± 0.09 Lux) ($p < 0.0001$) (Figure 2C). In solubility testing, MediNiK® was vastly more soluble than TISSEEL: 47.5% vs. 83.0%, residual, respectively ($p = 0.013$) (Figure 2D).

Conclusion: MediNiK® and TISSEEL exhibit similar tensile strength; however, MediNiK® offers superior transparency and solubility when considering removal of residual stone fragments.

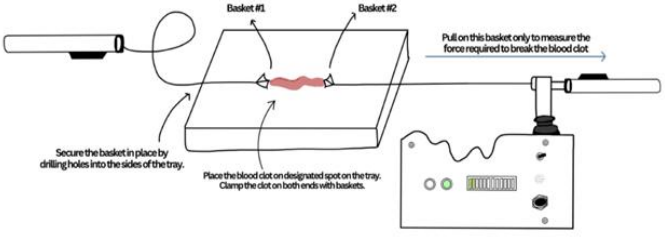

Figure 1: Tensile strength experimental setup showing two 1.7 F NGage® baskets (Cook Medical) grasping onto adhesive. Right-hand basket is connected to the UCI force sensor and pulled in a linear direction, while the left-hand basket remains stationery.

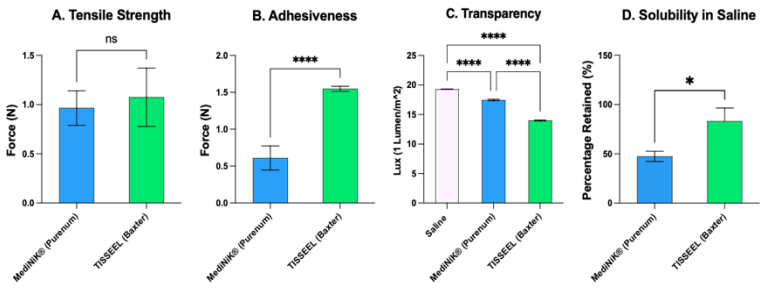

Figure 2: Comparison of MediNiK® (Purenum) and TISSEEL (Baxter)—in terms of tensile strength (A), adhesiveness to a stone (B), transparency (C), and solubility (D). Statistical significance is indicated by asterisks: *$p < 0.05$, ***$p < 0.001$, ****$p < 0.0001$.

ABSTRACT 22

AFTER ONE YEAR OF EXPERIENCE: COULD DISS (3.6 FR WORKING CHANNEL) MAKE EVERYTHING THAT SUCTIONING BENDABLE ACCESS SHEATH DOES?

Bogdan Geavlete[1,2,3], Cristian Mares[1,2], Razvan Multescu[1,2,3], Cosmin Ene[1,2], Valentin Iordache[1,2,3], Petrisor Geavlete[1,2,3]

[1]"Carol Davila" University of Medicine and Pharmacy, Bucharest, Romania
[2]"Saint John" Emergency Clinical Hospital, Bucharest, Romania [3]"Sanador" Hospital

Introduction: Minimally invasive techniques for renal stone management are constantly evolving. Direct In-Scope Suction (DISS^{TM}) technology from Pusen^{TM} offers improved intraoperative visualization and aspiration during flexible ureteroscopy (fURS). This study examines the efficacy of DISS (using a 3.6 Fr working channel) alone, compared to its combination with suctioning bendable access sheaths (FANS), in managing renal calculi.

Methods: A retrospective analysis of 75 consecutive patients undergoing fURS for renal calculi ≤25 mm between March 1, 2024 and July 31, 2024, was performed. Patients were divided into two groups: Group 1 (DISS with standard 10/12F access sheath - Flexor® Ureteral Access Sheath, n=35), and Group 2 (DISS with FANS, n=35). Outcomes assessed included stone-free rates (SFR) at three weeks post-operatively, operative time, need for postoperative stenting, and complication rates. Stone density measured in HU was between 460 and 1380, with a mean value of 980. In all cases Pusen PU3033AH fURS with 3.6 Fr working channel was used with direct in-scope suction DISS^{TM}. ClearPetra® Wellead Flexi Ureteral Access Sheath 10/12F or Elephant II (YiGao Med^{TM}) FANS were used. For lithotripsy we used Laser Mega Puls70 Quanta System Richard Wolf.

Results: The study demonstrated that DISS alone (Group 1) presented high SFR, operative time, and complication rates. However, the combination of DISS with FANS (Group 2) yielded superior results across all parameters. Specifically, Group 2 showed the highest SFR 1 case (2.85%) compared to 4 cases (11.42%) in Group 1, the shortest operative, and the lowest rates of postoperative stenting only 2 cases (5.71%) compared to 8 cases (22.85%) and overall complications – only 2 cases of mild hematuria compared to 4 cases of mild hematuria and one case of postoperative fever. In terms of visualization both groups presented excellent visualization during stone lithotripsy, considering the important help of dust suction through the scope in DISS technique alone.

Conclusion: While DISS^{TM} technology with a 3.6 Fr working channel offers significant advantages over standard fURS for renal stone management, combining DISS with FANS provides demonstrably superior outcomes. The synergistic effect of improved visualization and enhanced aspiration provided by FANS further optimizes stone removal, minimizes operative time, reduces complications, and improves overall patient experience. These findings support the clinical utility of integrating FANS technology into fURS protocols for managing renal calculi. Further research with larger, prospective, randomized studies is warranted to definitively establish the comparative effectiveness of these techniques.

ABSTRACT 23

CONCOMITANT URETERO-RENAL STONES TREATED WITH DISPOSABLE RIWO D-URS – FIRST EXPERIENCE

Bogdan Geavlete[1,2,3] Cristian Mares[1,2], Razvan Multescu[1,2,3], Cosmin Ene[1,2], Valentin Iordache[1,2,3], Petrisor Geavlete[1,2,3]

[1]"Carol Davila" University of Medicine and Pharmacy, Bucharest, Romania
[2]"Saint John" Emergency Clinical Hospital, Bucharest, Romania [3]"Sanador" Hospital

Introduction: The optimal approach for managing ureteral and renal calculi remains a subject of ongoing debate. Rigid ureteroscopes offer superior access and maneuverability in the ureter, while flexible ureteroscopes provide better navigation within the renal collecting system. The disposable RIWO D-URS (Richard Wolf ™) represents a novel hybrid approach, combining the advantages of both rigid and flexible ureteroscopes in a single instrument: a semi-rigid shaft with a flexible distal tip. This innovative design potentially allows for efficient treatment of both ureteral and renal calculi, streamlining the procedure and potentially improving outcomes. This study investigates the efficacy and feasibility of this novel device.

Methods: This prospective study was conducted three-month period. Seven patients with both renal and ureteral calculi and pre-existing JJ stents were enrolled. All procedures utilized the new RIWO D-URS ureteroscope, a semi-rigid ureteroscope with a flexible distal tip. Key features of the new ureteroscope include: a unique continuous irrigation system in a flexible ureterorenoscope; a third channel for constant irrigation backflow, even without a ureteral access sheath; maintained continuous irrigation flow even with laser fiber insertion; and a 9.0 Fr outer diameter with a 3.6 Fr working channel for auxiliary instruments and a 1.65 Fr channel for laser fibers, compatible with 9.5 Fr ureteral access sheaths. The device incorporates special boreholes on the distal tip to reduce intrarenal pressure. Laser Mega Puls70 Quanta System Richard Wolf was used for lithotripsy. Data collected included operative time, stone-free rate (SFR) at three weeks post-operatively (assessed via non-contrast CT), and the incidence of complications.

Results: A total of 7 cases of concomitant ureteral and renal lithiasis (less than 2 cm.) with prior JJ stenting were performed. Stone density was measured by CT with mean HU between 720 and 1280. Mean operative time was 55.5 minutes (range 45-75 minutes). All cases were performed without a ureteral access sheath - no-touch technique. Postoperative complications were minor; transient, mild hematuria (Clavien I-II) occurred in 2 patients (28.5%), and a JJ stent was placed for two weeks in 4 patients (57.1%). Minor residual fragment (3 mm) was observed in one patient (14.28%) in the inferior calyx but deemed clinically insignificant. No other complications occurred in the study group.

Conclusion: This prospective study demonstrates the feasibility and efficacy of the RIWO D-URS ureteroscope in managing both ureteral and renal calculi. The unique continuous irrigation system and flexible distal tip enabled efficient stone removal with minimal complications and acceptable operative times, even without the use of a ureteral access sheath. The results suggest that the RIWO D-URS effectively combines the advantages of rigid and flexible ureteroscopes, potentially improving outcomes for patients with complex urinary calculi. Further larger-scale studies are warranted to confirm these findings.

ABSTRACT 24

OPTIMIZING RADIOFREQUENCY THERAPY FOR OVERACTIVE BLADDER: IDENTIFYING HIGH NERVE DENSITY ZONES IN A CADAVERIC STUDY

Gamal Ghoniem[1], Mickey Karram[2], Muhammed A M Hammad[1]
[1]University of California, Irvine, CA, USA, [2]The Christ Hospital, Cincinnati, OH, USA.

Introduction: Targeted radiofrequency (RF) therapy is emerging as a promising treatment for overactive bladder (OAB), aiming to modulate autonomic nerve pathways to control symptoms. Identifying precise areas of high nerve density (HND) within the bladder and adjacent vaginal wall (AVW) is crucial for optimizing energy delivery. This study aims to determine the HND zone to support a minimally invasive RF intervention via the anterior vaginal wall.
Methods: Tissue samples were obtained from two adult female cadavers. Hematoxylin and eosin (H&E) staining confirmed anatomical structures, and S100 immunohistochemistry was used to visualize nerve distribution. Image analysis software quantified nerve size and density across the anterior and posterior bladder walls and the AVW. Statistical analyses, including one-way ANOVA and pairwise t-tests, were conducted to assess nerve differences within regions of the posterior bladder wall, stratified into "Towards Vagina," HND, and "Towards Bladder" at depths of 0-2.4 mm, 4.8-7.2 mm, and 7.2-9.6 mm from the vaginal surface.
Results: H&E staining confirmed intact tissue structures. S100 staining revealed significantly higher nerve density in the posterior bladder wall, particularly within the HND region at a depth of 4.8-7.2 mm. One-way ANOVA demonstrated significant differences in nerve size (p=0.0017 for T1, p=0.0006 for T2) and density (p=0.036 for T1, p=0.0007 for T2) within the HND region compared to adjacent regions. Pairwise t-tests further confirmed significant differences in nerve distribution, with the HND zone exhibiting the largest nerves and highest density across both specimens.
Conclusion: This study identifies the HND zone in the posterior bladder wall as an optimal target for RF therapy in OAB treatment. The findings suggest that applying RF energy at a depth of 4.8-7.2 mm via the anterior vaginal wall may enhance therapeutic efficacy, offering a minimally invasive approach for improved symptom relief. Further research is warranted to validate these findings in clinical settings.

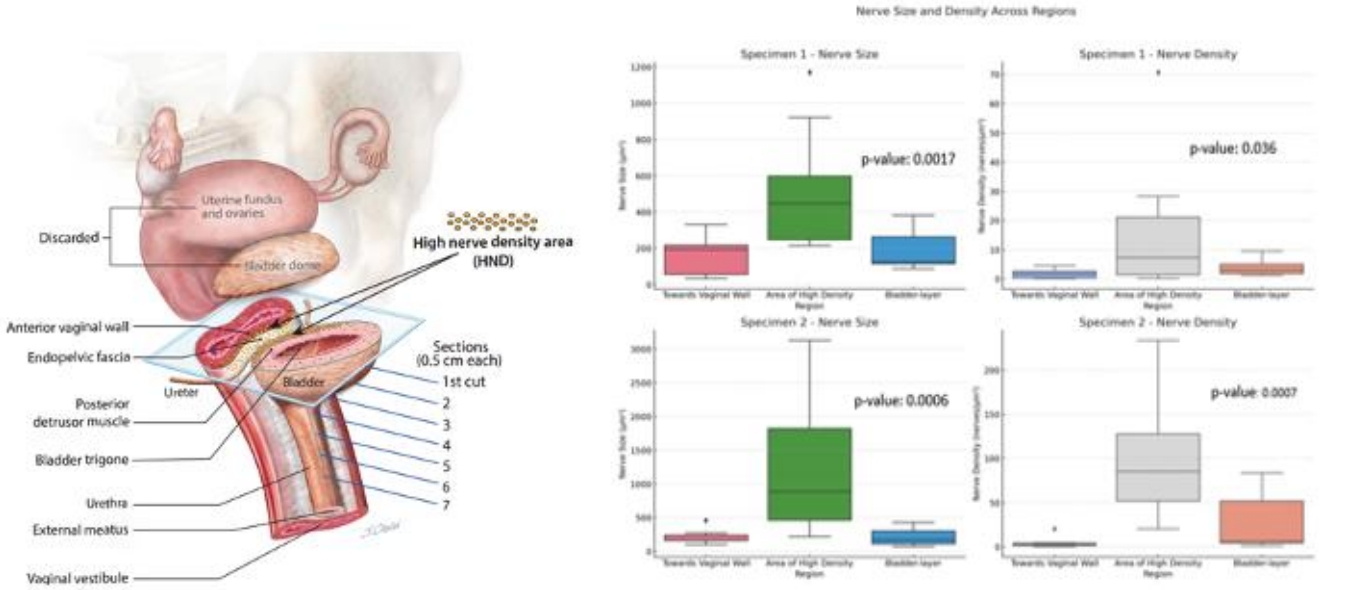

The box plots provide a comparison of the average nerve size & density across different regions in the posterior wall for Specimen 1 and Specimen 2. The variability within each region and between the two specimens is evident in the box plots with corresponding p-value for one-way ANOVA test.

ABSTRACT 25

ENHANCING SURGICAL SAFETY IN TELEOPERATED ROBOTICS RIRS SYSTEMS USING FORCE FEEDBACK

Jin-Hyeok Bae[1], Dong-Ho Lee[1]
[1] ROEN Surgical

Introduction: Remote robotic systems for Retrograde Intrarenal Surgery (RIRS) are emerging, enabling surgeons to manipulate both the ureteroscope and instruments on their own, thereby improving usability [1, 2, 3]. However, most systems lack force feedback, making it difficult to detect instrument-tissue interactions, increasing the risk of urinary tract injury (UTI). Prior studies measured the force applied during ureteral access sheath (UAS) insertion and found that when kept below 5N, the Post-Ureteroscopic Lesion Scale (PULS) score remained ≤1, indicating minimal injury [4]. This study integrates force feedback into robotic RIRS systems to enhance surgical safety through real-time force perception.

Methods: A teleoperation prototype was developed for experiments using a Becton Dickinson ureteroscope and a UAS for Flexible And Navigable Suction (FANS). A load cell (Dacell) was installed to measure the force along the UAS insertion axis. The force feedback system classified UAS status into three modes: Normal, Contact (≥0.5N), and Excessive Force (≥1.5N). Real-time alerts were provided to the operator to minimize excessive force. To simulate surgical conditions, a kidney model was fabricated using EcoFlex, mimicking the mechanical properties of real kidney tissue. In the experiment, the ureteroscope and the UAS was navigated to two target points in the kidney model under two conditions: with and without force feedback. Force exerted on the kidney's inner wall was measured. Twelve participants, with no medical background or prior force feedback experience, performed the task.

Results: Table 1 presents the peak force and duration of force warnings recorded for each participant. Overall, the results demonstrated that force feedback significantly reduced the peak force exerted on the kidney's inner wall (With force feedback: 2.07±0.38N, without force feedback: 4.78±1.44N) and noticeably shortened the duration of excessive force (With force feedback: 3.77±2.95 sec, without force feedback: 13.96±8.79 sec). Furthermore, when navigating into the calyx, participants using force feedback were able to perceive resistance from curved surfaces more effectively, allowing them to adjust their movements accordingly. These findings suggest that integrating force feedback into robotic surgical systems can improve surgical safety and minimize unintended tissue damage.

Conclusion: Force feedback in robotic RIRS significantly reduces unintended force on kidney tissue, enhancing surgical safety. By improving instrument control during navigation, it helps minimize the risk of ureteral damage. Further studies are needed to validate the system's effectiveness in clinical settings, assess its usability across surgeons with varying levels of expertise, and evaluate its performance in animal models to ensure its applicability in real-world surgical environments.

Table 1: Peak Force and Duration of Warning with/ without force feedback

Participant	Force Feedback Availability	Peak Force [N]	Duration of Warning [sec]	Participant	Force Feedback Availability	Peak Force [N]	Duration of Warning [sec]
A	O	1.94	2.26	G	O	2.74	1.15
	X	4.02	8.31		X	7.05	27.15
B	O	1.66	0.89	H	O	2.54	1.09
	X	3.04	30.83		X	4.27	7.01
C	O	1.93	6.23	I	O	1.61	3.36
	X	4.89	9.32		X	4.14	9.15
D	O	2.02	4.89	J	O	2.19	4.28
	X	5.86	11.01		X	5.75	10.28
E	O	1.49	0.00	K	O	2.01	9.44
	X	3.19	6.21		X	4.77	17.87
F	O	2.37	3.76	L	O	2.34	7.89
	X	3.14	6.09		X	7.23	24.27
Average	O	2.07±0.38	3.77±2.95	Both p-values are < 0.001. Thu, the differences are significant.			
	X	4.78±1.44	13.96±8.79				

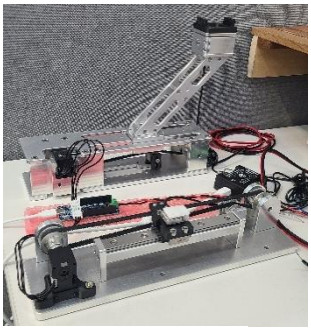

Figure 1 A teleoperation prototype

ABSTRACT 26

THE EFFECT OF CONTINUOUS FLOW IRRIGATION ON INTRARENAL PRESSURE DURING *EX VIVO* PORCINE RETROGRADE INTRARENAL SURGERY

Yezan F. Hadidi, Eman N. Chaudhri, Aymon Ali, Bruce M. Gao, Seyed Amiryaghoub M. Lavasani, Seyedamirvala Saadat, Harel C. Sims, Mariah C. Hernandez, Sohrab N. Ali, Pengbo Jiang, Roshan M. Patel, Jaime Landman, and Ralph V. Clayman
Department of Urology, University of California, Irvine, Orange, CA

Introduction: Traditional retrograde intrarenal surgery relies on one-way irrigation into a partially closed collecting system, leading to sustained increases in intrarenal pressure (IRP). Elevated IRP increases the risk of sepsis due to intra-renal reflux. This study evaluates a simulated, continuous flow ureteroscope (cfURS) with dedicated inflow and outflow channels to maintain IRP below 40 cmH_2O.

Methods: Using two 0.67 mm inner diameter (ID) and one 2.0 mm ID silicone tubes, and a 30 Fr PTFE insufflation tube, a simulated, multi-channel cfURS was assembled. With a SENCTRLä pressure transducer (Wenzhou, Zhejiang Province, China) percutaneously connected to the renal pelvis with an 8 Fr Pigtail catheter, saline irrigation (0.9% NaCl) was introduced through either or both 0.67 mm channels at pressures of 50, 100, 150, and 200 mmHg; the 2.0 mm channel was left open to drainage (**Figure 1)**. Irrigation was conducted for 3 minutes, during which a plateau pressure was reached at approximately 2 minutes, and IRP recordings were obtained from 15-second intervals within this range. Trials were performed in triplicate and a mean IRP was obtained under three common operative conditions: (1) two 0.67 mm inflow channels (Condition 1), (2) two 0.67 mm inflow channels (Condition 2), with a 200µ laser fiber in one (3) one 0.67 mm inflow channel, two outflow channels (0.67 and 2 mm) (Condition 3). Each scenario was tested at irrigant heights of 0 and 20.0 cm relative to the kidney, and with 45 and 65 cm URS lengths for a total of 144 IRP measurements.

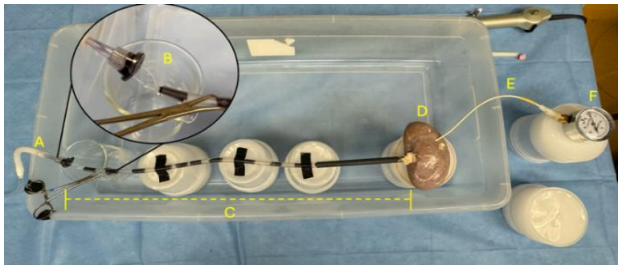

Figure 1: Experimental set-up with **A)** 0.9% saline

Results: Across all conditions, mean IRP remained below the 40 cmH_2O safety threshold. For the 45 cm URS, the highest mean IRP observed was at 20.0 cm above the kidney was at 200 mmHg irrigation pressure for Condition 2 (21.84 cmH_2O); the lowest mean IRP observed was at kidney height for both Conditions 2 and 3, regardless of irrigation pressure (0.00 cmH_2O) (Figure 2A).

For the 65 cm URS, the highest mean IRP observed was at 20.0 cm above the kidney at 200 mmHg irrigation pressure for Condition 1 (22.94 cmH_2O); the lowest mean IRP observed was at kidney height with Condition 3 regardless of irrigation pressure (0.00 cmH_2O) (Figure 2B).

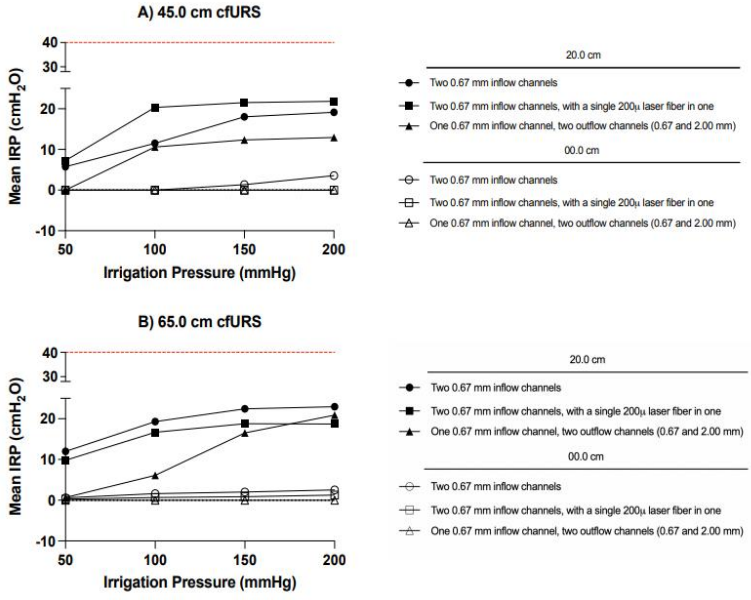

Figure 2: Mean IRP recorded at 50, 100, 150, and 200 mmHg irrigation through 45.0 and 65.0 cm (**2A** and **2B**, respectively) simulated, continuous flow ureteroscopes at 00.0 cm and 20.0 cm above, the kidney-ureter model.

Conclusions: A simulated multi-channel cfURS with a 2 mm aspiration port, allows for maintenance of IRP under 40 cm H_2O under common operative conditions and maximal irrigation pressures.

ABSTRACT 27

ROBO-CYSTO: FEASIBILITY OF A COMPUTER VISION MODEL TO IDENTIFY ANATOMIC LANDMARKS DURING CYSTOSCOPY

Maya Srinath[1], Iyla Bagheri [1], Charan Mohan [1], Louis Kavoussi [1] Arun Rai [2]
[1] Northwell Health, Smith Institute of Urology [2] Johns Hopkins, Brady Urological Institute

Introduction: Cystoscopy is the foundation of many urological procedures. Through cystoscopy, urologists can visualize the anatomy of the urethra and bladder and associated pathology. As we move toward embracing new technology in the practice of medicine, we hypothesize that artificial intelligence (AI)-based image identification systems can be taught to identify basic urethral and bladder anatomy. This study aims to test AI based image analysis models to identify basic anatomic landmarks visualized on cystoscopy of the male urethra and bladder.

Methods: Recorded cystourethroscopy videos from 6 patients were identified and segmented on a web-based system called Roboflow; a commercially available online platform allowing for the creation of computer vision models via machine learning [1]. The segmented videos were reviewed by 2 reviewers and images were manually annotated for various anatomic landmarks including bladder neck, bladder wall, left and right ureteral orifices, prostatic urethra, urethral sphincter, verumontanum, and penile urethra. Roboflow 3.0 Object Detection (YOLOv8 Derived) model was utilized in this study.

Results: 276 images from 6 videos were included in the final dataset. All were from rigid cystoscopy. 70% of the data was used to train the model, 20% to validate, and 10% used to test to model comprising 192 images in the training set, 57 images in the validation set and 27 in the test set. The final model was created over 264 epochs. The mean average precision (mAP) of the model was 79.9% with a recall of 74.4%. When looking at the precision of our computer vision model in identifying the ureteral orifices, it identified the left ureteral orifice with 100% precision and right ureteral orifice with 97% precision in the test set. Figure 1 provides mAP by anatomic location for the model.

Conclusion: A computer vision model can identify anatomic elements of the male urethra and bladder during cystoscopy with high degree of precision and recall. Further work can aim to refine this model for future diagnostic and therapeutic applications in cystoscopy.

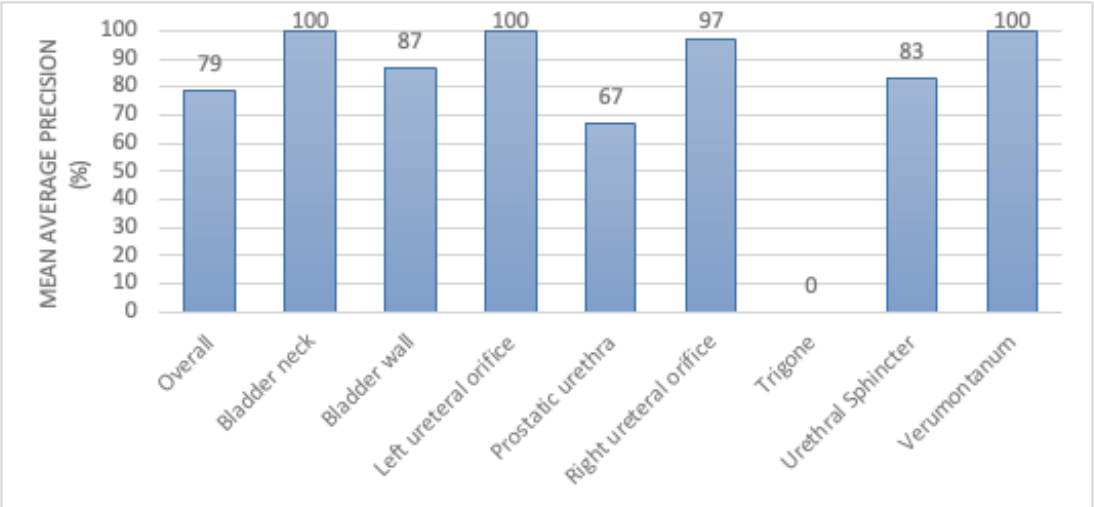

Figure 1: Average Precision by Anatomic Location

ABSTRACT 28

MEDIC: MACHINE LEARNING-BASED FEATURE EXTRACTION FOR INTELLIGENT CLIPPING IN ENDOSCOPIC KIDNEY SURGERY VIDEOS

Bradley French[1], Kanyifeechukwu Oguine[1], Greyson Wintergerst[1], Nicholas Kavoussi[2], Ipek Oguz
[1] Dept. of Computer Science, Vanderbilt University;
[2] Dept. of Urology, Vanderbilt University Medical Center, Nashville, TN

Introduction: The selection of endoscopic video segments, or clipping, is often performed manually by surgeons before being provided to researchers for downstream analysis. This selection introduces variability and possible bias, as surgeons may select too few or too many frames based on personal experience. Additionally, manually clipped videos may omit critical frames that contain subtle but clinically or computationally significant details, limiting the ability of computational models to learn robust features. Finally, the selection process is tedious and can inhibit studies on large datasets, which is problematic for modern deep learning models that thrive on large training datasets. To address these challenges, we propose MEDIC (Medical Endoscopy Data Intelligent Clipping), a deep learning-based classifier for video frames. This model serves as the first step in an automated and reproducible clipping process, ensuring that critical frames are retained while irrelevant ones are discarded.

Methods: We collected 12 ureteroscopy surgical videos for a total of 374,015 frames in 3 classes: (a) within collecting system anatomy (n=359,013), (b) before scope insertion/after scope removal (n=15,171), (c) menu screens (n=831). All videos were recorded using a digital ureteroscope (Storz XC). We trained a Convolutional Neural Network (CNN) for classification with 151,966/66,134/156,915 split for train/validation/test. We employed weighted sampling during training to overcome the class imbalance.

Results: The CNN was able to accurately describe each of (a), (b), and (c) frames with validation accuracies of 99.72%, 92.93%, and 100%, respectively, by epoch 60, as shown in Figure 1. The overall validation accuracy across all classes was 99.48%. Test accuracies were 99.99%, 98.58%, 100% respectively. The accuracy for class (c) indicates the model's ability to reliably identify menu screens, while the model shows strong performance for frames (a) inside and (b) outside the collecting system anatomy. However, the accuracy for class (c) was unstable, potentially indicating challenges related to the lack of frames compared to class (a).

Conclusion: This study demonstrates the feasibility of using deep learning to distinguish specific frame types and lead to the automation clipping of endoscopic surgical videos. The CNN effectively differentiates key visual components, providing a strong foundation for further temporal modeling in future work.

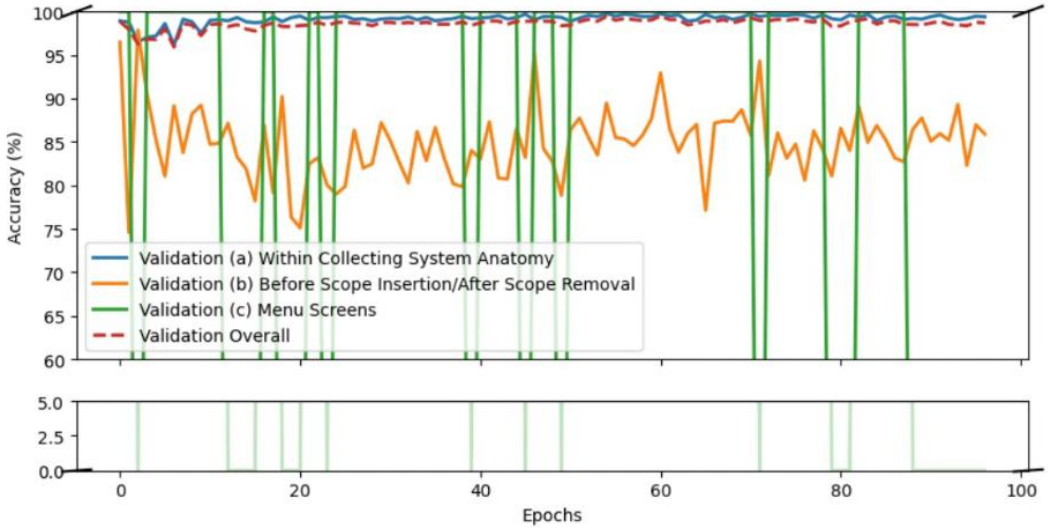

Figure 2. Accuracy plot for validation data. The model was validated on a subset of the total 408,030 frames (n = 66,134). The overall performance approached 99.5%.

ABSTRACT 29

AUTOMATED PREDICTION OF KIDNEY STONE-FREE STATUS USING DIGITAL URETEROSCOPY VIDEO ANALYSIS

Bradley French[1], Daiwei Lu[1], Nicholas Kavoussi[2], Ipek Oguz[1]
[1] Dept. of Computer Science, Vanderbilt University;
[2] Dept. of Urology, Vanderbilt University Medical Center, Nashville, TN

Introduction: Ureteroscopy (URS) with laser ablation via dusting (i.e., lower energy and high frequency) is the most common technique for kidney stone treatment worldwide [1]. Despite this, the analysis of treatment adequacy is inherently subjective and dependent on a surgeon's experience, visualization quality, and patient-specific features. These limitations contribute to variability in surgical outcomes, as up to 40% of patients have residual stone fragments after treatment [2, 3, 4]. We propose a method for computationally predicting kidney stone-free status using URS videos.

Methods: We collected forty-seven URS surgical videos depicting kidney stone dust at the conclusion of stone laser ablation. All videos were recorded using a digital ureteroscope (Storz XC). Stones were treated via dusting technique with a holmium laser by one of 4 endourologists. Median duration of videos was 13.01 seconds (5.075 seconds IQR). Each video was sampled at 30 frames per second. We compared three machine-learning models for predicting stone-free status: (a) a Convolutional Neural Network (CNN, to evaluate each frame independently), (b) a Long-Short Term Memory model (LSTM, to incorporate temporal dependencies in short-clips of videos), and (c) a Transformer model (to incorporate the contextual relationships across entire videos). We obtained ground truth stone-free status for each patient from computed tomography (CT) at 6 weeks. We evaluated each model's predictions against this ground truth. We also asked 16 urologists to visually predict the stone free status from a subset (n=14) of the clips. We compared these human expert predictions to the model performance.

Results: On a per frame analysis, the Transformer model (accuracy: 58%) outperformed both the CNN (50%) and LSTM (50%) in predicting residual stone fragment on postoperative imaging. Additionally, the Transformer model demonstrated fair accuracy (61%) in prediction on a per-video basis by combining per-frame predictions via majority vote. The Transformer model closely approached the performance of expert surgeons, who predicted full-video outcomes with an accuracy of 63±10% (mean ± stdev).

Conclusion: Our study demonstrates the potential of deep learning models for predicting kidney stone-free status using URS videos. The improved performance of the Transformer model is likely attributed to its analysis of temporal and contextual information. Its performance falls within the human expert variability and highlights the potential of data-driven decision-making to improve surgical outcomes.

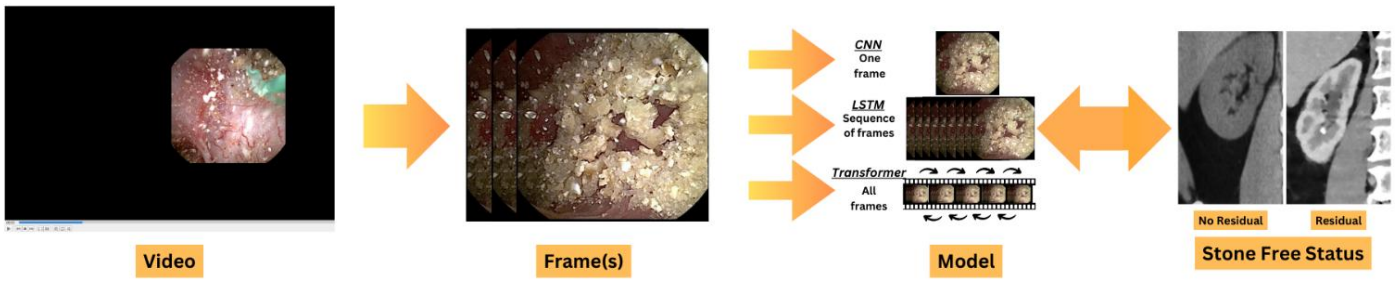

Figure 3. Deep learning prediction pipeline. We begin by collecting videos from endoscopic surgery. Once collected, we convert the videos to frames. We begin analysis of all frames on the three models: CNN, LSTM, and transformer. We then return individual frame predictions and aggregate video predictions.

ABSTRACT 30 **TOP 10 ABSTRACT**

FEASIBILITY OF WIRELESS CATHETER-FREE AMBULATORY URODYNAMICS IN MALE PATIENTS

Tyler Trump [1], Michael Gross [1], Kassandra Zaila [1], Madison Lyon [1], Steve Majerus [2,3], Brett Hanzlicek [2], Tyler Tevis [2], Ly Hoang-Roberts [1], Margot Damaser [1,2], Smita De [1]

[1] Glickman Urological and Kidney Institute - Cleveland Clinic; Cleveland, OH, USA
[2] Advanced Platform Technology Center - Louis Stokes VA Medical Center; Cleveland, OH, USA
[3] Department of Electrical, Computer and Systems Engineering, Case Western Reserve University, Cleveland, OH, USA

Introduction: Multichannel urodynamics (UDS) is the gold standard method to quantitatively evaluate the lower urinary tract (LUT). Despite being the gold standard, multichannel UDS has its limitations including creation of an uncomfortable, artificial environment for patients as well as reliance on complex equipment operated by trained staff. To overcome some of these limitations, a novel ambulatory system (the Urodynamics Monitor, UM) has been developed and previously described (Figure 1A) [1].The device has already been validated in female patients demonstrating accurate pressure data and ease of use. More recently, a method was developed for insertion into male patients. In this study, we seek to evaluate the tolerability of the UM and accuracy of UM data in male patients.

Methods: Male patients undergoing multichannel UDS and cystoscopy for evaluation of LUT symptoms were recruited. After baseline UDS and cystoscopy, the UM was inserted into the bladder through a sterile sheath. The sheath was advanced into the bladder in unison with the cystoscope. Following cystoscopy, the cystoscope was removed from the sheath and the UM was advanced through the sheath using the cystoscope as a "pusher," allowing for visual confirmation of placement. A second multichannel UDS was then performed with the UM simultaneously transmitting data followed by a period of catheter-free ambulation with physiological filling and voiding in private. A visual analogue pain scale was used to assess discomfort at each stage of the study.

Results: Six patients were recruited into the study with two excluded for urethral stricture diagnosed at time of cystoscopy. Conventional UDS findings are highlighted in Figure 1B. Figure 1C and 1D show representative data collection from the intravesical catheter and the UM taken simultaneously from 2 subjects. The highest mean pain score was 3 occurring at time of cystoscopy. A mean pain score of 1.5, 1.75, and 0 were identified with baseline UDS, UM insertion, and ambulation with UM in place, respectively. The mean pain score at 48-hour follow-up was 0.

Conclusion: Placement of the UM device in male patients is feasible and does not increase discomfort relative to standard evaluation. Clinically meaningful results appear similar with and without the UM in place. With further validation, the UM has the potential to provide UDS data on LUT symptoms during physiological filling and voiding with an improved patient experience.

1A

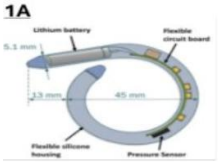

1B

	Baseline			With UM		
	Mean	Std Dev	Range	Mean	Std Dev	Range
Capacity (mL)	424.8	126.4	280 - 587	296	116.9	138 - 410
First Desire (mL)	267.3	78.5	161 - 345	216.5	87.2	102 - 301
Max flow (mL/s)	8.5	5.8	1.6 - 15.1	9.2	6.6	4.5 - 13.8
Pressure at max flow (cm H2O)	47.7	18.9	30.6 - 64.6	65.1	38.7	37.7 - 92.5
PVR (mL)	200	86.6	100 - 250	160.3	126.5	8 - 315
BOOI	37.3	27.3	4.4 - 63.5	30	36.2	4.4 - 55.6

1C

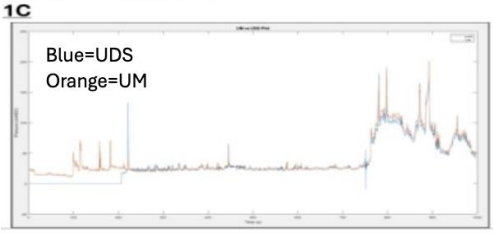

1D

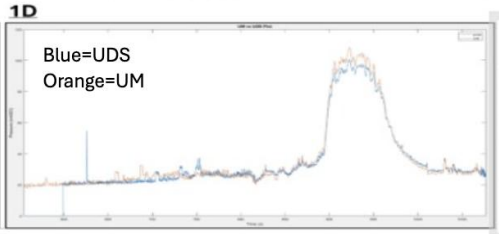

Figure 1A-1D
1A-Schematic of the UM device
1B-Conventional UDS data with and without UM device in place
1C and 1D-Data collection taken simultaneously from intravesical UDS catheter and UM device

ABSTRACT 31

EX-VIVO COMPARISON OF PIRANHA™ VS. CYBER BLADE™ MORCELLATORS IN A VALIDATED PROSTATE MODEL

Chloe Michel, Lauren Shepard, Ahmed Ghazi, Naren Nimmagadda

Introduction: Anatomic endoscopic enucleation of the prostate (AEEP) requires use of a morcellator for tissue evacuation unless in the exceptional case of open tissue extraction. Morcellation devices vary in their energy source and range of suction power. We performed an *ex-vivo* comparison of morcellation efficiency in a validated prostate model between the reusable Piranha™ morcellator and the disposable Cyber Blade™.

Materials and Methods: We created 50g hydrogel adenomas that were categorized as either nodular or non-nodular. Hydrogel adenomas were created using the same methodology as a previously validated model (Shepard et. al). For our study, 50g adenomas (10 non-nodular, 10 nodular) were created in a spherical shape. To mimic nodular prostatic adenomas, we included two 1cm spherical nodules that had been processed with additional freeze-thaw cycles to increase their density. The pieces were morcellated with the Piranha™ and Cyber Blade™ morcellators at manufacture-directed speed settings, 1500 RPM and 1300/1600 RPM, respectively. Additionally, the impact of suction source was tested with the Cyber Blade™ by comparing a Neptune™ and a D&C portable suction system.

Morcellation trials were completed using the aforementioned hydrogel model, which includes a prostatic fossa and bladder. Morcellation was completed using an offset nephroscope with two irrigation inflow sources. Irrigation collection cannisters and tissue cannisters were emptied in between each trial to standardize suction. Adenoma weights were recorded prior to each trial for correct calculation of morcellation efficiency. Two morcellation trials were run per combination of Cyber Blade™ speed setting, and suction source.

Results: Our trials revealed that the Cyber Blade™ was most efficient for nodular adenomas using a D&C portable suction machine at a speed of 1300 RPM. Morcellation efficiency with this combination yielded an average of 28.3g/min. The average efficiency for the Piranha™ with nodular tissue was 14.8g/min. For non-nodular tissue, Cyber Blade™ was most efficient using the portable D&C suction machine at a speed of 1600 RPM (26g/min). The Piranha™ demonstrated an efficiency of 12.7g/min with non-nodular tissue. Using an unpaired T-test model, this showed no significant difference in morcellator efficiency for the nodular group but a significant difference in efficiency for the non-nodular group favoring the Cyber Blade™.

Conclusion: In this *ex-vivo* model comparing morcellator efficiency at difference speeds and suction powers, we found that the Cyber Blade™ was more efficient than the Piranha™ for non-nodular tissue when used with a D&C portable suction machine at a speed of 1600 RPM. This may be in part due to the higher suction power achieved by the D&C machine (600mm Hg) compared to the Piranha™ (ranges between 487-562mmHg). This study will be expanded to larger size adenomas and eventually to an in-vitro model for better comparison of the morcellators.

ABSTRACT 32

A NOVEL CORE NEEDLE BIOPSY (CNB) INSTRUMENT DESIGNED FOR TARGETED PROSTATE BIOPSY

Eric Gwynn[1] Kevin Rackers[2]
[1] New River Urology, Hilton Head, SC [2]URO-1, Inc, Greensboro, NC

Introduction: Adoption of targeted prostate biopsy is accelerating due to increased detection of clinically significant prostate cancer[1]. However, two significant phenomena with existing standard of care (SoC) needles impede maximum sampling of the target – needle deflection and tissue displacement. (SoC) needles capture tissue in a notch located just proximal to the tip of the needle. Several studies have reported deflection of the needle tip as it traverses tissues of varying density. This impedes accurate sampling of target areas and reduces the volume of tissue captured within the notch.[2,3] The second is the shock wave generated by the needle when fired, which displaces tissues surrounding it[4].
A novel CNB instrument addresses both phenomena. The novel needle is coaxially centered in the outer cannula to prevent deflection. See Fig.1 To compensate for tissue displacement when the needle is fired the novel biopsy gun is designed to cause the needle to recoil twice when it reaches the end of its travel. A second feature delays deployment of the outer cannula by 5-8 msec after the needle reaches the end of its travel. See Fig.2

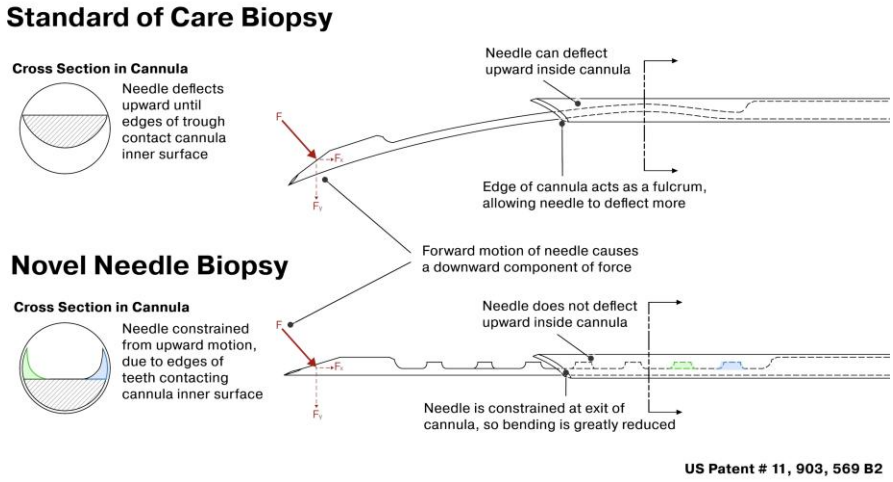

Methods: We report on five (5) men undergoing MRFUS guided trans perineal targeted biopsies enrolled in a multicenter randomized study (NCT05470127)*. Tissue deflection in a limited series of consecutive targeted biopsies was measured from frozen ultrasound image following sample acquisition

Results: The SoC instrument deflected 18 times out of 28 firing attempts (64%); the novel instrument 2 out of 25 (8%). SoC needle deflections ranged from 1- 4mm off target with a mean of 1.8mm; both deflections from the novel instrument were 1mm. Two tailed Z test comparing percentages of deflection resulted in a Z value of 4.22, $p<.00001$. Two tailed t-test comparing mean deflection results in a t value of 1.6752, $p<.00003$.

Conclusion: In this comparison of needle deflection in targeted prostate biopsy, the novel biopsy instrument performed significantly better than the SoC instrument in terms of frequency of deflection and distance from target. Accuracy in targeting suspected lesions may impact cancer detection rates. These promising results are being investigated in a large multicenter study.

ABSTRACT 33

EVALUATION OF A NOVEL WIRELESS MOTORIZED SINGLE-USE FLEXIBLE URETEROSCOPE IN PORCINE MODEL

Runhan Ren[1], Ali Algonaim[1], Victor KF Wong[1], Joseph C. Liao[2], Dirk Lange[1], Thomas Chi[3], Ryan F. Paterson[1], Brett Johnson[4], Connor M. Forbes[1], Mitchell R. Humphreys[5], Ben H Chew[1]
[1]University of British Columbia, [2]Stanford University, [3]University of Alabama, Birmingham, [4]University Texas Southwestern, [5]Mayo Clinic Arizona

Introduction: The use and availability of single-use flexible ureteroscopes has been increasing compared to traditional reusable scopes due to improvements in initial cost, sterilization, maintenance, and repairs. While advances in optics have been made, most single-use ureteroscopes still require a wired plugin connection to processing towers, despite advances in wireless technology. We evaluated the specifications of a newer generation wireless, motorized, single-use flexible ureteroscope (UroViu Corp, Los Altos CA).

Methods: A prototype of the ureteroscope was examined and assessed in a bench and porcine animal model.

Results: This ureteroscope consists of a reusable processor core with rechargeable battery and image capture, motor for scope rotation, and Wi-Fi transmitter housed within a disposable pistol-grip handle (Figure 1). The optical system consists of a camera with a 120-degree field of view and a 2-50 mm depth of field with two LEDs. The newer generation offers 7.5 Fr scope with a 67 cm long channel. It includes a separate instrument channel of 3.6 Fr. The disposable handle has a thumb-lever for upward and downward deflection of 270 degrees. 135-degrees of axial rotation in both directions is achieved through toggleable motorized control. This allows the physician's hand to remain in a neutral, ergonomic position. This ureteroscope transmits wirelessly to a13-inch portable screen with a low latency of 150 ms. Qualitative testing was done in porcine model with suction ureteric access sheath, basket, and laser fibers. It was found to be able to access and visualize all areas of the kidney in order to perform all necessary functions during ureteroscopy and laser lithotripsy.

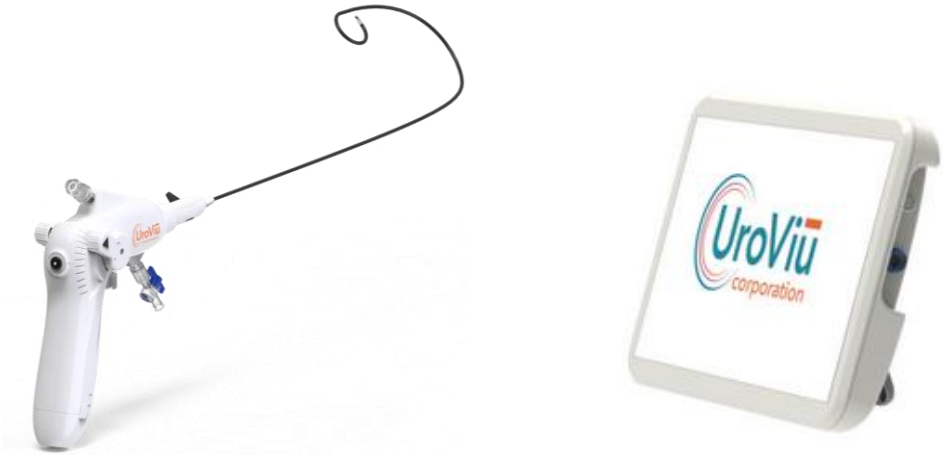

Figure 1. The UroViu single-use ureteroscope and portable relay station.

Conclusion: This novel, ergonomic, wireless, and portable single-use flexible ureteroscope system meets all requirements for ureteroscopic procedures as tested in a porcine model

ABSTRACT 34

UNDERSTANDING BIOMECHANICAL DIFFERENCES IN PENILE IMPLANT CYLINDER MATERIALS

Irwin Goldstein[1,2], Sue Goldstein[1], Bruna M. Couri [3]
[1] San Diego Sexual Medicine, San Diego, CA, USA
[2]Sexual Medicine, University of California San Diego Health East Campus, San Diego, CA, USA
[3] Coloplast, Minneapolis, MN, USA

Introduction: In 1973 the first inflatable penile prosthesis (IPP) was made from silicone. It was reported that during sexual activity that silicone cylinders often formed aneurysmal dilation from high intracavernosal pressures. Bioflex, an aromatic polyether urea urethane elastomer, was developed in 1982 as an alternative material. The aim of this study was to review biomechanical characteristics of Bioflex and silicone for use in an IPP to determine which cylinder material presents a more clinically relevant profile for sexual activity.

Methods: Published literature on Bioflex and silicone IPPs as well as Coloplast engineering documents have been reviewed.

Results: While literature comparing biomechanical characteristics of Bioflex and silicone are limited, studies consistently demonstrated that devices with Bioflex had higher resistance to penetration forces. Tensile strength of Bioflex is 7500 psi compared with 900 psi for silicone1. On a bench resistance test, with more than one thousand consecutive days of inflation and deflation, the Bioflex IPP showed no surface defects on scanning electron microscopy. In *in vitro* cyclic buckling studies, Bioflex cylinders underwent more than 6.5 million cycles without material failure, compared to silicone that failed after 1.1 to 1.2 million cycles. When Bioflex was tested regarding potential aneurysm failure, there were no aneurysms through various-sized wall defects up to one cm at up to 20 psi. To address the aneurysm problem with silicone, a dacron-lycra sleeve was developed to surround the cylinder. This sleeve restricts girth expansion to only 18 mm, unlike the Bioflex cylinder that allows expansion up to 21 mm, a 17% greater width. For longer penile lengths, Bioflex cylinders have been shown to have more axial rigidity and wider girth than silicone cylinders surrounded by the dacron lycra sleeve, while maintaining excellent elasticity. Concerning clinical relevance, anal intercourse requires a penile prosthesis with high axial strength as the force needed for anal penetration is more than 2-fold that for vaginal penetration, and mechanical stress is higher. For a female partner, reports reveal that greater pressure against the visceral afferent pelvic nerve in the vagina correlates with greater pleasure.

Conclusion: It is important for implanters to understand the biomechanical differences in the properties of the cylinder materials, including strength, girth expansion, and durability, which play a clinically relevant role for sexual activity. Further studies are needed.

ABSTRACT 35

WHAT IS "TENSION-FREE"? UTILIZING BLACK LIGHT ASSESSMENT OF SURGICAL TECHNIQUE (BLAST) TO QUANTIFY SUTURE TENSION IN AN ADVANCED URETERAL REPAIR SIMULATOR

Roach VA[1], Gong AT[1], Burke DM[1], Hagedorn JC[1], Hananel DM[1], Leuschke R[1], Skokan AJ[1], Speich JR[1], Traina DJ[1], Valovska MT[1], Wessells H[1], Wingate JT[1,2], Sweet RM[1].
[1] University of Washington, Seattle, WA.
[2] Madigan Army Medical Center, Tacoma, WA.

Introduction: A "tension-free" anastomosis is frequently emphasized in surgical training as a crucial measure to reduce the risk of tissue damage and anastomotic leakage. This is particularly important in traumatic ureteral repairs. However, the term "tension-free" with respect to anastomoses, has yet to be meaningfully quantified. To address this need, an advanced ureteral repair trainer was developed that incorporates black light assessment of surgical technique (BLAST) technology in the synthetic ureteral tissue to quantify what an expert would otherwise qualitatively identify as a "tension-free" anastomosis.

Methods: A UV-reactive fluorescent paint (BLAST) was mixed into the synthetic ureter solution before casting it into a mold. This mold created reproducible 10 mm spaced lines along the ureter, visible under UV light (365 nm). The completed ureteral repair puck was then integrated into the trainer. International expert urologists at the Society of Genitourinary Reconstructive Surgeons 2024 Academic Congress were invited to perform ureteral-ureteral (UU) anastomosis and reimplantation repairs. After each procedure, wing dividers were used to transfer the in-situ distance between the BLAST lines under UV light to a set of calipers for measurement. To quantify the expert's tension-free technique, a lab-developed uniaxial tensile tester employing a strain gauge (Reb7 load cell; Loadstar Sensors, Fremont, CA) was utilized to measure the tension of three individual synthetic ureters until the distance between the BLAST lines matched the expert's results.

Results: Sixteen expert international urologists performed a "tension-free" anastomosis on the ureteral repair trainer. Eight completed a ureteral-ureteral (UU) anastomosis, while eight completed a ureteral reimplantation. The mean distance between the lines of the BLAST markers was 10.35 ± 0.46 mm (range: 7.84 – 11.24 mm) and 10.80 ± 0.67 mm (range: 8.60 – 11.40 mm) for the UU, and reimplantation, which corresponded to a mean force of 0.013 N and 0.120 N, respectively at these distances. Two urologists that completed the reimplantation were excluded from analysis, as they indicated that their anastomosis was under "too much tension" (11.56 and 12.22 mm).

Conclusion: A "tension-free" anastomosis promotes healing while reducing the risk of leakage and damage. This study quantifies the actual force of a "tension free" anastomosis, anchored by expert performance for UU and reimplantation.

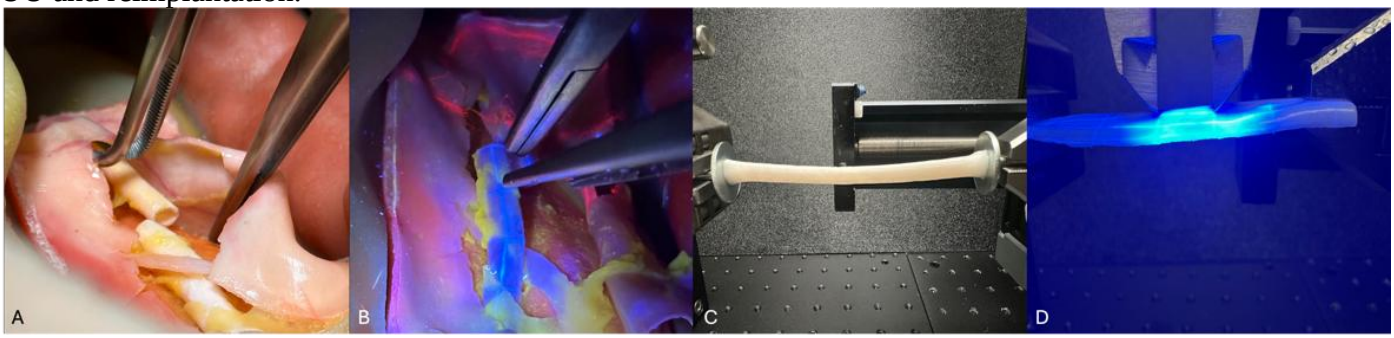

Figure 5: A) Synthetic ureter (cut), embedded in ureter repair trainer. B) Synthetic ureter, captured under black light (365 nm) to visualize embedded gridlines. C) Uniaxial tensile testing to measure tension in synthetic ureters. D) Measuring displacement of gridlines using black light, when synthetic ureter is placed under tension.

ABSTRACT 36

CAN A SURGEON WEAR A MONITOR: PHYSICAL ATTRIBUTES OF AN EXTENDED REALITY (XR) NEAR-EYE HEADSET

Steven Griffith[1], Henry Shields[1,2], Nathan Kriegel[2], Jonathan J. Stone[3], Michael P. Wilson[1], Nelson N. Stone[4]

[1]Viomerse, Inc, Pittsford, NY, [2]Northeastern University, [3]University of Rochester Medical Center, Rochester, NY, [4]Icahn School of Medicine, New York, NY

Introduction: When performing image guided procedures, surgeons need to look at one or more monitors. A heads-up display (HUD) designed with XR technology could offer the surgeons the opportunity to look directly at the operative field and their hands during the procedure. While the potential to improve hand-eye coordination is attractive, the XR HUD would also need to either replicate or exceed the visual acuity of current operating room monitors. We designed a system to meet these expectations.

Methods: The following attributes were considered necessary for the design of the HUD. 1) high transparency stereoscopic reflective waveguides to receive the video images; 2) large field of view to give surgeon the same visual experience when looking at a monitor; 3) adequate resolution and brightness, 4) high definition miniature projectors to display the images onto the lenses, and 5) software designed to arrange image position on the lenses, to generate real-time 2D/3D images and to control image opacity so the surgeons could look simultaneously at the operative site and the projected image (i.e. live ultrasound, fluoroscopic or endoscopic). The Normalized Angular Resolution (NAR) metric was used to evaluate display performance by considering both pixel distinguishability and resolution in relation to human vision for the HUD vs. a standard OR monitor. For 4K monitors positioned at least 7" from the surgeons, the NAR demonstrated consistent power-law behavior, expressed as: $-1.759\ y = 349,174,716 * x$ where y is the total effective pixels. This relationship provided crucial insights into long-term performance characteristics and helped predict system behavior across various surgical scenarios.

Results: A near-eye stereoscopic wearable display was developed with see-through optics which were housed in a 3D-printed frame (figure 1). The specifications of the lenses included: a fixed viewing distance (20 mm), resolution of 1920 x 1080 (2,073,600 pixels), dimensions 13 x 10 mm, pixel density 10,290,798.4 pixels/in², bit-depth 24 for RGB and for grayscale 8. The angular resolution of 1.02 arc minute/pixel (0.017°/pixel) closely matched human visual acuity. The graph shows superior color and greyscale depth advantage across almost the entire distance domain (figures 2,3). Beyond 11.5" the near-eye display exceeds resolution and color acuity of current OR monitors.

Conclusion: Our near-eye display system demonstrated measurable advantages in medical visualization through both theoretical analysis and practical validation. Our research established clear performance thresholds through intersection points at parity, order of magnitude, and two orders of magnitude improvement for RGB with the key thresholds being clinically significant as 11.5", 42.5"and 157.5"; and for greyscale 21.5",79.4" and 294" respectively.

Figure 1

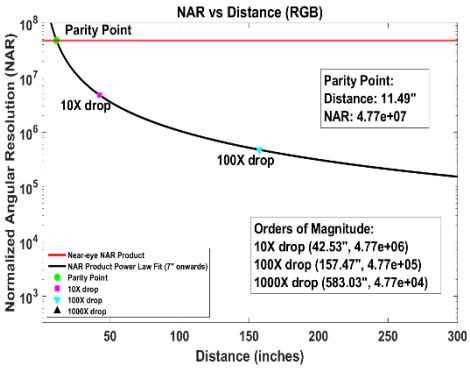

Figure 2

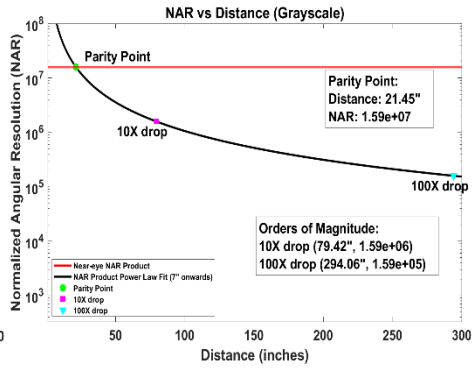

Figure 3

Figure 1: Resident wears HUD during image-guided procedure. Figures 2 & 3: Solid black regression line for 4K monitor demonstrating decreased acuity at greater distances vs. no change for near-eye HUD (solid red line), RGB and greyscale respectively.

ABSTRACT 37

TRANSPACIFIC TELESURGERY: A PRECLINCAL FEASIBILITY STUDY OF LONG-DISTANCE ROBOTIC SURGERY BETWEEN THE USA AND CHINA

Marcio Covas Moschovas[1], Shady Saikali[1], Mischa Dohler[2], Travis Rogers[1], Michael Mcdonald[1], Vipul Patel[1]

[1]AdventHealth Global Robotics Institute, Celebration, FL
[2]Advanced Technology Group, Ericsson Inc., Santa Clara, USA, Santa Clara, CA

Introduction: The 2001 Lindbergh operation demonstrated the feasibility of transatlantic telesurgery, and recent advancements in robotic platforms, 5g networks, and fiber optics have reignited interest in the field. We conducted a pioneering telesurgery study to assess connectivity and robotic performance between Orlando (USA) and Shanghai (China), with surgeons in both locations operating simultaneously on the same live animal models.

Methods: On July 23rd and 24th, 2024, we conducted a prospective telesurgery study utilizing four live porcine models, connecting Orlando and shanghai via the MicroPort Toumai robotic system. The study involved four surgeons in Orlando and one in Shanghai. The primary endpoint was to evaluate long-distance connectivity stability and surgical performance as surgeons—separated by 13,000 km—alternated control of the robotic console mid-procedure. This setup effectively simulated a real-world telesurgery scenario in which a remote surgeon assumes control in the event of complications or technical challenges.

Results: Multiple surgical procedures were successfully performed on four animal models (see table 1). Figure 1 illustrates the connectivity details. Day 1: mean latency: 139 ms (range: 137–216 ms). Day 2: mean latency: 139 ms (range: 137–185 ms). No connectivity failures, robotic malfunctions, or intraoperative complications were observed. The telesurgery connection remained stable throughout the entire trial.

Conclusion: This study is the first to demonstrate the feasibility of transpacific telesurgery done by two surgeons simultaneously. The ability to seamlessly switch robotic control between geographically distant surgeons without complications or delays reinforces the potential clinical viability of long-distance telesurgery. While our findings highlight the humanitarian and practical promise of this technology, they also emphasize the technical and logistical complexities that must be addressed before widespread clinical is possible.

Procedure Type	Animal Model	Surgeon Location	Animal Location	Connection Used	Platform Used	Latency (Milliseconds)	Complications	Troubleshooting with the Robot	Total Operative time (Minutes)
2 partial nephrectomies 2 radical nephrectomies 2 ureteroureterostomies 1 pyeloplasty	Porcine	Orlando (USA)	Shanghai (China)	Fiber	Microport Medbot Toumai	139 (137-216)	no	no	180 minutes
2 partial nephrectomies 2 radical nephrectomies	Porcine	Shanghai (China)	Orlando (USA)	Fiber	Microport Medbot Toumai	139 (137-216)	no	no	150 minutes
2 partial nephrectomies 2 radical nephrectomies	Porcine	Shanghai (China)	Orlando (USA)	Fiber	Microport Medbot Toumai	139 (137-185)	no	no	140 minutes
2 partial nephrectomies 2 radical nephrectomies 1 ureteroureterostomy 1 pyeloplasty	Porcine	Orlando (USA)	Shanghai (China)	Fiber	Microport Medbot Toumai	139 (137-185)	no	no	170 minutes

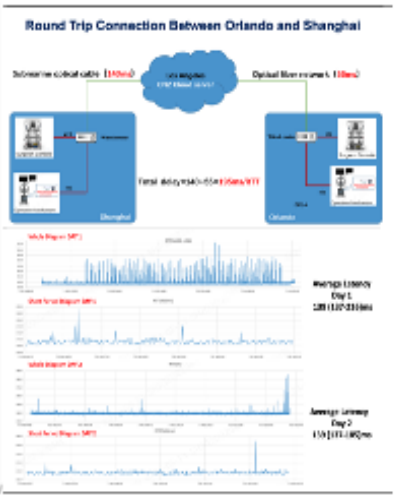

ABSTRACT 38

PRESSURE CHARACTERIZATION OF BENCHTOP MODEL WITH SIMULATED FANS OPERATION

Anya Chase, Alycia Abbott, Jessica Williams, Aditi Ray
Boston Scientific Inc

Introduction: The introduction of flexible and navigable suction ureteral access sheaths (FANS) to the clinical environment of ureteroscopy presents additional variables that impact intra-renal pressure (IRP). A comparison between IRP in a benchtop model and an *in-vivo* porcine model during a simulated FANS procedure was performed to characterize a rigid closed chamber pressure environment.

Methods: For the benchtop study, a sealed version of the previously presented Boston Scientific Bench (BSB) model chamber (with a 3-D printed "kidney" insert) [1, 2] was used to simulate the clinical environment with the FANS providing the only path for fluid outflow. A Comet™ II Pressure Guidewire was used to measure the chamber pressure. An 11/13 F commercially available FANS was inserted into the chamber near the Comet™ II Pressure Guidewire and a LithoVue™ Elite (LVE) Single-Use Digital Flexible Ureteroscope System with intrarenal pressure monitoring was inserted through the FANS. Prototype software was used with the LVE scope. A prototype fluid management system provided irrigation with a pump pressure setpoint of 200 mmHg. A vacuum pump was connected to the FANS with a pressure sensor in line with the suction. Initial vacuum source setpoint was -200 mmHg. Tape was placed over the vent of the FANS to ensure a seal. Simulated use of FANS was performed by moving the distal tip of the LVE scope from the BSB chamber to the FANS hub then moving it back to the chamber without moving the FANS. This was repeated five times. Pressure behavior was compared to a similar setup in an *in-vivo* porcine model using the same irrigation and vacuum setpoints. The vent of FANS was controlled by physicians. Two physicians retracted the LVE scope three times each.

Results: When the LVE scope was fully inserted in the BSB, kidney chamber pressure was between -5 and -50 mmHg. When the LVE scope was retracted, kidney chamber reached pressures of approximately -170mmHg to -210 mmHg. In the *in-vivo* porcine model, when the LVE scope was in the kidney, kidney pressure was between 10 and 100 mmHg. When retracting the LVE scope through the FANS, the renal pressure often remained closer to 0 mmHg gauge pressure. However, the minimum renal pressure recorded from the Comet pressure guidewire with the LVE scope tip retracted in FANS was -128 mmHg indicating that FANS tip position with respect to the Comet pressure guidewire location could affect this measurement.

Conclusion: Kidney chamber pressures during simulated FANS operation with the BSB are more negative than renal pressure measured in the *in-vivo* model likely due to the ability to create an airtight environment in the BSB. In the *in-vivo* model, pressures between sensors varied depending on both LVE scope and FANS tip position. This highlights the importance of spatial variation of renal pressure, and that pressures near the FANS tip may be lower than pressures elsewhere.

Disclaimers: Prototype fluid management system and prototype LVE software used in this study were concept device/technologies, which were not available for sale at the time the study was conducted. Pressures measured from the LVE and Comet pressure guidewire extend beyond the specified operating range for each device. Bench and preclinical testing results may not necessarily be indicative of clinical performance. Testing was performed by Boston Scientific. Data on file.

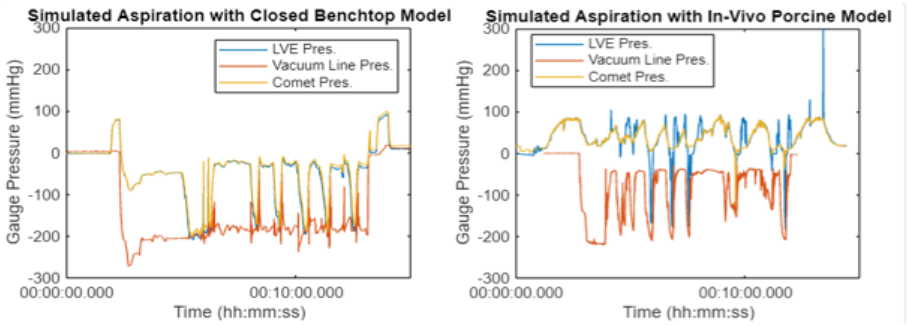

Figure 1: Pressure environment in benchtop model (left) Pressure environment in *in-vivo* porcine model (right)

ABSTRACT 39

AUTOMATED DETECTION OF LASING ACTIVITY FOR POST-OPERATIVE CASE ANALYSIS IN MiniPCNL PROCEDURES WITH THE MONARCH™ PLATFORM

Saif Sayed[1], Camilla Gomes[1,2], Brandon Cowan[1,2], Hedyeh Rafii-Tari[1]
[1] Research & Development, Johnson & Johnson MedTech Surgery, Santa Clara, CA
[2] Department of Surgery, University of California, San Francisco, CA 94143

Introduction: Case review serves as an educational tool and method for identifying areas for improvement in procedural self-analysis for both faculty and learners; however, lengthy procedures like ureteroscopy and/or percutaneous nephrolithotomy (PCNL) often yield hours of video footage from which to isolate relevant procedural steps. We aim to develop a computer vision algorithm to autonomously detect the active lasing phase during robotic-assisted ureteroscopy and PCNL, facilitating a more efficient analysis of lasing-related activities.

Methods: Clinical experts reviewed MONARCH™ Platform, Urology case videos to identify frames corresponding to "laser-idle" and "laser-active" states. These expert-labeled frames provided the essential action labels required for training the deep learning model. The proposed architecture comprises a UNet-based tool detector, a fine-tuned ActionCLIP model for spatial feature extraction, and a temporal feature tracking model (TCN) as shown in Figure 1.

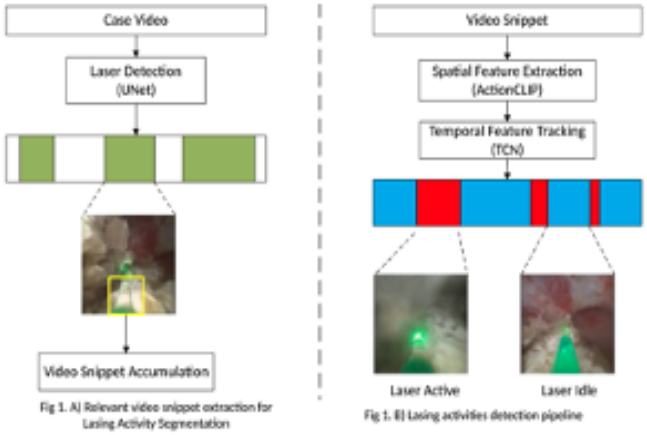

Fig 1. A) Relevant video snippet extraction for Lasing Activity Segmentation
Fig 1. B) Lasing activities detection pipeline

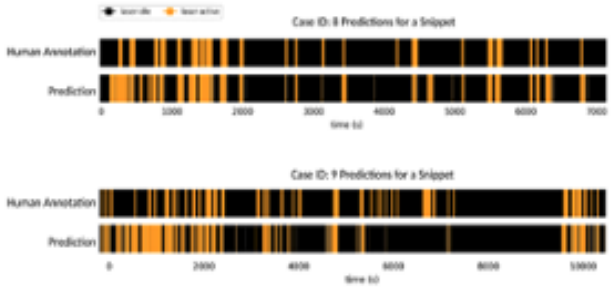

Fig 2. Sample snippets activity detections from test Cases

Results: The dataset comprised of 12 randomly selected MiniPCNL Procedures with the MONARCH™ Platform, each varying in stone burden and case duration. The human labels and model prediction outputs areas shown in Figure 2. The model was trained & validated on 10 cases and tested on 2 mini-PCNL cases. For the total test duration of 580 seconds of lasing activations, the model was able to detect 350 seconds correctly. For both *laser-idle* and *laser-active* states, the model gave a detection test accuracy of 75.16% per video frame.

Conclusion: This is the first reported computer vision model to detect lasing activity in stone procedures, and its promising accuracy in a visually challenging scene is an exciting development as we enable proceduralists to quickly pinpoint the lasing-specific segments of the procedure.

ABSTRACT 40

DOES LUBRICATION OF BRAIDED AND MONOFILAMENT SUTURE WITH BACITRACIN-PETROLATUM AND SALINE, RESPECTIVELY, REDUCE SUTURE DRAG AND, PRESUMABLY, TISSUE TRAUMA? A QUANTITATIVE PULL-FORCE MEASUREMENT STUDY

Alejandro D. Lopez[1], Diba Nayeri[2], Michael Zaliznyak[3], Cedric A.R. Bailey[4], Maurice M. Garcia[5]
[1]School of Medicine, University of California San Francisco, San Francisco, CA
[2]School of Medicine, University of Southern California, Los Angeles, CA
[3]Department of Urology, University of California San Francisco, San Francisco, CA
[4]Department of Pathology and Laboratory Medicine, Cedars-Sinai Medical Center, Los Angeles, CA
[5]Department of Urology, Cedars-Sinai Medical Center, Los Angeles, CA

Introduction: It is always desirable to reduce trauma to tissues during surgery. This is especially important with fine tissues such as urethra, vascular-anastomotic sutures, micro-surgery, and sutures in organs such as kidney and liver. Tissue drag during suturing reflects friction between suture and tissue and presumably correlates with greater trauma to tissue. We routinely coat braided sutures with Bacitracin-petrolatum ointment. However, some surgeons are skeptical of the safety of this practice. Strategies to reduce suturing tissue drag/trauma are poorly standardized and studied. Our aim is to measure whether lubrication of braided and mono-filament sutures with Petrolatum or saline, respectively, reduce suture drag.

Methods: Ten 2-0 and Ten 4-0 Vicryl™ (braided) and Monocryl™ (monofilament) sutures (total: 40) were passed through unique needle entry/exit sites in a 4"x4" area of a silicone-cast pelvis. Each suture was passed three times: #1, dry (no lube); #2: lubricated with Bacitracin [petrolatum] (braided) or continuous saline irrigation (monofilament), and #3: repeat of #2, but without additional lubricant. A handheld digital force meter with a hook attachment was then hooked through a slipknot in the suture adjacent to the needle, to measure peak pull-force (N). A two-tailed, unpaired t-test was used as a test of significance.

Results: Relative to passage of either suture type without lubrication (*dry*), lubrication with either Bacitracin or continuous irrigation reduced suture drag to below the limit of detection, whereas repeat passage of the same suture without reapplication of lubricant significantly reduced drag, to 54% of dry for braided 4-0 & 2-0, and to 38% of dry for 4-0 monofilament and 59% of dry for 2-0 monofilament.

Conclusion: Lubrication of brained and monofilament sutures with Bacitracin-petrolatum or saline, respectively, significantly reduces drag- and presumably, tissue damage. Repeat lubrication appears to maximize benefit. To date, no study has shown that petrolatum-coating impairs wound healing. These data are the first to quantitatively measure the effect of lubrication on the required suture pull force. Histologic tissue and microsurgical-suture follow-up studies are warranted.

Table 1 **Measured Suture Pull-Force for Braided and Monofilament Suture With and Without Lubrication Using Bacitracin-Petrolatum Coating and Saline-Irrigation**

	A.			B.			C.			D.		
Trial #	4.0 Braided (Vicryl) Suture			2.0 Braided (Vicryl) Suture			4.0 Monocryl Suture			2.0 Monocryl Suture		
	Dry	Bacitracin Ointment-Coated		Dry	Bacitracin Ointment -Coated		Dry	Wet		Dry	Wet	
	(N)	First Pass (N)	Second Pass (N)	(N)	First Pass (N)	Second pass (N)	(N)	First Pass (N)	Second Pass (N)	(N)	First Pass (N)	Second Pass (N)
1	1.1	<0.0098	0.5	1	<0.0098	0.9	1.8	<0.0098	0	2.4	<0.0098	1.2
2	1	<0.0098	0.7	1.3	<0.0098	0.3	1.5	<0.0098	0.7	1.8	<0.0098	1.1
3	1	<0.0098	0.6	1	<0.0098	0.9	1.6	<0.0098	0.9	1.7	<0.0098	1
4	1	<0.0098	0.7	1.1	<0.0098	0.3	1.5	<0.0098	0.7	1.6	<0.0098	0.9
5	1.5	<0.0098	0.6	1.4	<0.0098	0.4	1.6	<0.0098	0.7	2.3	<0.0098	1.3
6	1.1	<0.0098	0.5	1.4	<0.0098	0.6	1.4	<0.0098	0.6	1.7	<0.0098	1
7	1.2	<0.0098	0.6	1.7	<0.0098	0.6	1.4	<0.0098	0.5	1	<0.0098	1.3
8	1.3	<0.0098	0.5	0.9	<0.0098	0.7	1.1	<0.0098	0.4	2.2	<0.0098	0.8
9	0.9	<0.0098	0.6	1	<0.0098	0.7	1.1	<0.0098	0.4	1.4	<0.0098	1
10	0.9	<0.0098	0.6	0.9	<0.0098	0.9	1.2	<0.0098	0.5	1.9	<0.0098	1
Mean	1.1	<0.01	0.59	1.17	<0.01	0.63	1.42	<0.01	0.54	1.8	<0.01	1.06
			Percent of dry: 54%			Percent of dry: 54%			Percent of dry: 38%			Percent of dry: 59%
		*p** <0.0001	*p** <0.0001		*p** <0.0001	*p** <0.0001		*p** <0.0001	*p** <0.0001		*p** <0.0001	*p** <0.0001

ABSTRACT 41 **TOP 10 ABSTRACT**

HIGH-PRECISION DETECTION OF DIFFICULT-TO-DETECT LESIONS IN BLADDER CANCER DIAGNOSIS USING A LIGHTWEIGHT AI MODEL

Ryotaro Okazaki[1], Atsushi Ikeda[1], Wonjik Kim[2], Hirokazu Nosato[2], Hiroyuki Nishiyama[1]
[1] University of Tsukuba, Ibaraki [2] National Institute of Advanced Industrial Science and Technology, Ibaraki, Japan

Introduction: The current standard method for bladder cancer diagnosis, white light cystoscopy, misses 10-30% of lesions. Particularly flat lesions, small tumors, and carcinoma in situ (CIS) are frequently overlooked, resulting in high recurrence rates of 40-80%[1]. Despite advances in deep learning for medical imaging, existing models have not solved this challenge: these difficult lesions are either underrepresented in datasets or entirely absent, leading to significantly low detection rates[2, 3, 4, 5, 6]. Furthermore, some current state-of-the-art models employ complex architectures such as Transformers with hundreds of millions of parameters, making real-time application in clinical settings virtually impossible[5, 6, 7]. This research directly addresses this dual challenge: detecting the most diagnostically difficult lesion types while maintaining computational efficiency suitable for actual clinical environments.

Methods: We designed a novel lightweight diagnostic framework that balances clinical utility and computational efficiency. This approach integrates EfficientNetV2[8] and U-Net[9] architectures, but the true innovation lies in our pioneering loss function fusion strategy. Through extensive experimentation, we discovered that specific loss function weighting models excel at detecting specific lesion characteristics. We developed a fusion model that strategically combines the complementary strengths of each weighted model to optimize detection performance for difficult-to-detect cases while maintaining overall performance. Our comprehensive dataset, consisting of 10,332 normal images and 1,411 tumor images (40.2% flat lesions), was labeled by urologists and pathologists according to shape, size, T classification, and malignancy grade, enabling detailed analysis based on lesion characteristics.

Results: Our fusion model achieved remarkable detection improvements for cases that clinicians struggle most to identify (Figure); detection rates for small tumors increased from 39.9% to 61.7%, flat lesions from 56.6% to 76.2%, and CIS lesions from 70.6% to 89.2%. These achievements were accomplished while maintaining excellent overall performance metrics of 95.8% sensitivity, 98.8% specificity, and an average Dice coefficient of 0.822. Most notably, the model achieved this with just 53 million parameters—less than one-third the size of models with comparable performance[6]—and a processing speed of 14.9 frames per second on a standard laptop. This performance breakthrough demonstrates the first viable approach to providing real-time clinical support for the most challenging cases of bladder cancer.

Conclusion: Our research overcomes two fundamental limitations that have hindered AI implementation in bladder cancer diagnosis: low detection rates for clinically difficult lesions and impractical computational requirements. By developing a groundbreaking fusion approach that precisely targets cases where clinician performance declines, we have created a system that provides meaningful diagnostic assistance rather than merely confirming obvious findings. The model's lightweight architecture and processing speed remove implementation barriers for actual clinical deployment. This breakthrough has profound implications for bladder cancer management—reducing missed diagnoses, improving recurrence monitoring, and enhancing patient outcomes through early intervention for CIS, the most aggressive cancer frequently missed by conventional methods.

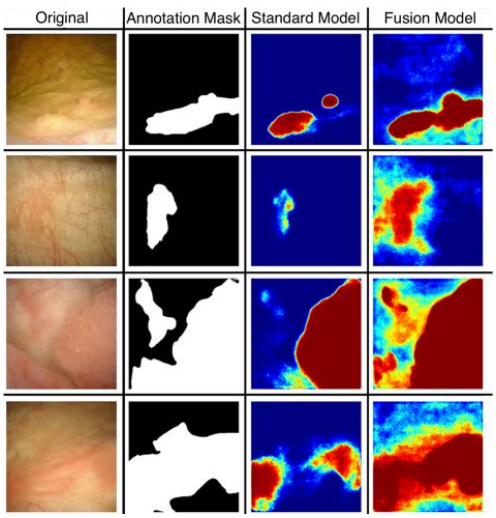

Figure: Fusion model detection of challenging bladder cancer lesions.

ABSTRACT 42

THE FIRST-IN-HUMAN TRANSCONTINENTAL TELESURGERY COLLABORATION FOR HIGH-INTENSITY FOCUSED ULTRASOUND (HIFU): A NEW ERA IN GLOBALIZING FOCAL CANCER TREATMENT FOR PROSTATE CANCER

Nicolas A Soputro[1], Waleed Hassan[2], Christopher J Weight[1], Georges-Pascal Haber[2], Jihad Kaouk[1], Ruben Olivares[1]
[1] Department of Urology, Cleveland Clinic Main Campus, Cleveland, OH, USA
[2] Department of Urology, Cleveland Clinic Abu Dhabi, United Arab Emirates

Introduction: The advent of telesurgery has opened a new frontier within minimally invasive surgery, allowing surgeons to complete procedures from a remote location and providing new opportunities for the delivery of care. Herein, we sought to describe the first clinical experience of telesurgery using High-Intensity Focused Ultrasound (HIFU) to treat prostate cancer.

Methods: The HIFU procedure was performed using the Focal One® device (Focal One, Austin, Texas, USA) on a 72-year-old with an ISUP Grade Group 2 prostate cancer from a single biopsy core that corresponds to a PIRADS 4 lesion in the left mid-apical region. A secure remote connection was established using the Software-Defined Wide Area Network (SD-WAN) infrastructure between the purpose-built virtual desktop for the console surgeon in Cleveland (Ohio, USA) and the operating room in Abu Dhabi (United Arab Emirates), spanning a total distance of 7,091 miles (or 11,412 km). The virtual desktop was specifically developed to mirror the two screens of the Focal One® device. On the day of the surgery, the local team was responsible for placing the Foley catheter, patient positioning, and the insertion of the Focal One® ultrasound probe into the patient's rectum. Following this, control was given to the remote surgeon, who completed the routine steps of HIFU, which included the fusion of preoperative MRI images with real-time ultrasound images, contouring of the prostate, identification and mapping of the region of interest, as well as the subsequent ablative treatment, employing the double-tap technique. A separate audiovisual field was also established and maintained during the surgery, ensuring consistent and fluid communications between the two locations.

Results: The procedure was completed successfully within 100 minutes, with 50 minutes of ablation time and an estimated ablation volume of 26.4 cm^3. Intraoperative blood loss was minimal, and there was no evidence of intraoperative complications. The patient had an uneventful postoperative recovery, and he was discharged home four hours after the surgery without any opioid analgesia. Foley catheter was removed on postoperative day 5. With the total recorded round-trip latency of 115 milliseconds, there remained no perceptible disruptions that were noted during the procedure.

Conclusion: This collaborative effort marked a significant milestone that underscored the safety and feasibility of HIFU telesurgery for the management of localized, clinically significant prostate cancer. This remote surgery model using an already established network infrastructure, offers significant promise for expanding access to specialized, high-quality medical care, particularly in underserved regions.

Figure 4. First transcontinental HIFU telesurgery experience between Cleveland, Ohio (USA) and Abu Dhabi (UAE)

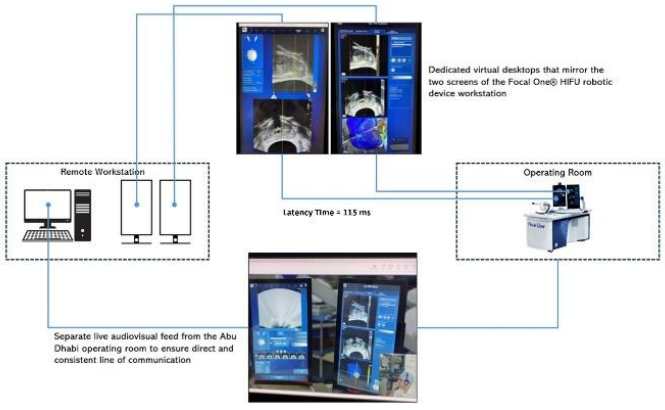

Figure 2. Schematic of remote workstation set-up for the surgeon console in Cleveland and the network infrastructure

ABSTRACT 43 **BEST ABSTRACT AWARD**

ROBOTIC TRANSURETHRAL BLADDER TUMOR RESECTION: A NEW ERA OF NATURAL ORIFICE TRANSLUMINAL ENDOSCOPIC SURGERY (NOTES)

Nicolas A Soputro[1], Carter D Mikesell[1], Lin Wang[1], Adriana M Pedraza[1], Salim K Younis[1], Megan Griffith[2], Jason YK Chan[3], Jane K Nguyen[1,2], Christopher J Weight[1], Jihad Kaouk[1], Nima Almassi[1]

[1] Glickman Department of Urology, Cleveland Clinic, Cleveland, OH, USA

[2] Diagnostics Institute, Pathology & Laboratory Medicine, Cleveland Clinic, Cleveland, OH, USA

[3] Chinese University of Hong Kong (CUHK), Hong Kong

Introduction: Transurethral Resection of Bladder Tumor (TURBT) represents the current gold standard for diagnosis, clinical staging, and initial management of bladder cancer. Nevertheless, the procedure carries risk of complication, including bleeding, bladder perforation, and suboptimal resection, which may compromise oncological outcomes and necessitate re-resection. Cautery artifact and difficulty orienting specimen may also compromise assessment of depth of tumor invasion. With an aim to reduce perioperative morbidity and enhance surgical precision and clinical staging, we sought to demonstrate our first experience of robotic TURBT using a novel, endoluminal robotic system.

Methods: All procedures were completed using the purpose-built robotic platform (Agilis Robotics, Hong Kong), which comprised two ultra-thin and flexible instruments with a purpose-built grasper on the left hand and hook bipolar diathermy on the right hand. Both instruments were introduced through a standard 27Fr resectoscope sheath, together with a 12º 4mm rigid endoscopic camera, as often used for TURBT procedures. Our pre-clinical experience consisted of both ex-vivo trials on a porcine bladder, as well as resections within the bladder of a female cadaver. For the latter, the cadaver was positioned in a supine lithotomy position with the robotic system placed between the legs. The surgeon console chair was placed on the right side of the bed, ensuring easy access to adjust the cystoscope at all times.

Results: A total of five *ex-vivo* and one cadaveric procedures were completed successfully without any need for additional ports, conversion to other techniques, or evidence of intraoperative complications. All participants were able to complete the resections across various locations within the bladder, including the posterior wall, bladder dome, anterior wall, as well as the right and left lateral walls. All specimens were resected en bloc, with an average resected area and resection speed of 35.9 mm^2 and 7.6 mm^2/min, respectively. We did not identify any significant differences in the performance between the participants. The cadaveric trial was performed by an experienced robotic surgeon (N.A.), who achieved an average resection area of 65 mm^2 at 10.9 mm^2/min without evidence of bladder perforation. The en-bloc specimen from the cadaver was evaluated by our Genitourinary Anatomical Pathologist (J.K.N.), who confirmed the presence of detrusor muscle in all samples with minimal evidence of electrocautery artifact. Procedural workload was assessed using the NASA-TLX, with all participants reporting favorably low scores across all six domains of the validated questionnaire.

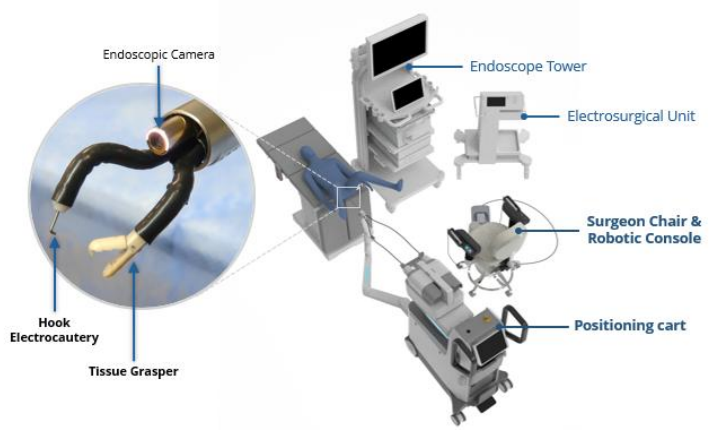

Figure 1. Intraoperative room configuration with the novel purpose-built transurethral robotic system.

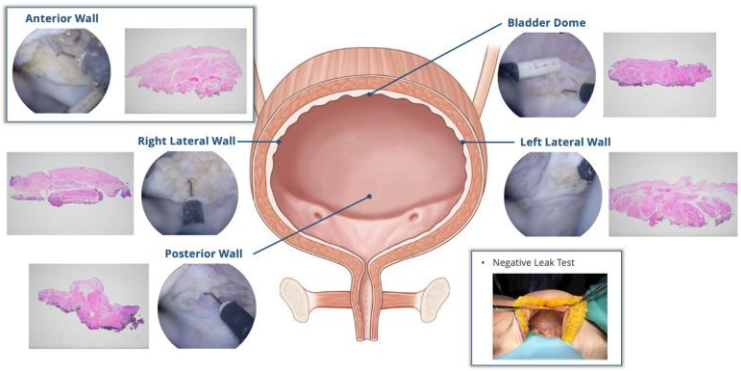

Figure 2. The different resection sites during the robotic TURBT procedure on a female cadaver. The purpose-built robotic grasper was shown for its utility to provide additional retractions that allowed for improved specimen orientation and assessment of potential muscle invasion.

Conclusion: This study highlighted the feasibility and efficacy of robotic TURBT using a purpose-built system, showing strong potential for enhanced surgical precision and improved histopathological assessment for muscle invasion. While this pre-clinical experience yielded promising results, further studies remain necessary to assess clinical applications, learning curves, and procedural safety of this innovative endoluminal robotic approach.

ABSTRACT 44 **TOP 10 ABSTRACT**

PROSTATE DUCTAL ANATOMY AS A CANCER CONTRAST MECHANISM FOR ULTRASOUND

Dan Luca[1], Jake W. Pensa[1], Derrick Ushko[2], Griffith Hughes[1], Adam Kinnaird[3], David Kuppermann[1], Anthony Sisk[1], Leonard Marks[1], Rory Geoghegan[1], Wayne G. Brisbane[1]
[1]Department of Urology, University of California, Los Angeles [2]University of Victoria, British Columbia, Canada
[3]University of Alberta, Alberta, Canada

Introduction: Conventional ultrasound (US) with a frequency of 6-9MHz and a resolution of ~200µm, has poor sensitivity and specificity for detecting prostate cancer (PCa) [1], [2]. Micro-ultrasound (microUS) at 29MHz (~70µm resolution), has recently been introduced as a potential alternative. The higher resolution enables visualization of prostate ductal anatomy, which is disrupted in PCa tissue (Figure 1) [2], [3]. The aim of this study is to analyze whole-mount (WM) pathology slides and to evaluate prostate ductal anatomy as a contrast mechanism for visualization of prostate cancer using micro-ultrasound.

Methods: Ten men scheduled to undergo radical prostatectomy for PCa were enrolled in an IRB-approved study (IRB-19-1136). After prostatectomy, prostates were grossed, sectioned, and stained. All clinically significant PCa lesions were annotated by an experienced pathologist. The scanned slides were then analyzed using a custom computer vision script (MATLAB) to identify and quantify ductal features. Using the annotated lesions, binary masks were made to delineate benign and PCa groups. A color thresholding step was then applied to the tissue within each mask to select the white space where the prostate ducts are located. We extracted two main features: the duct equivalent diameter, and the ductal ratio.

Results: A total of 54 slides were processed with 145,150 benign and 9,245 PCa ducts identified. The mean equivalent diameter of benign ducts was 155.7 ± 147.8 µm. PCa ducts had a mean equivalent diameter of 129.4 ± 94.3 µm (Figure 2A). The average ductal ratio for benign tissue was 0.086 ± 0.029 and 0.039 ± 0.017 for PCa tissue (Figure 2B).

Conclusion: Prostate ducts are large enough to be resolved on microUS, but too small for conventional ultrasound. In addition, PCa tissue exhibits an approximate 50% reduction in ductal ratio, which highlights the potential of ductal anatomy as a contrast mechanism for PCa visualization using micro-ultrasound.

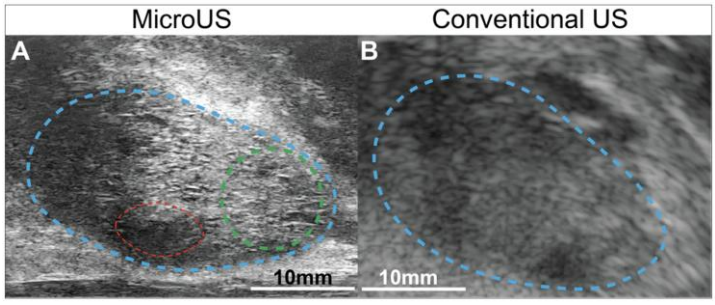

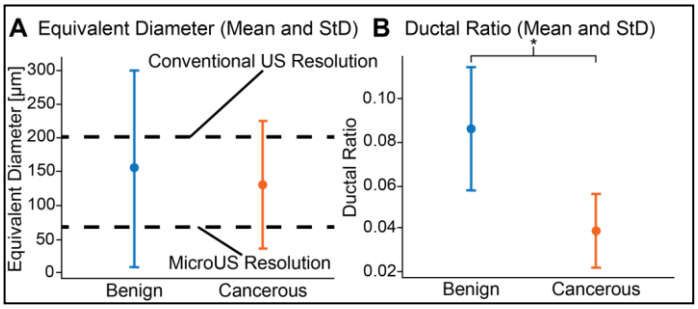

Figure 1A. MicroUS image of a prostate (outlined in blue) with visible prostate ducts (outlined in green), and visible cancer (red)
Figure 1B. Conventional US image of the same prostate tissue (outlined in blue) with no visible prostate duct

Figure 2A. The equivalent diameter for benign and PCa prostate ducts.
Figure 2B. The ductal ratio for benign and PCa tissue. *p-value << 0.001 for two-sample T-test.

ABSTRACT 45

ASSESSING PERSONAL STATEMENTS FOR UROLOGY RESIDENCY APPLICANTS GENERATED BY ARTIFICIAL INTELLIGENCE COMPARED TO APPLICANT WRITTEN PERSONAL STATEMENTS

Iyla Bagheri[1], Alexandra Tabakin[1], Louis Aghanwa[2], Kaitlyn Sbrollini[3], Andrew Chen[4], Michael D Gross[5], Jason Kim[3], Wai Lee[1]

[1]The Smith Institute for Urology at Northwell Health, New Hyde Park, NY, [2]Donald and Barbara Zucker School of Medicine at Hofstra/Northwell, Hempstead, NY, [3]Stony Brook, Stony Brook, NY, [4]Cedars Sinai, Beverly Hills, CA, [5]Cleveland Clinic, Cleveland, OH

Introduction: The use of artificial intelligence (AI) to facilitate tasks has grown in popularity and can generate written material, including personal statements (PS) for residency applications. The objective of our study was to assess how urology faculty would evaluate PS written by AI compared to actual personal statements written by urology applicants.

Methods: A survey was conducted on academic urology faculty assessing four PS — 2 written by human applicants and 2 generated by ChatGPT 4.0. The AI-generated PS were created by a first- and fourth-year medical student with minimal faculty or resident oversight. The two PS written by actual applicants were provided by urology applicants that matched their first-choice residency program at least 5 years prior to this study. Participants ranked the statements using a Likert scale (1-5) on originality, clarity, and personal insight/self-awareness. They also indicated whether they believed each statement was generated by AI and commented on how they would rank the applicant.

Results: Our questionnaire generated a 45% participation rate (68/151). Seventeen questionnaires were excluded for incomplete responses. The final cohort included 51 complete questionnaires. Faculty were more likely to highly rank applicants with human-written PS than AI-generated PS (66.6 vs 33.3%, $p<0.01$). Faculty were also more likely to accurately identify human-written PS than AI-generated PS (73.2 vs 26.8%, $p<0.01$). When stratified by those with academic leadership roles (department chairs and resident program directors), there was no difference between academic leaders and other faculty in accuracy for predicting human vs AI-generated PS (45.3 vs 54.7%, $p=0.65$).

Conclusions: This study provides insight into the perceptions of academic urology faculty regarding AI-generated PS. Although human-written PS outperformed AI-generated PS with respect to originality, personal insight, and rankings, the findings underscore the necessity for residency programs to develop clear criteria for evaluating PS amidst the growing use of AI tools in application submissions.

ABSTRACT 46

THE FIRST EXPERIENCE USING 5.1 FR. WORKING CHANNEL WITH SUCTION (SINGLE-USE FLEXIBLE URETEROSCOPES PU 400A) AND BENDABLE ACCESS SHEATH 12/14 FR. IN COMPLETE 2-3 CM RENAL STONE REMOVAL

Bogdan Geavlete[1,2,3], Cosmin Ene[1,2], Catalin Bulai[1,2,3], Razvan Multescu[1,2,3], Adrian Militaru[1,2,3], Valentin Iordache[1,2,3], Petrisor Geavlete[1,2,3]

[1]"Carol Davila" University of Medicine and Pharmacy, Bucharest, Romania [2]"Saint John" Emergency Clinical Hospital, Bucharest, Romania [3]"Sanador" Hospital

Introduction: Renal lithiasis continues to represent a frequent pathology, so the technology improvement is essential for developing new methods of treatment that are less invasive and more effective. The aim of this study was to evaluate for the first time the single-use flexible ureteroscopes PU 400A with a 5.1 Fr. working channel with suction and a bendable access sheath 12/14 Fr. in patients having 2-3 cm renal stones.

Methods: We enrolled 68 cases, which were performed using a single-use digital flexible ureteroscope Pusen PU400A 9.2 Fr. with a suction system (5.1 Fr. working channel). The stones were fragmented using Laser Mega Puls70 Quanta System Richard Wolf with a 200-μm laser fiber and an energy setting of <30 W. The access sheath was ClearPetra® Wellead Flexi Ureteral Access Sheath 12/14F (with suction). The suction pressure was controlled at 80–120 mmHg. A 6-Fr indwelling double-J stent was placed postoperatively and retained for 2–4 weeks, depending on the condition of the ureter. The pyelocaliceal kidney stones (single) had maximum dimensions between 11 mm and 34 mm, 1.121 to 2.420 mm^3, HU between 1.120 and 1.480. Average age 52.1 years. 65 patients (95.6%) were previously stented.

Results: The suction system was used both during the lithotripsy, improving visualization, and at the end to achieve a complete stone-free status in real time. The median IRP was 19.4 mmHg (10.1-39.7). Operative time (OP) was between 31 and 88 min (average 47.2 min). In 19 cases (27.9%) mild hematuria was described (Clavien I-II). No urinary tract infections (UTI) were found. No other complication was determined in the studied group. The evaluation of the postoperative stone-free status was performed in all cases 3 weeks after the date of the procedures by non-enhanced CT. The stone-free rate at 3 weeks was 89.7 % (61 cases). Residual fragments are considered significant if they are larger than 2 mm; in cases where residual fragments are detected, a second flexible ureteroscopy was performed with 100% of stone-free.

Conclusion: Preliminary data seem to be favorable, with significant improvement in terms of safety and of the stone-free rate, but larger multicenter studies are necessary for determining the best place of this method in the urological field.

ABSTRACT 47

A COMPARATIVE *IN VITRO* STUDY OF STANDARD VERSUS FLEXIBLE SUCTION URETERIC ACCESS SHEATH

Mario Basulto-Martínes and John Denstedt
Western University, London, ON, Canada

Introduction and Objectives
Surgical management of urinary stones has advanced significantly, with flexible ureterorenoscopy (fURS) and percutaneous nephrolithotomy (PCNL) becoming key techniques for complex stones, particullary in the lower pole stones with challenging renal anatomy. fURS is often favored due to its lower risk of bleeding. The emergence of flexible and navigable suction ureteric access sheaths (FANS) offers potential advantages for fURS in improving stone clearance and reducing operative time. This study aimed to evaluate the effectiveness of a novel FANS compared to a standard UAS in an *in vitro* lower urinary tract model.

Methods
This *in vitro* study was carried out using a urinary tract model containing artificial stones to simulate a lower pole calyx with complex anatomy. Fourteen procedures were performed, using either a standard UAS (n=7) or a FANS (n=7). Surgical time, laser time, total energy output, laser energy time, laser ablation speed, and stone clearance were recorded. Each procedure was conducted with single-use 8.4 Fr ureteroscope, and a Holmium:YAG laser set to 0.5 J, 25 Hz, and short pulse.

Results
Complete stone clearance was achieved in 5 of 7 procedures using FANS, while none of the procedures with the standard UAS reached this outcome. Median laser time [1442 (1285 – 1504) vs. 1653 (1566 - 1704) s, p=0.017] and total energy output [18270 (16069 - 18931) vs. 20663 (19575 - 21325) J, p=0.017] were significantly lower in the FANS group, with comparable overall surgical times between the two groups.

Conclusions
This *in vitro* study demonstrates that FANS significantly enhances stone clearance in a complex lower pole model, achieving higher SFRs, reduced lasering time, and lower energy output compared to a standard UAS, while maintaining similar operative times. FANS appears promising for improving fURS outcomes, particularly in anatomically challenging cases. Clinical trials are warranted to validate these findings *in vivo*.

ABSTRACT 48 **TOP 10 ABSTRACT**

IMPROVED CONTROL OF RENAL PELVIS PRESSURE USING A PROTOTYPE FLUID MANAGEMENT SYSTEM INCORPORATING URETEROSCOPE PRESSURE FEEDBACK

Leilane Glienke[1], Anthony F Bonzagni[1], Timothy L Hall[2], Khurshid R Ghani[1], William W Roberts[1]
Departments of [1]Urology and [2]Biomedical Engineering University of Michigan, Ann Arbor, MI, USA

Introduction: During ureteroscopy it is desirable to maintain renal pelvis pressure (P_{RP}) below 40 cmH_2O - the threshold for pyelovenous backflow - to decrease risk of infectious complications and postoperative pain. P_{RP} is dependent on both outflow resistance (R_{OUT}) and irrigation rate. R_{OUT} varies between patients as well as during a ureteroscopy case based on anatomic features and instrumentation used. Therefore, irrigation rate should be continually adjusted for optimal P_{RP} control. A prototype fluid management system (FMS) has been developed that adjusts irrigation rate based on pressure feedback. We sought to characterize P_{RP} in a silicone kidney ureter model using this prototype FMS compared to conventional pressure-driven irrigation across a range of R_{OUT} values.

Methods: A LithoVue™ Elite ureteroscope (Boston Scientific, Marlborough, MA) was inserted into a silicone kidney ureter model with its tip in the renal pelvis. Irrigation was delivered from the prototype FMS with P_{RP} limit set to 40 cmH_2O or from conventional gravity irrigation at 50, 75, 100, 125, or 150 cmH_2O irrigation pressure. P_{RP} was measured at steady state. Trials were conducted in triplicate for each irrigation setting and five outflow resistance scenarios (R_{OUT} = 0.9, 2.0, 2.9, 4.0, and 4.9 cmH_2O/(ml/min)).

Results: For conventional irrigation, P_{RP} increased as irrigation pressure increased and as R_{OUT} increased (Figure). For prototype FMS irrigation, the mean P_{RP} remained below 40 cmH_2O – specifically 31.9, 36.9, 38.3, 39.2, and 39.7 cmH_2O as R_{OUT} was incremented from 0.9-4.9 cmH_2O/(ml/min) respectively (Figure). For example, when R_{OUT} was 2.0 cmH_2O/(ml/min), P_{RP} was 37 cmH_2O with both 125 cmH_2O conventional irrigation pressure and the prototype FMS. However, with greater R_{OUT} of 2.9, 4.0, and 4.9 cmH_2O/(ml/min)), mean P_{RP} increased to 47, 57, and 60 cmH_2O respectively with 125 cmH_2O conventional irrigation pressure but was maintained below 40 cmH_2O with the prototype FMS.

Conclusion: Mean P_{RP} with the prototype FMS was maintained below the 40 cmH_2O threshold across different R_{OUT} values, while P_{RP} with conventional irrigation frequently exceeded the 40 cmH_2O pressure threshold. Adjusting irrigation rate based on pressure feedback is an effective way to control P_{RP} and may reduce risk of infectious complications and postoperative pain.

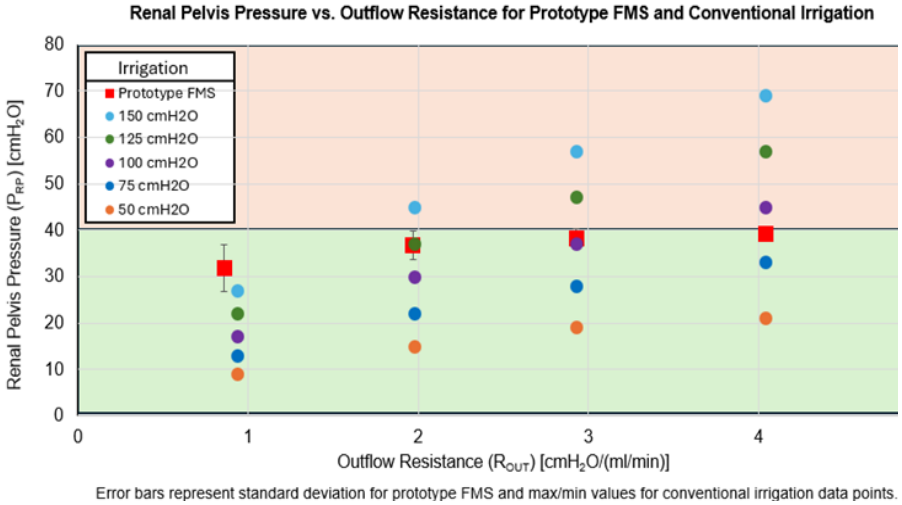

Funding: Research Grant from Boston Scientific

ABSTRACT 49

LASER LITHOTRIPSY OF A BRUSHITE CRYSTALLINE AGGREGATE STONE MODEL: FRAGMENT DISTRIBUTION VS. BEGOSTONE AND HUMAN STONES

Leilane Glienke[1], John W. Robinson[2], Tim L. Hall[3],
Khurshid R. Ghani[1], Adam J. Matzger[2,4], and William W. Roberts[1]
Departments of Urology[1], Chemistry[2], Biomedical Engineering[3], and the Macromolecular Science and Engineering Program[4] at the University of Michigan, Ann Arbor, MI, USA

Introduction: Laser research is hampered by a lack of accurate stone models that replicate fragmentation during laser lithotripsy. We sought to assess the distribution of stone fragments from laser ablation of new brushite crystalline powder and brushite crystalline aggregate stone models and compare with human stones and BegoStone. Samples of 15:3 and 15:5 BegoStone, powder, and aggregate model stones were tested alongside human CHPD and COM stone samples.

Methods: All samples were secured and hydrated before Ho:YAG laser energy was delivered (Lumenis P120H) using a 200-micron D/F/L fiber. Lithotripsy was performed by repeatedly translating the fiber automatically through a predetermined grid of points (MATLAB program) until >50% of each sample was ablated. Fragments were separated by sieving.

Results: For each stone type, 70.2–96.9% of the mass of fragments consisted of particles smaller than 0.25 mm. The percentage by mass of fragments greater than 1 mm in trials with 0.8 J x 10 Hz settings was 0.5%, 0.0%, 1.1% and 5.1% for BegoStone 15:3, BegoStone 15:5, powder model, and aggregate model respectively, compared to 5.5% for CHPD and 16.2% for COM (Figure 1). Only the aggregate model, CHPD and COM samples produced fragments > 2mm.

Conclusion: The new aggregate model stone better replicates the fragment distribution of human stones after laser lithotripsy. The method of producing the aggregate model stone - incorporating crystal and chemical components found in urinary stones - holds promise for developing better stone models needed to address a range of important lithotripsy research questions.

Funding: Research Grant from Boston Scientific

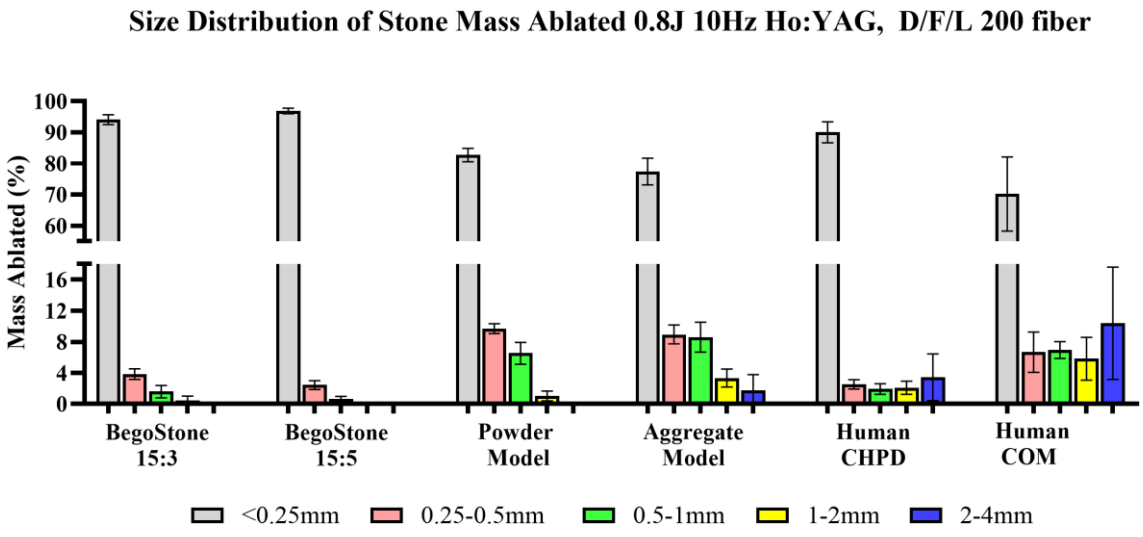

Figure 1

ABSTRACT 50

AUGMENTED REALITY ASSISTED MRI-ULTRASOUND FUSION FOR NON-RECTAL FULLY-TRANSPERINEAL PROSTATE BIOPSY

Jaskirat Saini, Braden Millan, Ruben Blachman-Braun, Baris Turkbey, Sheng Xu, Ming Li, Sandeep Gurram, Bradford Wood, Peter A. Pinto
Urologic Oncology Branch, Center for Interventional Oncology, National Cancer Institute, NIH

Introduction: Augmented reality technologies enable the superimposition of imaging anatomy upon the patient during procedures. We sought to demonstrate the feasibility of using an augmented reality (AR) system (XR90, MediView XR Inc, Cleveland, OH) to fuse ultrasound and multi-parametric MRI (mpMRI) segmentation in real-time to perform a non-rectal fully trans-perineal, AR-assisted prostate biopsy.

Methods: A fiducial grid was used to place pen marks at fixed distances in the suprapubic region, where MRI-compatible fiducial markers (MR-Spot, Beekley Corporation, Bristol, CT) were placed before the patient underwent a pre-biopsy mpMRI. Anatomic segmentation of the fiducial markers, target lesion, prostate, bladder, rectum, pelvic vasculature, and pelvic/lower extremity bones was performed using third-party software (Axial 3D, Belfast, UK). An electromagnetic (EM) field generator was integrated onto the operating table (Aurora, Northern Digital Inc, Waterloo, Canada). EM and optically tracked registration markers were placed at the 3 fiducial marker locations and used to register the patient-specific segmentation and tracked instruments, which include the ultrasound probe (Vivid iq, GE HealthCare, Chicago IL) and trocar (E-Trax, Civico, Coralville, IA). The FDA-cleared AR headset-based system was used to perform a targeted biopsy after performing our standard mpMRI/ultrasound (US) fusion-guided prostate biopsy (Figure 1) (UroNav, Koninklijke Philips N.V., Amsterdam, Netherlands).

Results: Using an AR headset, a 3D volumetric rendering of patient-specific mpMRI was registered and successfully deployed in a targeted prostate biopsy. To account for differences in positioning during the preoperative mpMRI and the surgical procedure, registration was further manually adjusted by correlating a position on the ultrasound and segmented anatomy. Biopsy of the target lesion was performed via a non-rectal fully trans-perineal approach using AR as an adjunct to US guidance. AR-assisted biopsy results were congruent with our standard mpMRI/US fusion biopsy results showing benign prostate tissue. AR assistance helped the operator adjust the placement of the cannula for biopsy. No adverse events were noted.

Conclusions: This use case demonstrates the feasibility of using AR to perform a non-rectal fully trans-perineal targeted prostate biopsy. Limitations include the current pre-procedural workflow with imaging segmentation and system registration with the patient in dorsal lithotomy, the size of the EM generator, and a non-specialized ultrasound probe.

Acknowledgement: Supported by the Center for Cancer Research of the NCI, Intramural Research Program of the NIH, the Center for Interventional Oncology, and devices supplied by MediView XR, Inc. (Cleveland, OH).

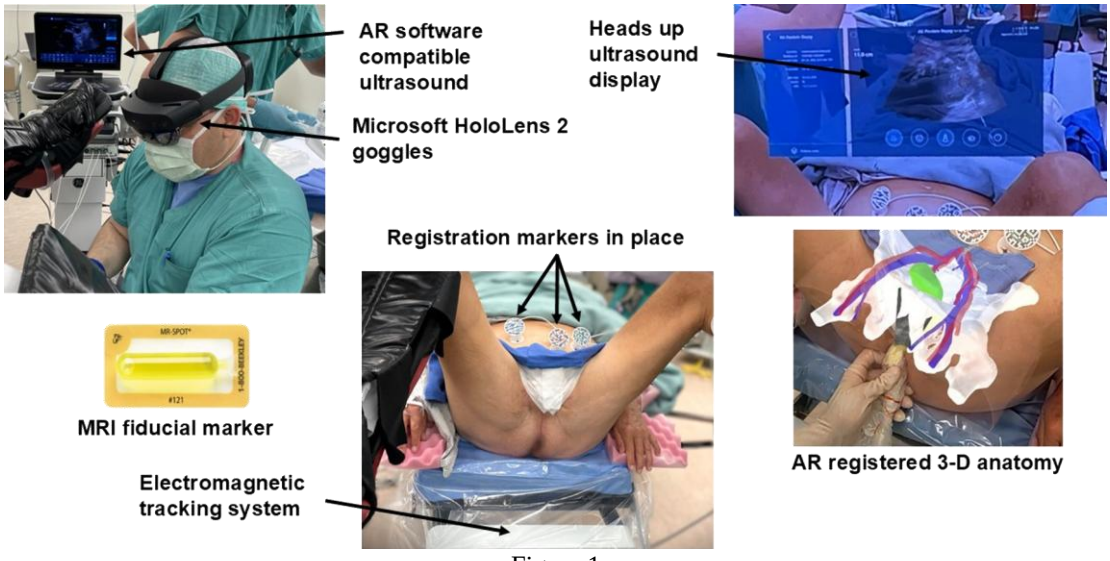

Figure 1

ENGINEERING AND UROLOGY SOCIETY OFFICERS:

PRESIDENT
Jihad Kaouk

SECRETARY
Margaret Pearle

TREASURER
Chandru Sundaram

COUNCILOR
Louis Kavoussi

EXECUTIVE DIRECTOR
Dan Stoianovici

ADVISORY BOARD
Jeffrey Cadeddu

Ralph Clayman

Jean de la Rosette

Misop Han

Pilar Laguna

Thomas Lawson

Manoj Monga

Pierre Mozer

Stephen Nakada

Jens Rassweiler

Koon Ho Rha

William Roberts

Arthur Smith

Li-Ming Su

Gerald Timm

Hessel Wijkstra

Kevin Zorn

AWARDS:

BEST ABSTRACT AWARDS:

ROBOTIC TRANSURETHRAL BLADDER TUMOR RESECTION: A NEW ERA OF NATURAL ORIFICE TRANSLUMINAL ENDOSCOPIC SURGERY (NOTES)

Nicolas A Soputro[1], Carter D Mikesell[1], Lin Wang[1], Adriana M Pedraza[1], Salim K Younis[1], Megan Griffith[2], Jason YK Chan[3], Jane K Nguyen[1,2], Christopher J Weight[1], Jihad Kaouk[1], Nima Almassi[1]
[1] Glickman Department of Urology, Cleveland Clinic, Cleveland, OH, USA
[2] Diagnostics Institute, Pathology & Laboratory Medicine, Cleveland Clinic, Cleveland, OH, USA
[3] Chinese University of Hong Kong (CUHK), Hong Kong

BIOPSY NEEDLE DESIGN MATTERS: 96% REDUCED BACTERIAL TRANSFER AND SIGNIFICANTLY IMPROVED TARGETING MAY CHALLENGE TR vs TP PROSTATE BIOPSY PARADIGMS

Andreas Forsvall[1,2,3] for the Lund/Xaga study group
[1] Faculty of Medicine, Department of Clinical Sciences, Infection Medicine, Lund University, Lund, Sweden
[2] Department of Urology, Helsingborg Hospital, Helsingborg, Sweden
[3] Xaga Surgical AB, Eslov, Sweden

AWARDS:

TOP 10 ABSTRACTS:

FEASIBILITY OF WIRELESS CATHETER-FREE AMBULATORY URODYNAMICS IN MALE PATIENTS

Tyler Trump [1], Michael Gross [1], Kassandra Zaila [1], Madison Lyon [1], Steve Majerus [2,3], Brett Hanzlicek [2], Tyler Tevis [2], Ly Hoang-Roberts [1], Margot Damaser [1,2], Smita De [1]
[1] Glickman Urological and Kidney Institute - Cleveland Clinic; Cleveland, OH, USA
[2] Advanced Platform Technology Center - Louis Stokes VA Medical Center; Cleveland, OH, USA
[3] Department of Electrical, Computer and Systems Engineering, Case Western Reserve University, Cleveland, OH, USA

A STEERABLE KIDNEY STONE BASKET

Peter Connor[1], Joshua Gafford[2], Scott Webster[2], S. Duke Herrell[1,2,3], Nick Kavoussi[3], Kim Maciolek[3], Amy Reed[3], Kent Chevli[4], Jake Childs[2], Tyler Efird[2], and Robert J. Webster III[1,2,3]
[1] Vanderbilt University, [2] EndoTheia Inc.
[3] Vanderbilt University Medical Center, [4] WNY Urology Associates

IMPROVED CONTROL OF RENAL PELVIS PRESSURE USING A PROTOTYPE FLUID MANAGEMENT SYSTEM INCORPORATING URETEROSCOPE PRESSURE FEEDBACK

Leilane Glienke[1], Anthony F Bonzagni[1], Timothy L Hall[2], Khurshid R Ghani[1], William W Roberts[1]
Departments of [1]Urology and [2]Biomedical Engineering University of Michigan, Ann Arbor, MI, USA

OPTIMIZATION OF GOLD-SILVER NANOPARTICLE COATINGS WITH ANTIMICROBIAL AND ANTIBIOFILM PROPERTIES

Alejandro Bautista-Perez-Gavilan[1], Jorge Gutierrez-Aceves[1], Smita De[1], Aaron W. Miller[1,2], Vijay Krishna[3]
[1] Urology Department, Cleveland Clinic Glickman Urological Institute, Cleveland, OH, USA
[2] Cardiovascular and Metabolic Sciences Department, Cleveland Clinic Lerner Research Institute, Cleveland
[3] Biomedical Engineering, Cleveland Clinic Lerner Research Institute, Cleveland, OH, USA

HIGH-PRECISION DETECTION OF DIFFICULT-TO-DETECT LESIONS IN BLADDER CANCER DIAGNOSIS USING A LIGHTWEIGHT AI MODEL

Ryotaro Okazaki[1], Atsushi Ikeda[1], Wonjik Kim[2], Hirokazu Nosato[2], Hiroyuki Nishiyama[1]
[1] University of Tsukuba, Ibaraki [2] National Institute of Advanced Industrial Science and Technology, Ibaraki, Japan

A NEW ULTRASOUND PROBE AND ROBOT FOR PROSTATE BIOPSY

Dan Stoianovici[1,2], Katarzyna J. Macura[3], Doru Petrisor[1,2], Arvin K. George[1], Misop Han[1]
[1]Brady Urological Institute, [2]Robotics Laboratory, [3]Department of Radiology, Johns Hopkins University

PROSTATE DUCTAL ANATOMY AS A CANCER CONTRAST MECHANISM FOR ULTRASOUND

Dan Luca[1], Jake W. Pensa[1], Derrick Ushko[2], Griffith Hughes[1], Adam Kinnaird[3], David Kuppermann[1], Anthony Sisk[1], Leonard Marks[1], Rory Geoghegan[1], Wayne G. Brisbane[1]
[1]Department of Urology, University of California, Los Angeles [2]University of Victoria, British Columbia, Canada
[3]University of Alberta, Alberta, Canada

THE EFFECT OF PROSTATE SIZE AND NUMBER OF CORES AT SYSTEMATIC PROSTATE BIOPSY – STUDY UPDATE

Dan Stoianovici[1,2], Katarzyna J. Macura[3], Bruce Trock[1],
Amin Herati[1], Christian Pavlovich[1], Arvin George[1], Misop Han[1]
[1]Brady Urological Institute [2]Robotics Laboratory, [3]Department of Radiology, Johns Hopkins University

AWARDS:

BEST REVIEWER AWARDS (LAST 5 YEARS):

		2021	2022	2023	2024	2025
George	Aninwene II			☼		
Atieh	Ashkezari					☼
Jeffrey	Cadeddu		☼			
Ralph	Clayman			☼	☼	
John	Denstedt				☼	
Oscar	Fugita				☼	☼
Petrisor	Geavlete	☼			☼	
Bogdan	Geavlete		☼			
Bradley	Gill					☼
Philippe	Grange			☼		
Dylan	Isaacson	☼				
Louis	Kavoussi					
Jaime	Landman		☼		☼	
Thomas	Lawson		☼			
Salvatore	Micali	☼				
Cristian	Mirvald		☼			
Steven	Monda			☼		
Razvan	Multescu				☼	☼
Naren	Nimmagadda	☼				
Christian	Pavlovich		☼			
Thomas	Polascik					☼
Roxana	Ramos				☼	
Koon Ho	Rha					☼
Abhishek	Singh		☼			
Nicolas	Soputro	☼				
Renea	Sturm				☼	

AWARDS:

REVIEWERS:

We gratefully acknowledge the contribution of the following reviewers to the success of the meeting and thank them for taking the time to promote the best science.

Atieh Ashkezari	Leilane Glienke	Doru Petrisor
Alejandro Bautista-Perez-Gavilan	Muhammed Moukhtar Hammad	Thomas Polascik
Akash Chauhan	Misop Han	Koon Ho Rha
Ralph Clayman	Atsushi Ikeda	William Roberts
Brandon Cowan	Kathleen Kieran	André Santos
Margot Damaser	Avaneesh Kunta	Harel Sims
John Denstedt	Seyed Amiryaghoub Lavasani	Nicolas Soputro
Kristin Ebert	Thomas Lawson	Maya Srinath
Cosmin Ene	Dong-Ho Lee	Dan Stoianovici
Andreas Forsvall	PAUL Merguerian	Nelson Stone
Oscar Fugita	Adrian Militaru	Zachem Tanner
Petrisor Geavlete	Mahdi Mottaghi	Tyler Trump
Ahmed Ghazi	Razvan Multescu	Marie-Therese Valovska
Bradley Gill	Amy Pearlman	Felix Yiu

GRANTS, EXHIBITORS, AND ACKNOWLEDGEMENTS:

The Society of Urological Robotic Surgery (SURS) thanks the following company for providing an Independent Educational Grant for the Society of Urological Robotic Surgery (SURS) Meeting

BOSTON SCIENTIFIC
EXACT IMAGING
KOELIS
INTUITIVE
VASCULAR TECHNOLOGY, INC.

EXHIBITORS

COOK MEDICAL

THANKS

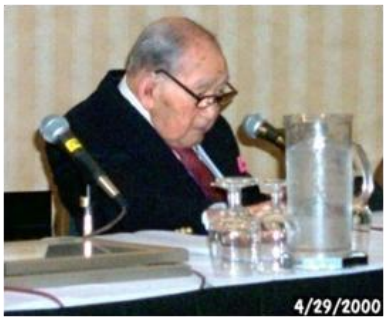

George Nagamatsu, MD founded the Engineering and Urology Society in 1985

Jack Vitenson, MD was the first Society Treasurer in 1985

Special thanks to Dr. Thomas Lawson for his help in formatting the abstracts and to Michelle Paoli and Debra Caridi for organizing this Annual Meeting.

ACCME ACCREDITATION:

Engineering Urology Society Meeting at the AUA2025
Accreditation Information

Accreditation: The American Urological Association (AUA) is accredited by the Accreditation Council for Continuing Medical Education (ACCME) to provide continuing medical education for physicians.

Credit Designation: The American Urological Association designates this live activity for a maximum of 2.0 *AMA PRA Category 1 Credits*™*.* Physicians should claim only the credit commensurate with the extent of their participation in the activity.

Learning Objectives
After participating in this CME activity, participants will be able to:

1. Initiate engagement in multidisciplinary collaboration, recognizing the important interplay between technological and technical innovations with improved patient outcomes.
2. Evaluate new innovations and techniques in Urology, including emerging robotic platforms and medical devices to further improve diagnostic and procedural accuracy and accessibility.

Analyze the application of new and emerging technologies in various patient care settings.

ACCME ACCREDITATION:

Focal Therapy Society Meeting at the AUA2025
Accreditation Information

Accreditation: The American Urological Association (AUA) is accredited by the Accreditation Council for Continuing Medical Education (ACCME) to provide continuing medical education for physicians.

Credit Designation: The American Urological Association designates this live activity for a maximum of 2.0 *AMA PRA Category 1 Credits*™*.* Physicians should claim only the credit commensurate with the extent of their participation in the activity.

Learning Objectives
After participating in this CME activity, participants will be able to:

1. Describe the evolving standards in prostate cancer diagnosis and risk stratification as of 2024.
2. Explain the role of advanced imaging modalities, including micro-ultrasound and artificial intelligence, in planning and monitoring focal therapy.
3. Evaluate the benefits and challenges of integrating imaging techniques into clinical workflows for partial gland ablation.
4. Discuss the principles and applications of cryotherapy, irreversible electroporation, and robotic partial prostatectomy in focal therapy.
5. Compare the efficacy, safety, and practical implications of these technologies in treating localized prostate cancer.

Formulate strategies for incorporating advanced focal therapy techniques into clinical practice to improve patient outcomes.

ACCME ACCREDITATION:

Society of Urologic Robotic Surgeons Meeting at the AUA2025
Accreditation Information

Accreditation: The American Urological Association (AUA) is accredited by the Accreditation Council for Continuing Medical Education (ACCME) to provide continuing medical education for physicians.

Credit Designation: The American Urological Association designates this live activity for a maximum of 4.5 *AMA PRA Category 1 Credits*™*.* Physicians should claim only the credit commensurate with the extent of their participation in the activity.

Learning Objectives
After participating in this CME activity, participants will be able to:

1. Implement at least one new technique or strategy for robotic urinary tract reconstruction (e.g., fistula repair, ureteral stricture management, buccal mucosa ureteroplasty) to improve surgical outcomes in their practice.
2. Apply updated knowledge of nerve-sparing techniques and strategies for optimizing continence and sexual function preservation during robotic cystectomy to enhance patient quality of life.
3. Evaluate the benefits and challenges of different robotic kidney transplantation approaches (including robotic donor nephrectomy and single-port techniques) to determine the optimal approach for individual patients.
4. Select appropriate patients for transvesical and extraperitoneal single-port robotic prostatectomy based on an understanding of the indications, surgical techniques, and comparative outcomes of these approaches.
5. Analyze complex robotic urologic surgery cases and formulate effective surgical plans based on expert recommendations and evidence-based practices discussed during case presentations and panel discussions.

Integrate emerging technologies, such as AI and simulation, into their robotic surgery practice to enhance surgical precision, efficiency, and patient safety.

ACCME ACCREDITATION:

Evidence-Based Content: It is the policy of the AUA to ensure that the content contained in this CME activity is valid, fair, balanced, scientifically rigorous, and free of commercial bias.

Disclosures of Relevant Financial Relationships: All persons in a position to control the content of a CME activity are required to disclose to the AUA, as the ACCME-accredited provider, all financial relationships with any ineligible companies during the previous 24 months. An ineligible company is defined as one whose primary business is producing, marketing, selling, re-selling, or distributing healthcare products used by or on patients. The AUA must determine if the individual's relationships are relevant to the educational content and mitigate any conflicts of interest prior to the commencement of the educational activity. The intent of this disclosure is not to prevent individuals with relevant financial relationships from participating, but rather to provide learners with information so they can make their own judgments. All relevant financial relationships for this educational activity are available at auanet.org/AUA2024/speakers/disclosures.

AUA Disclosure Policy: Please visit auanet.org/AUA2025/attendee-info/cme-credits/cme-information to review the complete policy related to disclosure of relevant financial relationships with ineligible companies and mitigation of identified conflicts of interest.

Off-Label or Unapproved Use of Drugs or Devices: The audience is advised that this CME activity may contain reference(s) to off-label or unapproved uses of drugs or devices. Please consult the prescribing information for full disclosure of approved uses.